UNIVERSITY OF NAPLES "FEDERICO II"

PhD Program
Molecular Pathology and Physiopathology
XXVIII Cycle

School of Molecular Medicine

"Characterization of an autoimmune condition associated with AEC syndrome"

SUPERVISOR
Prof.ssa Missero Caterina

CANDIDATE
Dr.ssa Cirillo Luisa

PhD COORDINATOR
Prof. Vittorio Enrico Avvedimento

Academic Year 2014-2015

"Characterization of an autoimmune condition associated with AEC syndrome"

TABLE OF CONTENTS

LIST OF PUBLICATIONS

Research Techniques Made Simple: Skin Carcinogenesis Models: Xenotransplantation Techniques. Maria Rosaria Mollo, Dario Antonini, **Luisa Cirillo** and Caterina Missero, *J Invest Dermatol. 2016 Feb;136(2):e13-7. doi: 10.1016/j.jid.2015.12.015.*

LIST OF ABBREVIATIONS

AEC syndrome Ankyloblepharon- Ectodermal defects- Cleft lip/palate syndrome
WT Wild Type
+/L K14-Cre; $p63^{+/FloxL514F}$
L514F K14-Cre; $p63^{FloxL514F/FloxL514F}$
L514F; Tslp eKO K14-Cre; $p63^{floxL514F/floxL514F;}$ $Tslp^{FloxL2/FloxL2}$
EEC Ectrodactyly Ectodermal defects Cleft lip/palate syndrome
LMS Limb Mammary Syndrome
ADULT Acro Demato Ungual Lacrimal Tooth Syndrome
RHS Rapp Hodgkin Syndrome
E17.5 Embryonic day 17.5
P0 Post-natal day 0
P3 Post-natal day 3
P5 Post-natal day 5
P8 Post-natal day 8
P10 Post-natal day 10
P16 Post-natal day 16
P90 Post-natal day 90
AER Apical Ectodermal Region
Krt1 Keratin 1
Krt5 Keratin 5
Krt6 Keratin 6
Krt10 Keratin 10
Krt14 Keratin 14
Krt15 Keratin 15
Krt16 Keratin 16
Krt17 Keratin 17
Lor Loricrin
Ivl Involucrin
Flg Filaggrin
Dsg1 Desmoglein 1
Dsc3 Desmocollin 3
Dsp Desmoplakin
DBD DNA binding domain
SAM Sterile-α-Motif
PS Post-SAM domain
KCs Keratinocytes
ECs Epithelial Cells
ED Ectodermal Dysplasia
Cdh1 E-cadherin
H&E Haematoxylin and Eosin
TEM Tissue-electron microscopy
qRT-PCR quantitative Real Time-Polymerase Chain Reaction

Tslp Thymic Stromal Lymphopoietin
AMPs Anti Microbial Peptides
LC Langerhans Cells
DCs Dentritic cells
DDCs Dermal Dentritic cells
NK Natural killer cells
DETCs Dentritic Epidermal T cells
DAMPs Danger-Associated molecular patterns
TH T helper cells
APCs Antigen-Presenting Cells
IFN-γ Interferon-γ
IL-1a Interleukin-1a
IL-1b Interleukin-1b
IL-2 Interleukin-2
IL-4 Interleukin-4
IL-5 Interleukin-5
IL-10 Interleukin-10
IL-13 Interleukin-13
IL-20 Interleukin-20
IL-25 Interleukin-25
IL-33 Interleukin-33
TNF-α Tumor Necrosis Factor-α
TLRs Toll-like receptors
HMGB1 High Mobility Group Box 1
G-CSF (Csf3) Granulocyte-Colony Stimulating Factor (Colony Stimulating factor 3)
GM-CSF (Csf2) Granulocyte Macrophage-Colony Stimulating Factor (Colony Stimulating factor 2)
DefB1 Defensin B1
DefB3 Defensin B3
DefB4 Defensin B4
DefB6 Defensin B6
PAR2 Protease Activated Receptor 2
AD Atopic Dermatitis
NS Netherton Syndrome
Klk5 Kallikrein 5
Klk6 Kallikrein 6
Klk7 Kallikrein 7
Klk9 Kallikrein 9
Klk10 Kallikrein 10
NFAT Nuclear Factor of Activated T cells

ABSTRACT

Ankyloblepharon- Ectodermal defects Cleft lip/palate (AEC) syndrome, also known as Hay-Wells syndrome, is a severe genetic disorder caused by mutation in p63 gene and characterized by congenital erythroderma and severe skin erosions in infants that resolve very slowly leaving scars. To identify molecular mechanisms underlying the severe skin defects, we generated a conditional knock-in mouse carrying an inducible p63 mutation (L514F). AEC conditional mutant mice showed a strong phenotype including focal skin erosions, crusting and complete hair loss. A high percentage of mutant mice died between 8 and 15 days after birth. Epidermis was hyperplastic and hyperkeratotic, and massive infiltration of macrophages and mast cells was observed in the dermis. At the molecular level, reduced mechanical stress resilience was accompanied with a progressive skin inflammation due to strongly elevated level of Thymic stromal lymphopoietin (Tslp), an IL-7 like cytokine. Epidermal-derived Tslp was circulating in the bloodstream, causing a dramatic expansion of immature B-cells (pre B-cells) in the bone marrow and spleen, leading to the insurgence of an autoimmune lymphoproliferative disorder. Genetic ablation of Tslp in the epidermis ameliorated the general health condition of mutant mice, significantly reducing skin inflammation, rescuing B-cell differentiation, and increasing survival in AEC mice.
Mechanistically, massive Tslp release was accompanied by strong induction of kallikrein-6 (Klk6) and NFAT accumulation in mutant epidermis. Klk6 is repressed by wild-type p63 in epidermis and NFAT overexpression strongly induced Tslp in keratinocytes. Taken together these data indicate that in AEC mutant epidermis, Klk6 upregulation leads to massive Tslp induction by an NFAT-dependent mechanism. We propose that since extended skin erosions in AEC patients can also be associated with an autoimmune proliferative disorder, controlling Tslp in severely affected patients may be therapeutically beneficial.

1. BACKGROUND

1.1 The skin: the body natural barrier

The skin performs many important functions: protect us from trauma, ultraviolet radiation, microorganisms and chemicals agents. Prevents the loss of liquid; participates in the mechanism of thermoregulation, increasing (vasodilatation) or slowing down (vasoconstriction) the dispersion of heat.
It is composed of three main layers that from the outside inwards are: epidermis, dermis and hypodermis (subcutaneous layer).
The epidermis is the outermost layer of the skin, composed of a stratified squamous epithelium that rest on top of a basement membrane, rich in extracellular matrix, which separate it and its appendages, including the hair follicles and sweat glands from the underlying dermis. The epidermis and its appendages provide a protective barrier. It has a thickness comprised between 50 μm and 1.5 μm. The epidermis is composed of 4 layers: the cornified layer also known like stratum corneum, granular layer, spinous layer and basal layer (Fig. 1). The stratified squamous epithelium of the epidermis is maintained by cell division within the basal layer. During the epidermal maturation the cells undergo a complex series of morphological and biochemical changes that result in the production of the stratum corneum, the highly cornified outermost layer of the tissue composed by cornified cell envelopes assembled by cross-linking of structural proteins and lipids. More in detail, the cells of the basal layer remain attached to an underlying matrix through a series of adhesion molecules such as hemidesmosomes, laminin and anchoring fibrils, and proliferate. Some of their daughter keratinocytes enter the spinous layer through asymmetric mitoses, where they exit the cell cycle, grow larger and establish robust intercellular connections (Simpson et al, 2011). The cells switch expression of basal layer specific keratins, Keratin5 (Krt5) and Keratin 14 (Krt14), to Keratin1 and Keratin10 (Krt1; Krt10) typical of the spinous layer (Fuchs & Green, 1980). In addition other keratins are also expressed suprabasally, as Keratin6 (Krt6), Keratin16 (Krt16) and Krt17 (Krt17), but only in hyperproliferative condition such as wound healing. The spinous layer also contains Langerhans cells, which are derived from a precursor in bone marrow and are involved in immune response. Above the spinous layer, keratinocytes contain numerous keratohyalin granules packed with the protein profilaggrin in their cytoplasm, hence the name “stratum granulosum”. Cells in the granular layer flatten and assemble a water-impermeable cornified envelope underlying the plasma membrane and express filaggrin (Flg) and loricrin (Lor) as markers. In addition, cornified envelope proteins, which are rich in glutamine and lysine residues, are synthesized and deposited under the plasma membrane of the granular cells. As response to the increased permeability to the calcium, the cells activate transglutaminase, generating γ-glutamyl ε-lysine crosslinks to create an indestructible barrier. Finally, stratum

corneum keratinocytes release lysosomal enzymes to degrade major organelles, including the nucleus. The final steps of terminal differentiation involve also the extrusion of lipid bilayers, packaged in lamellar granules, onto the scaffold of the cornified envelope. The dead stratum corneum cells create an impenetrable layer that is continually replaced (Fuchs, 2007).

Keratinocytes move from the proliferative basal layer through the granular layer and continually replaced the cells of the outward layers. Indeed, as the body's outer frontier, the epidermis is subject to repeated trauma that must be repaired after wounding (Shen et al, 2013). Within this layer, epidermal stem cells divide to self-renew and produce transient amplifying (TA) cells, which are able of a more limited proliferative capacity. Transit amplifying cells constitute the major cell type in the basal layer of the developing and mature epidermis and after few rounds of cell division they exit from the cell cycle, and initiate a terminal differentiation program, as they migrate outward toward the tissue surface.

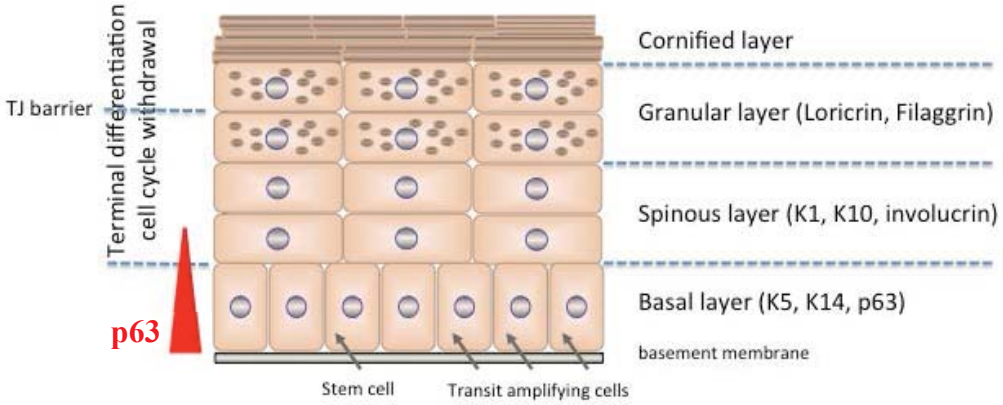

Figure 1. The epidermis. The epidermis is a stratified squamous epithelium composed by the indicated layers: the basal layer on top of the basement membrane consisting of proliferating, transit-amplifying cells interspersed to epidermal stem cells; spinous layer, granular layer and the cornified layer. Upon withdrawal from the cell cycle, basal keratinocytes detach from the basement membrane and undergo a terminal differentiated program to become corneocytes in the outer layers of the epidermis. The gene mainly expressed in the basal layer is p63, the master regulator of epidermal development. In the intermediate stratum spinosum, the cells reinforce their keratin filament network, and adjacent cells interact via many desmosomes. In the stratum granulosum, keratinocytes become more flattened and express certain proteins such as filaggrin and loricrin, which aggregate to form the typical keratohyalin granules of the granular layer. The epidermis is separated from the dermis by the basement membrane.

1.2 p63, the master regulator of epidermal gene expression: structure and function

p63 belongs to the p53 gene family consisting of three genes, p53, p63, and p73, that show significant homology (Yang et al, 2002). They share three functional domains: an N-terminal transactivation domain which shares 25% homology with N-terminal part of p53, a central DNA binding domain which shares 65% of homology with the corresponding p53 domain and C-terminal tetramerization domain, which shares 35% of homology with the oligomerization domain of p53 (Yang et al, 2002). In addition, all family members share some functions and bind to a canonical p53-binding site, thus controlling the expression of a subset of p53 target genes (Fig 2). p63, p53 and the third member p73, constitute a family of key transcriptional regulators in cell growth, differentiation and apoptosis. Indeed, while p53 is a major player in tumorigenesis (Kemp et al, 1994), p63 and p73 are involved in embryonic development (Mills et al, 1999; Yang et al, 2000). p63 has a crucial role in embryonic development of stratified epithelia where it can function either as an activator or a repressor (Koster & Roop, 2004; LeBoeuf et al, 2010). In particular, p63 is a master regulator of epidermal gene expression and it is critical for cell proliferation (Antonini et al, 2010; Senoo et al, 2007; Truong et al, 2006), cell adhesion (Carroll et al, 2006; Koster et al, 2007) and stratification (Koster & Roop, 2004; Truong et al, 2006) while suppressing terminal differentiation (Nguyen et al, 2006).

The p63 gene encodes a tetrameric factor that can be expressed in at least six isoforms with widely different transactivation potential that share an identical DNA binding domain (Yang et al, 1998). p63 is composed of 16 exons located on chromosome 3q28 and it has two independent transcriptional start sites that give rise to two different N-terminal isoforms: TA and ΔN that in turn produce α, ß or γ ends as the result of alternative splicing events towards the C-terminal region. In particular, TAp63 contains an acidic N-terminal transactivation domain similar to the one found in the canonical full-length p53. TAp63 is expressed at very low levels in most tissues, whereas it is constitutively expressed in female germ cells where it is activated by phosphorylation upon DNA damage, inducing oocyte death (Gonfloni et al, 2009; Kerr et al, 2012; Suh et al, 2006). In contrast ΔNp63 is widely expressed in the basal regenerative layer of the epidermis and other stratified epithelia, (Yang et al, 1998). ΔNp63 is the most abundant protein in the epidermis whereas the TAp63 is barely detectable by RNA-seq (Rizzo et al, 2014). The first 26 amino acids of the N-terminal region in ΔNp63 are required for its transcriptional activity, together with the proline-rich domain (PR) and a domain (TA2) located between the OD and the sterile-α-motif (SAM) domain (Dohn et al, 2001; Ghioni et al, 2002; Helton et al, 2006). The main isoform expressed in stratified epithelia is the p63α that contains at the C-terminal end a SAM domain and a post-SAM domain (PS) absent in p63ß, p63γ, or in p53 (Yang et al, 1998). SAM domains have several functions; they can interact with

themselves, bind to other SAM domains, bind to non–SAM domain proteins, or to RNA (Qiao & Bowie, 2005). p63's SAM domain is a five helical bundle domain that is unable to form homodimers (Chi et al, 1999; McGrath et al, 2001) and its function remains uncovered. The PS domain, also known as transcriptional inhibitory domain (TID), consists of two regions. The former interacts with the TA domain of another TAp63 molecule, establishing a closed and inactive dimer that can be activated by phosphorylation, resulting in an active tetramer (Deutsch et al, 2011; Su et al, 2010). The latter region holds p63 protein concentration via a sumoylation-dependent mechanism (Straub et al, 2010). However, the functional role of the PS domain is poorly understood.

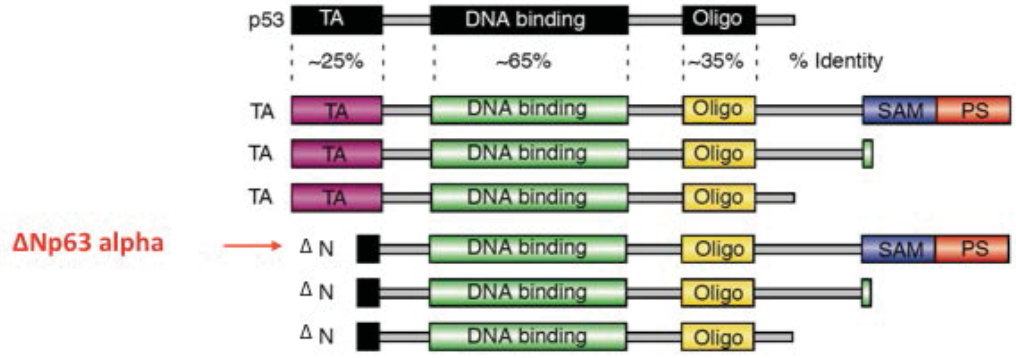

Figure 2. **Functional domains and isoforms of the *p53* family proteins.** Comparison between p53 and p63 proteins. Conserved protein domains are: TA, Trans-Activation domain; DNA binding domain; Oligomerization domain; SAM, Sterile- α -motif domain; PS, Post-SAM domain. TA, isoforms are transcribed from the upstream promoter; and ΔN, isoforms transcribed from the cryptic promoter within intron 3. The percentage of identity is indicated for each domain.

1.3 p63-deficient mice

In the 1999, two independent groups obtained a p63-deficient mouse model. Using these models they could explore the unique roles of p63 in development of ectodermal derived tissues. $p63^{-/-}$ mice die for dehydration soon after birth and display severe defects of all stratified epithelia and their derivatives, facial clefting and impaired limb formation, suggesting that p63 plays a pivotal role in these tissues (Mills et al, 1999; Yang et al, 1999). Defects in the surface epithelium of $p63^{-/-}$ mice have been ascribed to loss of proliferative potential of keratinocyte stem cells (Senoo et al, 2007; Yang et al, 1999), and/or altered

epidermal stratification and cell differentiation associated with reduced expression levels of Krt5/Krt14 and Krt1/Krt10 (Koster & Roop, 2004; Mills et al, 1999; Romano et al, 2009). p63-deficient newborns show striking limb defects. The fore limbs were truncated and hind limbs were completely absent and the structures dependent upon epidermal-mesenchymal interactions during embryonic development, such as hair follicles, teeth and mammary glands, are absent. Phalanges and carpals were absent in both the p63-homozygous mutant, whereas more proximal forelimb structures were slightly heterogeneous in the extent of the truncation in the two models. The femur and all distal skeletal elements were also absent. These defects are caused by a failure of the apical ectodermal ridge (AER) to differentiate. The lack of a proper AER limb buds in p63 null mice results from a failure of the ectoderm to undergo growth and differentiation that give rise to this stratified epithelium. Indeed, several genes that are important in limb-bud outgrowth are not expressed, such as Fgfr8, a marker of the AER, and Msx-1 which expression in the mesenchyme depends on an ectodermal signal, or abnormally expressed, such as Lmx-1, a marker of the dorsal limb mesenchyme (Mills et al, 1999; Yang et al, 1999).

The skin in the knock-out mouse model generated by McKeon's group lacks expression of the basal layer markers as Krt5 and Krt14 and also spinous layer markers Krt1 and Krt10. Even though, isolated patch of the epidermis showed the expression of late differentiation markers such as Loricrin, Involucrin and Filaggrin. The authors prove that p63 is required for the initial development and continued regeneration of the epidermis and that the loss of p63 in the tissues failed to maintain the proliferative potential of stem cells in skin (Fig. 3) (Yang et al, 1999). In addition, to reinforce this hypothesis the same authors in another study demonstrate that p63 is fundamental to maintain the proliferative potential of epithelia stem cells of both thymus and epidermis (Senoo et al, 2007).

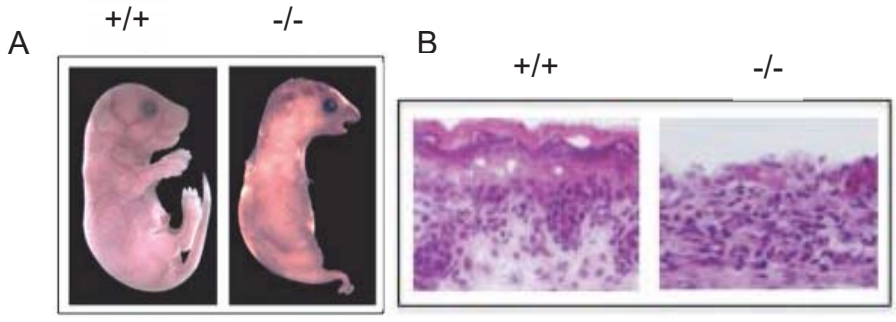

Figure 3. Phenotype of p63 knock out mouse generated by McKeon's group. A) The newborn p63 null mice show defects in skin stratification, limb formation and craniofacial defects. B) H&E staining of the skin at E17 display p63-/- mice lacking squamous stratification in the epidermis compared to wild-type skin which shows extensive stratification. (Adapted from (Yang et al, 1999)).

The p63 knock out mice generated by Mills's group developed aberrant skin and appendages due to lack of stratification and differentiation (Fig. 4)(Mills et al, 1999). The authors showed that in p63 null mice all structures that required the ectodermal mesenchymal signal were compromised because the ectoderm failed to receive the signal. They showed that the skin of p63 null mice were covered by a single disorganized layers of ectodermal cells or flattened epidermal cells in which they did not detect the expression of any early or late differentiation markers. Their results suggested that p63 is the determining factor of stratification, and supported the hypothesis that p63 is required for simple epithelial cells to commit to a stratified epithelial lineage during development (Mills et al, 1999).

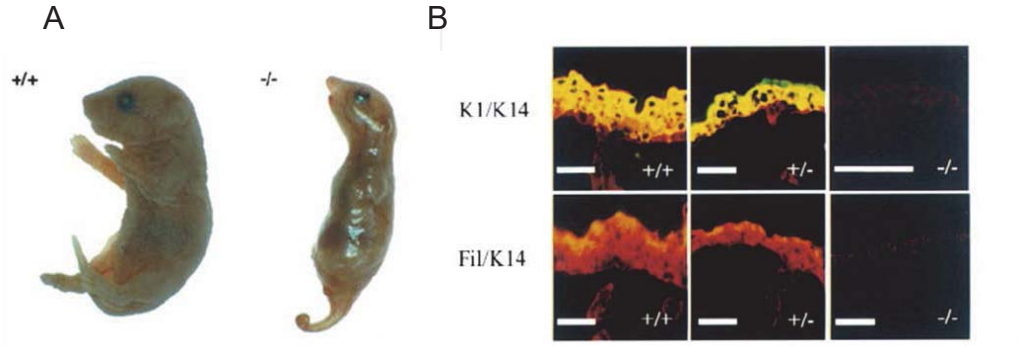

Figure 4. The phenotype of p63-deficent newborn mice generated by Mills's group. A) p63 null mice show severe limb and skin defects. B) Expression of different markers in the epidermis of p63 null mice: staining for Krt14 in red and Krt1 and Filaggrin (Fil) in green. Krt14 is weakly express in p63 null mice, whereas Krt1 and Fil are not detectable in the epidermis (Adapted from Mills et al., 1999).

1.4 p63-associated disorders

The crucial role of the transcription factor p63 in the formation of the epidermis and other stratifying epithelia is demonstrated by two lines of evidence. First, p63-deficient mice have no epidermis and aberrant squamous epithelia, and are also devoid of epithelial appendages, such as hair follicles and teeth. Second, heterozygous mutations in the human p63 gene are responsible for several ectodermal dysplasia (ED) syndromes, which are congenital disorders characterized by abnormalities of two or more ectodermal structures, such as hair, nails, sweat glands and digits. p63 expression is highest in the proliferative basal cell layer where epithelial progenitor cells are thought to reside in a range of stratified epithelia, including skin, in particular

in the nuclei of basal cells of the skin, cervix, tongue, esophagus, mammary glands, prostate and urothelium (Carroll et al, 2007).

Mutations in the p63 gene can cause at least five different syndromes: Ectrodactyly- Ectodermal defects-Cleft lip/palate syndrome (EEC, OMIM 604292), Ankyloblepharon- Ectodermal defects-Cleft lip/palate syndrome (AEC, OMIM 106260), Limb Mammary Syndrome (LMS, OMIM 603543), Acro- Dermato- Ungual- Lacrimal- Tooth syndrome (ADULT, OMIM 103285) and Rapp-Hodgkin Syndrome (RHS, OMIM 129400). Furthermore, two non-syndromic human disorders are caused by p63 mutations: isolated split hand/foot malformation (SHFM4, OMIM 605289) and recently non-syndromic cleft lip.

EEC syndrome is mainly caused by point mutation in the DNA binding domain (DBD) of the p63 gene. EEC syndrome comprises limb malformation, ectodermal dysplasia and orofacial clefting. Representative limb malformation are ectrodactyly and syndactyly (Rinne et al, 2007). Ectodermal dysplasia is seen as lightly colored, sparse hair and can be observed absence of eyelashes, eyebrows and alopecia. Skin is thin and dry, sometimes resembling dermatitis.

LMS was the first p63 syndrome linked to chromosome region 3q27. Mutations in LMS are located in the N- and C-terminus of the p63 gene. LMS phenotype comprises malformations of the hands and/or feet and hypoplastic nipples and/or mammary glands. Ectodermal defects are much less prominent than in EEC syndrome but mammary gland hypoplasia or aplasia is more frequent in LMS than in EEC.

ADULT syndrome phenotype is most similar to LMS syndrome, although clear differences can be seen when observing larger families or patient population. The main difference is the absence of orofacial clefting and the presence of hair and skin defects in the ADULT syndrome. Neverthless, teeth, skin, nail, hair and lacrimal duct defects are constantly present in ADULT syndrome (100, 91, 100%, 53% and 67%, respectively). A point mutation in exon 8, changing R298 in the DNA binding domain into either a glutamine or a glycine has been found. While EEC syndrome mutations in the DNA binding domain impair the binding of p63 protein to DNA (Celli et al, 1999), arginine 298 is not located close to the DNA-binding interface, and mutation of this arginine does not affect DNA binding (Duijf et al, 2002). Two other mutations are located in the N-terminus.

RHS was first described in 1968 by Rapp and Hodgkin in three individuals from one family with sparse eyebrows, slow-growing wiry scalp hair, nail dystrophy, hypodontia, clefting, hipohidrosis, and a characteristic facies. RHS share most features with AEC, but is differentially classified because of the lack of skin erosions and the absence of ankyloblepharon. Other ED symptoms, such as orofacial clefting and the absence of limb malformations are similar to AEC. In both syndromes clefting in lip and/or palate is equally frequent. The strong overlap between AEC and RHS suggest that they are variable manifestations of the same clinical entity (Bertola et al, 2004; Rinne et al, 2007). AEC and RHS mutations are located in the C-terminus of the p63

protein. They are either point mutations in the SAM domain or deletions in the SAM or PS domains (Barrow et al, 2002; Celli et al, 1999; Kantaputra et al, 2003; McGrath et al, 2001; van Bokhoven & Brunner, 2002). In 2001, heterozygous missense mutations in the TP63 gene were identified as the molecular basis for AEC syndrome and, in 2003, the first TP63 gene mutation was reported in RHS.

SHFM is a pure limb malformation (ectrodactyly and syndactyly) condition, without orofacial clefting or ectodermal dysplasia. The non-syndromic SHFM4 is caused by several mutations, which are dispersed throughout the p63 gene and probably it is caused by altered protein degradation, even though different degradation routes are involved (Rinne et al, 2007). A non-syndromic orofacial clefting type was also linked to p63 gene, R313G is the first mutation discovered (Leoyklang et al, 2006).

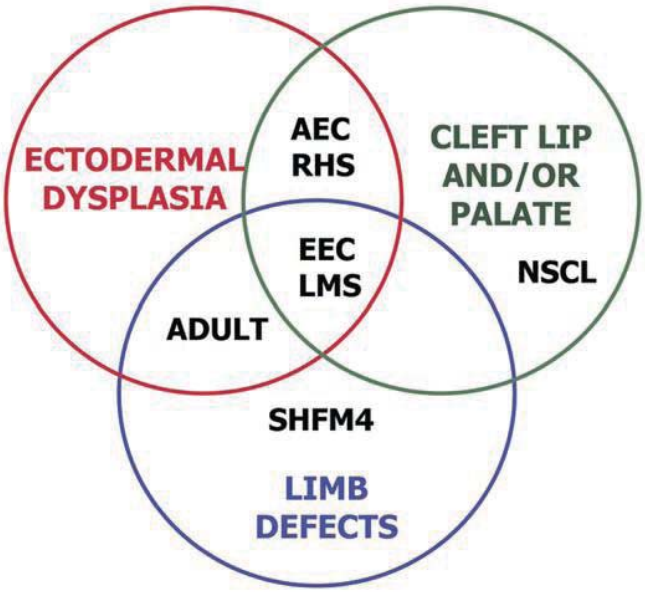

Figure 5. Various combinations of ectodermal dysplasia, orofacial clefting and limb malformations are the hallmark of p63-associated syndromes. EEC syndrome is the prototype of these syndromes and together with LMS shows all three hallmarks. ADULT syndrome patients never show orofacial clefting, whereas AEC and RHS never show limb defects. Non-syndromic limb defect condition (SHFM4) and non-syndromic cleft lip/palate (NSCL) are also caused by mutations in the p63 gene. (From Hans van Bokhoven et al, 2007)

1.5 AEC syndrome

Ankyloblepharon-Ectodermal defects Cleft lip/palate syndrome (AEC), also known as Hay–Wells syndrome, was first reported by Hay and Wells in 1976

(Hay & Wells, 1976). It is a rare autosomal dominant disorder, characterized by congenital fusion of the eyelids (ankyloblepharon), ectodermal dysplasia with severe involvement of the skin, and cleft palate with or without cleft lip. Clinical manifestations have different penetrance: about 75% of patients have severe skin erosions at birth, with some AEC patients reported to have up to 70% denuded skin. By 4 – 5 years age erosions could disappear, except for the head and auricular region. Clefting occurs approximately in 80% of AEC patients. The ankyloblepharon occurs only in 44% of AEC cases (Fig. 6). Hearing loss has been reported in about 40% of the patients. AEC patients have nails and teeth defects in about 75–80% of cases (Fig. 6). About half of the patients have lacrimal duct atresia. Dermatological features include thin and dry skin, often associated with congenital erythroderma, widespread skin erosions at or soon after birth, and erosive keratoderma of palms, soles and thin hair and/or alopecia. The most severe cutaneous manifestation of this disorder is the skin fragility associated with severe skin erosions after birth. Erosions typically involve the scalp, head and neck, skin folds, palms, and/or soles and are often accompanied by crusting and secondary infections (Fig. 6). Skin lesions are a distinctive signs of AEC syndrome. Adult patients can be affected by palmoplantar hyperkeratosis and erosive palmoplantar keratoderma with bleeding after extensive walking. The biological mechanisms underlying the skin erosions remain unveiled, and treatment is limited to gentle wound care and antibiotic treatment to prevent or cure infections. Healing is slow and recurrent breakdown is typical.

In AEC syndrome pathogenic mutations mainly fall in the C-terminus of p63 protein and include twenty-five missense and only two frameshift mutations in the SAM domain, whereas in the PS domain predominate the frameshift mutations that extend p63 protein (Rinne et al, 2009). These mutations give rise to mutant p63α proteins with dominant effects towards their wild-type counterparts. Recently, novel AEC causative mutations have been identified that result in translation re-initiation downstream of the non-canonical transactivation domain in the ΔN-specific isoforms, leading to expression of truncated ΔNp63 protein with dominant negative effects (Rinne et al, 2008).

AEC syndrome differs from the other conditions by the severity of the skin phenotype, the occurrence of ankyloblepharon, and the absence or mild limb malformations.

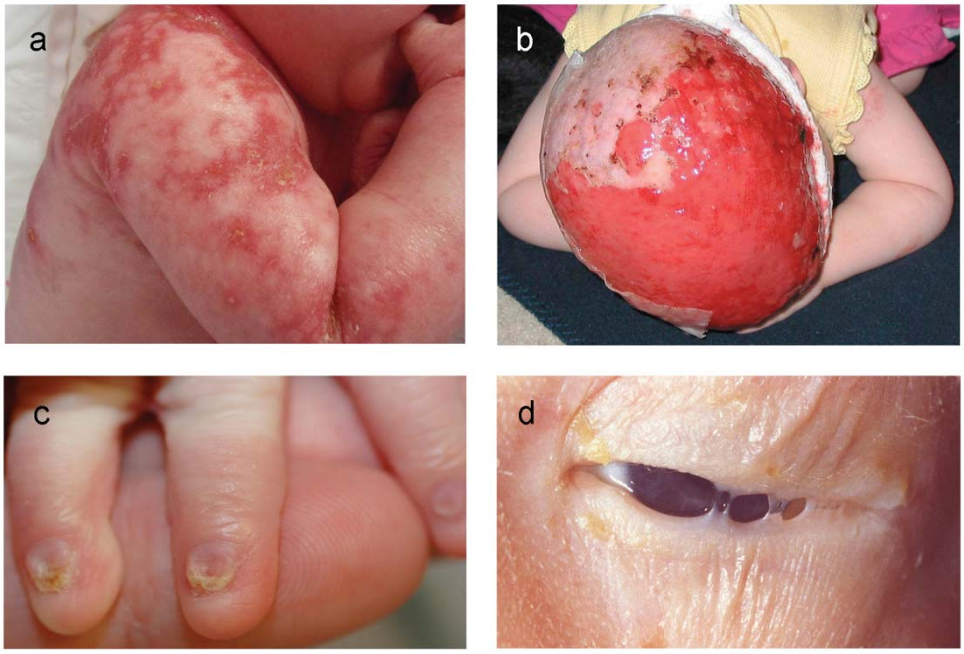

Figure 6. Clinical appearance of a child affected by AEC syndrome. a) A close up of reticulated scarring that is typically seen in AEC patients as the results of skin erosions healing processes. b) Scalp erosions with hemorrhagic crusting, granulation tissue and secondary infection. c) Dystrophic fingernails of AEC patients, characterized by small nails with partial loss/absence and distal fraying of the nail plate. d) Focal fusion of the eyelids (ankyloblepharon) (Adapted from Ferone et al., 2015).

1.6 AEC mouse models

To study the functional activity of mutant p63 in AEC syndrome a first knock-in mouse model ($p63^{+/L514F}$) was generated in our laboratory (Ferone et al, 2012).
This model carries a phenylalanine substitution in position 514 (L514F) and closely resembles the human disease (Ferone et al, 2012). This mutation falls in the first helix of the SAM domain and disrupts the folding of the protein. Among the AEC causative mutations we decided to focus our attention on L514 amino acids for three reasons: first of all, this amino acid is mutated in three different amino acids (phenylalanine, valine or serine); this mutation affects an amino acid that is predicted to be buried inside the protein and has a small solvent accessible surface, so any mutation in this region is likely to affect the overall structure and stability of the protein by altering the packing of the helices, and moreover the substitution of a leucine with a phenylalanine probably cause a severe steric clash between two phenylalanine rings that are located close to each other (McGrath et al, 2001; Rinne et al, 2007).

$p63^{+/L514F}$ mouse model is characterized by hypoplastic and fragile skin, ectodermal dysplasia and cleft palate (Fig. 7). Ferone et al., 2012, found that epidermal hypoplasia and cleft palate are associated with a transient reduction in epithelial cell proliferation during development. These defects closely resemble those observed in the Fgfr2b-/- mice (Candi et al, 2006; De Moerlooze et al, 2000; Petiot et al, 2003; Rice et al, 2004; van Bokhoven et al, 2001). Since p63 transcriptionally controls the Fibroblast growth factor receptors Fgfr2 and Fgfr3 and their expression, they found that impaired FGF signaling downstream of p63 is likely an important determinant of reduced ectodermal cell proliferation and defective self-renewing compartment in AEC syndrome. Unfortunately, a neonatal lethality due to cleft palate prevented the generation of a mouse line and the studying of the adult phenotype.

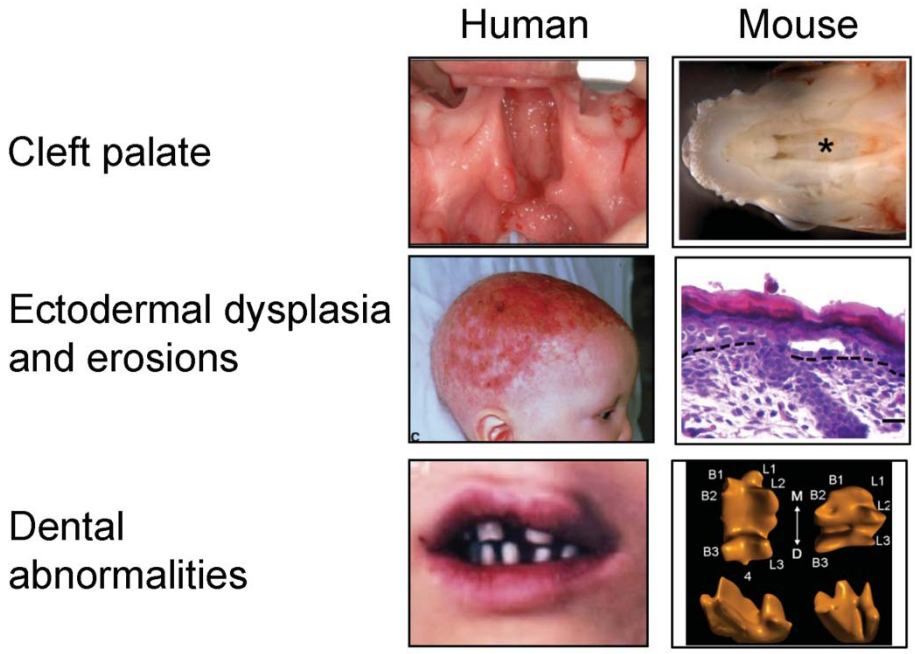

Figure 7. Child affected by AEC syndrome compared to the constitutive AEC mouse model. Comparison between AEC syndrome phenotype and constitutive AEC mouse model indicated that the mouse model faithfully recapitulated some human features, as cleft palate, skin erosions and dental abnormalities.

1.7 Skin immune function

The function of the skin as a physical and biochemical barrier is due by terminally differentiated epidermal keratinocytes (KCs) and by the acidic, hydrolipidic nature of the skin, as a result of sweat, sebum, lipids, and antimicrobial peptides (AMPs).

In the epidermis are present also melanocytes and immune cells such as Langerhans cells (LCs) and T lymphocytes. By the other hand, the dermis is composed of a stratum papillare and a stratum reticulare containing thin and thick collagen fibers, respectively. The collagen fibers offer a mechanical barrier as well as a structural framework in which to host blood vessels and many immune cells such as dermal dendritic cells (DDCs), αβ T cells, γδ T cells, natural killer (NK) cells, B cells, mast cells, and macrophages. Moreover mice, but not humans, possess Vγ5Vδ1 T cells, named dendritic epidermal T cells (DETCs) for their morphology and location. DETCs constitute more than 90% of epidermal T cells, forming an interdigitating network with keratinocytes and LCs (Di Meglio et al, 2011) (Fig 8).

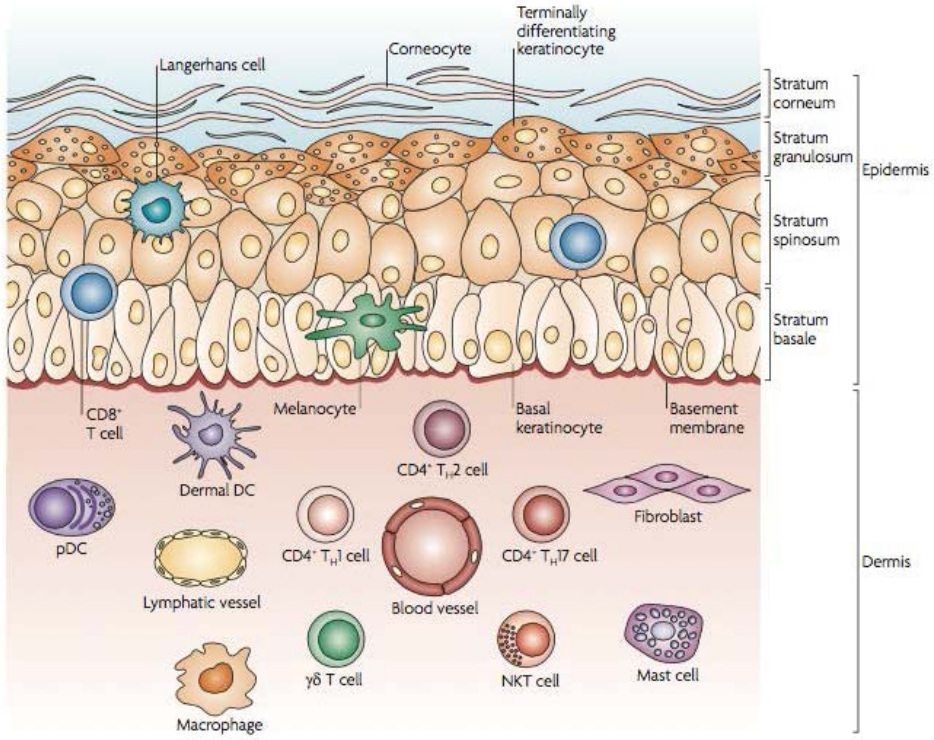

Figure 8. Skin cellular effectors involved in inflammation response. The skin covers an active role in the immune system. The epidermis is responsible for the maintenance of epithelial barrier integrity. It is also populated by melanocytes, which produce pigment (melanin), Langerhans cells and CD8+ T cells in the basal layer and in stratum spinosum. The dermis is constituted of collagen, elastic tissue and reticular fibers. It is populated by specialized cells, such as dendritic cells (DCs) and T cells, but also by macrophages, mast cells, and fibroblasts (Adapted from Nestle et al, 2009).

The skin contains two distinct T cells populations: a population of epidermis-resident memory CD8+ T cells, also known as cytotoxic T cells and a population of recirculating memory CD4+ T cells, recognized as T helper cells (TH). Once infection has resolved and immunological memory has taken place, memory CD8+ T cells remain sequestered in the epidermis, close to the original infection site. In contrast, memory CD4+ T cells rapidly circulate through the dermis, re-enter the circulation, and rapidly reach previously uninvolved skin in the case of secondary infection (Gebhardt et al, 2011).

Upon the activation by immunogenic peptides presented by antigen-presenting cells (APC), naive TH lymphocytes can differentiate into two TH cell populations, TH1 and TH2. TH1 cells typically produce interleukin-2 (IL-2) and interferon-γ (IFN-γ), induce macrophage activation, and are very ejective in controlling infection with intracellular pathogens. By contrast, TH2 cells secrete IL-4, IL-5, and IL-13 and they are excellent helpers for B cells in the antibodies production, and they are required to eradicate helminths and extracellular parasites.

In addition to these cytokines, IL-20, a member of IL‑10‑related cytokines also involved in TH2 inflammatory response, is released properly by keratinocytes. In particular, it is an autocrine signal that leads to keratinocyte proliferation, epidermal thickening, and it is associated with inflammatory skin diseases such as psoriasis and atopic dermatitis. Engagement of the IL-20 receptor activates STAT3 and promotes wound healing, epithelial proliferation and elaboration of antimicrobial peptides (Gebhardt et al, 2009).

Keratinocytes can be considered the first immune sentinels encountered by pathogens and are therefore, quick and efficient in sensing and responding to danger (Nestle et al, 2009). On first encountering a microbe, KCs are alerted to potential danger by recognizing conserved microbial structures known as pathogen-associated molecular patterns (PAMPs) via their pattern recognition receptors (PRRs) (Takeuchi & Akira, 2010) such as Toll-like receptors (TLRs), which keratinocytes express on their surface (TLR-1, TLR-2, TLR-4, TLR-5, and TLR-6) and in their endosomes (TLR-3 and TLR-9). TLR engagement triggers activation of nuclear factor- kappa B (NF-kB) and interferon regulatory factor (IRF), which in turn induces immune and inflammatory genes, namely, tumor necrosis factor (TNF) and type I IFNs (Di Meglio et al, 2011).

Another way in which KCs try to limit the immediate microbial threat is by releasing pro-inflammatory cytokines activating “the inflammasome”, a multiprotein complex (Feldmeyer et al, 2010). This in turn activates the enzyme caspase 1, which cleaves unprocessed pro-interleukin-1b (pro-IL-1b) and pro-IL-18, stored in KCs, into the active IL-1b and IL-18. Activated keratinocytes release processed IL-1 (Dombrowski et al, 2011), enabling neighboring epithelial cells to respond by amplifying the signal through further production of IL-1a, in addition to IL-1b, TNF, and IL-6.

Another critical role covered by KCs in the defense against invading microorganisms is the induction of AMPs. There are many cationic AMPs,

such as the cathelicidin, defensins, and S100 family proteins (Harder & Schroder, 2005). These cationic molecules destroy bacteria by creating holes in their anionically charged cell walls or by sequestrating iron required for bacterial growth (Glaser et al, 2005). Pro inflammatory cytokines (IL-1a, IL-1b, IFN-g, TNF) differentially regulate the expression of genes encoding for several AMPs, and IL-17A, IL-17F, and IL-22 are potent inducers of AMPs (Sonnenberg et al, 2011).

In response to most type-2-cell-mediated stimuli, barrier epithelial cells (ECs) produce cytokines such as IL-33, thymic stromal lymphopoietin (TSLP), and IL-25 that activate DCs to promote adaptive Th2 cell immunity, and license the innate type 2 cell response by activation of ILC2s, basophils, eosinophils, and mast cells (Allakhverdi et al, 2007) (Fallon et al, 2006) (Halim et al, 2012) (Schmitz et al, 2005). These cytokines represent an innate ‘‘pro-Th2’’ cell set of cytokines.

In addition to the polarizing cytokines IL-25, IL-33, and TSLP, ECs can regulate type-2-cell-mediated immunity through the production of endogenous danger-associated molecular patterns (DAMPs) or alarmins (Hammad & Lambrecht, 2015). The alarmins high mobility group box 1 (HMGB1), S100 family proteins, IL-33, and IL-1a are normally localized in the nucleus. However, they can be released by non-programmed cell death or be actively secreted in a process not requiring the classical cellular secretion pathway involving vesicular transport from the Golgi complex. It would be interesting to further investigate the role of these alarmins in skin diseases and also in homeostatic conditions.

Other important actors of barrier type 2 immunity are granulocyte macrophage colony stimulating factor (GM-CSF), known in mouse as Colony stimulating factor 2 (Csf2), and granulocyte colony stimulating factor (G-CSF), called in mouse as Colony stimulating factor 3 (Csf3). These growth factors are released by ECs and stimulate the proliferation, maturation, and function of antigen-presenting cells (APCs) like DCs and macrophages, and also promote eosinophil survival (Figure 9).

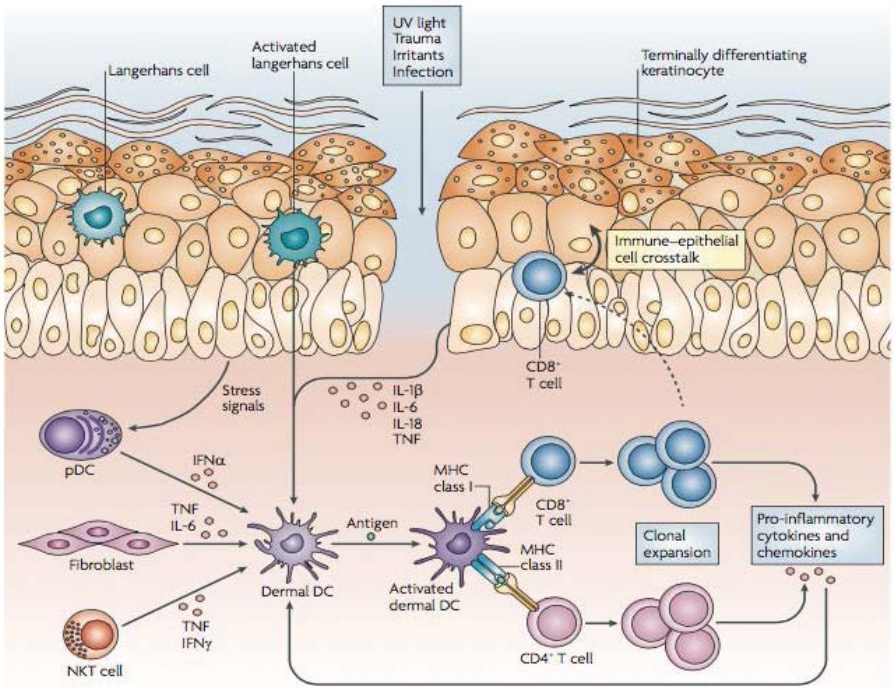

Figure 9. Skin-resident immune sentinels. Any type of barrier disruption such as ultraviolet (UV) light damage, trauma, skin infections or irritants triggers a coordinated immune response to maintain skin homeostasis. Skin-immune cellular components are considered key sentinels for restoring homeostatsis but can also be effector cells under skin inflammation conditions. Langherans cells, which also belong to the family of DCs, are key immunological sentinels. Keratinocytes sense and react to dangerous stimuli by producing pro-inflammatory cytokines (such as IL-1b, IL-6, IL-18 and TNF), which activate DCs. Dermal dendritic cells activate and promote the expansion of skin-resident memory CD4+ or CD8+ T cells. T cells produce pro-inflammatory cytokines and chemokines, thus amplifying the inflammatory reaction. Furthermore, skin-resident T cells can migrate into the epidermis, engaging in an immune-epithelial crosstalk (Adapted from Nestle et al, 2009).

1.8 Thymic stromal lymphopoietin (Tslp), one of the most important alarmins in skin inflammation

Thymic stromal lymphopoietin (TSLP) belongs to the interleukin (IL)-2 cytokine family, specifically it is a paralog of IL-7 (Leonard, 2002) (Friend et al, 1994). TSLP is involved in several immunoregulatory functions, but in particular it is able to stimulate thymocytes to induce the production of TH lymphocytes and the consequently differentiation of TH2 cells and the relative production of IL4 and IL13. TSLP, as IL-7, promotes the differentiation of B-

cells and it is also able to evoke itch in atopic dermatitis patients (Wilson et al, 2013). It is also implicated in the pathogenesis of asthma, as the agent sensitizing the lung to allergens (Demehri et al, 2009a).
Human and murine TSLP are very similar, in fact they share a high degree of homology (Reche et al, 2001) (Sims et al, 2000). During allergic inflammation, the primary producers of TSLP are epithelial cells, such as keratinocytes, and stromal cells although recent data have demonstrated that both dendritic cells (DCs) and mast cells are capable of TSLP production (Soumelis et al, 2002) (Watanabe et al, 2004) (Ying et al, 2005) (Kashyap et al, 2011) (Moon et al, 2011).
Several kind of cells, such as T cells, B cells, natural killer (NK) cells, monocytes, basophils, eosinophils and DCs, and non hematopoietic cell lineages such as epithelial cells respond to the TSLP regulation and express the Tslp Receptor (TSLPR) (Fig 10). TSLPR is constituted by two units: the former, the TSLPR subunit and the latter, the IL-7Rα chain both in humans and mice (Ziegler & Artis, 2010) (Reardon et al, 2011).

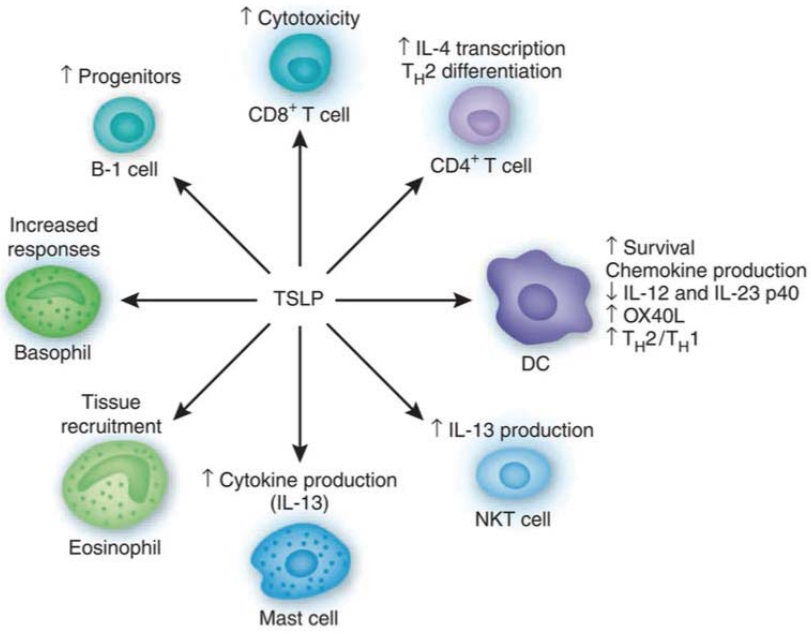

Figure 10. Tslp's cellular targets. Tslp acts on several cellular targets such as lymphocytes (B and T-cells), granulocytes, DCs, natural killer T cells (NKT), mast cells, eosinophils, and basophils.

The early studies characterizing TSLP showed that TSLP could support B-cell development (Friend et al, 1994) (Levin et al, 1999). Several groups demonstrated the association of TSLPR mutations with a subtype of B cell

leukemia confirming that altered TSLP expression can have a significant impact on B cells (Chapiro et al, 2010) (Roll & Reuther, 2010) (Tasian & Loh, 2011). In addition, elevated systemic levels of TSLP has been demonstrated to lead to aberrant B-cell lymphopoiesis, with direct actions on B cell development and indirect effects leading to autoimmune diseases (Astrakhan et al, 2007) (Iseki et al, 2012). Indeed, Demehri et al proved that in Notch1; Notch2 conditional knock out mice high systemic levels of Tslp caused the insurgence of a B-lymphoproliferative disorder, an autoimmune condition associated to Tslp (Demehri et al, 2008).

1.9 Signaling pathway involved in Tslp regulation

Nowadays, the mechanism of action of Tslp has not yet been defined. Several research groups are still working in this field. So far, Murthy et al have demonstrated that ADAM17 is involved in the basal Notch activation and it triggers Notch signaling to regulate c-Fos activation, monitoring so epidermal barrier homeostasis. Loss of this control induces the production of cytokines or alarmins, such as Tslp and IL33, which trigger immune responses. Independent studies have demonstrated that the loss of Notch, deregulation of AP-1 signaling pathway, or elevated production of epithelial TSLP results in inflammatory skin disease (Demehri et al, 2009a) (Dumortier et al, 2010).
Moreover, Wilson et al showed a new role covered by TSLP. They demonstrated that it might evoke itch behaviors directly by activating sensory neurons, and indirectly by activating immune cells, which secrete inflammatory mediators that target sensory neurons, or both. Indeed, keratinocytes may directly communicate with sensory neurons via neuromodulators (Ikoma et al, 2006). The release of TSLP by keratinocytes has been demonstrated that is correlated to the GPCR protease-activated receptor 2 (PAR2) and to Ca^{2+} influx that activates the NFAT/calcineurin pathway which triggers the activation of Tslp transcription (Wilson et al, 2013). TSLP secretion has been demonstrated be calcium dependent. Epithelial cells such as keratinocytes express Ca^{2+} channel on their surface like ORAI1, ORAI2. In keratinocytes, the ORAI1 signaling pathway connects PAR2 to TSLP release. The activation of PAR2 allows the release of Ca^{2+} from endoplasmic reticulum and the activation of ORAI1 regulator, called STIM1 (STromal Interaction Molecule 1) that opens ORAI1 channels to promote Ca^{2+} influx. Ca^{2+} activates calcineurin, a phosphatase involved in the NFAT dephosphorylation. NFAT dephosphorylated translocates from the cytoplasm to the nucleus and induces the transcription of TSLP. Wilson and colleagues found that TSLP is released by keratinocytes under Ca^{2+} influx and it activates sensory neurons directly to evoke itch behaviors. In addition, they identify the ORAI1/NFAT signaling pathway as a key regulator of PAR2-mediated TSLP secretion by epithelial cells. Instead, Furio et al (Furio et al, 2015) showed that patients affected by Netherton syndrome (NS) presented elevated systemic levels of Tslp. They demonstrated that the overproduction of Tslp in NS syndrome is related to the

activation of PAR2-NF-κB axis by kallikrein 5 (KLK5) activity. NS is a disorder characterized by severe skin inflammation, scaling and atopy for which physicians and scientists do not have a complete understanding. In NS patients, an intrinsic mechanism takes place in keratinocytes and leads to increased expression of TSLP, TNF-α, IL-8 and ICAM-1 as a result of PAR2 activation by active KLK5. Overall, the mechanisms underlying Tslp action are tricky and involve several pathways. It will take some time for scientists to understand the pawn genes involved in this mechanism.

1.10 Kallikrein proteases involved in the activation of PAR2 receptor

Kallikreins (KLKs) or kallikrein related peptidases are a subgroup of extracellular serine proteases. They have been divided in two major categories: the former corresponds to plasma KLK (only KLK1B belongs to this category), the latter corresponds to the tissue KLK family (KLK1-KLK15) (Prassas et al, 2015).
KLK1B, the only example of plasma KLKs, is produced in liver and it has a conformation and a structure completely different from tissue kallikreins.
Tissue KLKs in turn can be divided in two different families, the chemotrypsin and the trypsin-like serine proteases.
KLKs are synthesized as inactive zymogens, pre-pro-KLK proteins, which are then autoactivated or activated by different KLKs or by other proteases. The activation of pro-KLK zymogens happens extracellulary thanks to the trypsin-like cleavage of the pro-peptide and it is a key mechanism in regulating KLK activity in tissues. Once activated, KLKs play their role of serine proteases in catalytic mechanism.
Tissue KLKs can acts by their selves or they are involved in tissue-specific proteolytic cascades. Altered expression of KLKs activity is correlated to different-specific pathologies.
In the epidermis are present both trypsin- and chemotrypsin-like serine protease, about nine KLKs, such as KLK1, KLK5-KLK8, KLK10, KLK11, KLK13 and KLK14, are co-expressed in the stratum corneum and upper stratum granulosum of normal human epidermis. In normal condition, pro-KLKs are required and activated to maintain skin-barrier integrity. They are involved in three main functions: 1) promotion of skin desquamation and/or keratynocites proliferation, regulating skin renewal and barrier thickness; 2) regulation of lipid metabolism by controlling lipid-processing enzymes and the activation of PAR2; 3) processing of pro-cytokines and antimicrobial peptides involved in innate immune responses.
The activity of KLKs family in epidermis is played by KLK5, also known as stratum corneum tryptic enzyme (SCTE), KLK7, also called as stratum corneum chymotryptic enzyme (SCCE), KLK8, and KLK14. These KLKs are secreted by keratynocytes into stratum corneum and after secretion they participate in a proteolytic cascade. KLK5 is able to auto-activate and to

initiate the proteolytic cascade. It subsequently activates pro-KLK7, pro-KLK8 and pro-KLK14 by cleaving their pro-peptides (Fig. 11). After the activation, KLK5 and KLK7 cleave corneodesmosomes, which are composed by DSG1, DSC1 and corneodesmosin, let's starting the skin desquamation process or shedding of SC corneocyte cells. Matriptase, an activator of serine-protease and the lympho-epithelial Kazal type inhibitor (LEKTI), which is a protease inhibitor, regulate KLK activity both in normal and pathologic condition.
KLK5, KLK6 and KLK14 are able to activate the keratinocyte-expressed proteinase-activated receptor 2 (PAR2), beginning an inflammation process mediated by NFAT/calcineurin/Tslp signaling pathway (Wilson et al, 2013).

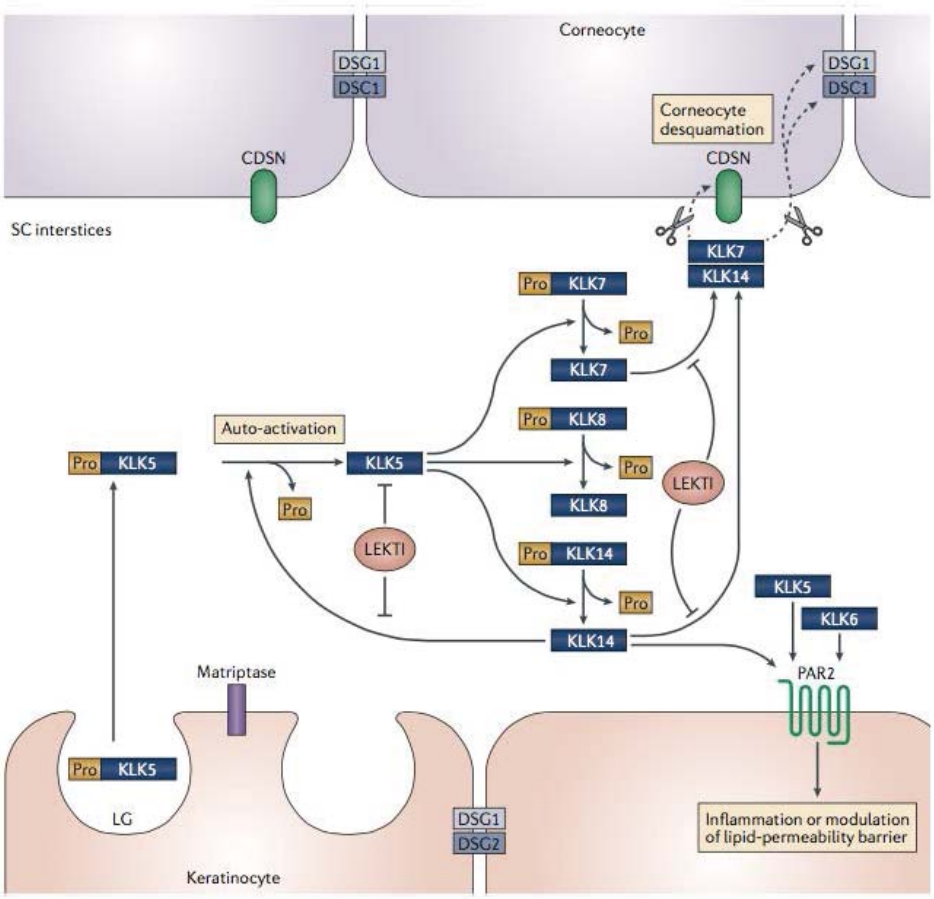

Figure 11. The proteolytic cascade of kallikreins in skin epidermis. KLKs in the epidermis are secreted by lamellar granules (LG) of keratinocytes in the stratum granulosum into the stratum corneum (SC). Upon secretion it starts their activation and the related proteolytic cascade (Adapted from Prassas et al, 2015).

2. AIM OF THE STUDY

The aim of my project was to study the conditional AEC mouse model in post-natal life and to understand the molecular mechanism underlying the AEC syndrome. In particular, my study focused on the characterization of the inflammatory state associated with the severe phenotype of AEC conditional mice and the generation and characterization of a novel conditional model for AEC syndrome in a Tslp null background. Tslp is an alarmin, involved in the insurgence of the inflammatory state and it plays an important role in AEC syndrome. For this reason, we decided to generate an AEC mouse model in a Tslp null background to understand what happens in AEC conditional mice in the absence of this particular cytokine.

3. MATERIALS AND METHODS

3.1 Generation of conditional $p63^{+/FloxL514F}$ mouse model

We recently generated a conditional knock-in model ($p63^{+/FloxL514F}$), in which the L514F mutation is expressed only in the presence of the CRE recombinase. The knock-in/replacement strategy was designed to replace the wild-type amino acid Leucine (Leu, L) encoded by codon 514 with a sequence coding for Phenylalanine (Phe, F) in the p63 protein in murine embryonic stem (ES) cells by homologous recombination. The targeting construct contained two LoxP flanking fused wild-type exons 13 and 14 placed upstream a neomycin resistance cassette flanked by FRT loci and a mutant exon 13 followed by the exon 14 and an immune epitope tag (3xFlag) at the end of this.

3.2 Mouse genotyping

Conditional knock-in $p63^{+/FloxL514F}$, $p63^{FloxL514F/FloxL514F}$, K14Cre;$p63^{+/FloxL514F}$ (+/L) and K14Cre;$p63^{FloxL514F/FloxL514F}$ (L514F) were genotyped by PCR using genomic DNA isolated from mouse tails.
Oligonucleotide primers used for PCR:
Conditional knock-in $p63^{+/FloxL514F}$, $p63^{FloxL514F/FloxL514F}$

Forward primer (5'-3')	**Reverse primer (5'-3')**
CAGCGTATCAAAGAGG AAGGAGA	AGCCAGAATCAGAATCAGGTG AC

The expected bands were of 250bp for the wild-type mice, 337bp for the mutant homozygous mice and both for the heterozygous ones.

To distinguish the presence of K14-Cre recombinase in p63 heterozygous and homozygous mice we used the following primers for PCR:

Forward primer (5'-3')	**Reverse primer (5'-3')**
AGGGATCTGATCGGGA GTTG	CTTGCGAACCTCATCACTCG

L514F; Tslp eKO mice were obtained by crossing K14-Cre; $p63^{+/FloxL514F}$ with Tslp $^{FloxL2/FloxL2}$ received from Pierre Chambon (Li et al, 2009).
Primers used to genotype Tslp line:

Forward primer (5'-3')	Reverse primer (5'-3')
CCCAGGCTACCCTGAAACTGAG	GTTTCAGGAGCCAGGAGAACAATCTG

The expected bands corresponded to 333bp for the wild-type mice, 450bp for the mutant homozygous mice and both for the heterozygous ones.

3.3 Western blot

For immunoblotting cells were lysed in sample buffer (10% glycerol, 0.01 % Bromophenol Blue, 0.0625 M Tris-HCl pH 6.8, 3 % SDS, 5 % ß-mercaptoethanol) supplemented with protease inhibitors. For immunoblotting of epidermal extracts, epidermis was isolated from dermis by producing a thermal shock at 55°C or by floating skin biopsies, epidermis side up in a dispase solution. After isolation from dermis, epidermis was snapped frozen in liquid nitrogen and then homogenized with a tissuelyser in lysis buffer supplemented with phosphatase and protease inhibitors. Proteins were run on a denaturing SDS-PAGE gel and subsequently transferred to Immobilon-P transfer membranes (Millipore) probed with primary antibodies and detected by chemiluminescence (ECL, GE Healthcare Life Sciences). Antibodies used for immunoblotting were: p63 (4A4 Santa Cruz Biotechnology), Cdh1 (BD Bioscience), Krt5, Krt14, Krt1, Krt10, Ivl, Lor (all Covance), Krt15 (a gift from doct. Langbein), β-actin (Santa Cruz Biotechnology), Klk5 and Klk7 (R&D Systems), Klk6 (a gift from doct. Mari Kishibe).

3.4 Real-time RT-PCR

Mouse epidermis was isolated from dermis by digestion with dispase solution. Total RNA was extracted from primary keratinocytes or epidermis using TRIzol reagent (Invitrogen). cDNA was synthesized using SuperScript Vilo (Invitrogen). Two-step real-time reverse transcription RT-PCR was performed using the SYBR Green PCR master mix in an ABI PRISM 7500 (Applied Biosystems). Levels of the target genes were quantified using specific oligonucleotide primers and normalized for Actin (ß-actin) or RPLP0 expression.

Oligonucletide primers used for Real-Time RT-PCR on mouse samples:

Gene	Forward primer (5'-3')	Reverse primer (5'-3')
ß-actin	CTAAGGCCAACCGTGAAAAGAT	GCCTGGATGGCTACGTACATG

p63 wt	ACTCTCCATGCCCTCCAC	GAGCAGCCCAACCTTGCT
p63 L514F	ACTCTCCATGCCCTCCAC	GAGCAGCCCAACCTTGCA
Krt5	CAACGTCAAGAAGCAGTGTGC	TTGCTCAGCTTCAGCAATGG
Krt14	ACCACGAGGAGGAAATGGC	TGACGTCTCCACCCACCTG
Csf2	CAGCCAGCTACTACCAGACATACTG	CGCATAGGTGGTAACTTGTGTTTC
Csf3	GCCCAGAGGCGCATGA	TCCTGACCATAGTGCACTTTGC
Cxcl5	TGGCATTTCTGTTGCTGTTCAC	TTGCGGCTATGACTGAGGAA
IL1F5	GGAGGACTGCACGCAGAGA	GCCCGATTTGGGACAACAC
IL1F6	GAAAGAGCAAACAGTTCCAGTCACTA	TGTTCGTCTCAAGAGTGTCCAGAT
IL1F9	CCCTTGTGACAGTTCCACGAA	GGGTACTTGCATGGGAGGATAG
DefB1	TGATATGTTTTCTTTTCTCCCAGATG	TGTTCTTCGTCCAAGACTTGTGA
DefB3	CTGTCTCCACCTGCAGCTTTTA	TGCCTCCTTTCCTCAAACAACT
DefB4	CTGTCTCCACTTGCAGCCTTTA	GCTCCATTGGTCATGCATGTT
DefB6	CCATTACCTGCTCTTTGCCTTTA	TGGGAAAAGGCTGCAAGTGG
Tslp	GCCAGGGATAGGATTGAGAGTATAGT	GACTGTGAGAGCAAGCCAGCTT
IL1b	CATGAGCACCTTCTTTT	CACACACCAGCAGGTTATCATC

	CCTTCA	A
IL4	GACTCTTTCGGGCTTTTCGA	GTGGACTTGGACTCATTCATGGT
IL6	TCGGAGGCTTAATTACACATGTTC	TGCCATTGCACAACTCTTTTCT
IL13	TTGAGGAGCTGAGCAACATCA	ACCATGCTGCCGTTGCA
IL20	GCAATGGAGAAATACAACCAAATTC	TTTACCACCGCTGCCTGAA
IL25	GGATGGCCCCCTCAACA	CAAGTCCCTGTCCAACTCATAGC
IL33	TGGTCCCGCCTTGCAA	CAGTAGACATGGCAGAATTCTTTGG
INFγ	TTGCCAAGTTTGAGGTCAACAA	TGGTGGACCACTCGGATGA
IL17	TCAGACTACCTCAACCGTTCCA	CCAGATCACAGAGGGATATCTATCAG
TNFα	CAGCCGATGGGTTGTACCTT	GGCAGCCTTGTCCCTTGA
S100a8	AATGACTTCAAGAAAATGGTCACTACTG	ACTATTGATGTCCAATTCTCTGAACAAG
S100a9	ACAAATGGTGGAAGCACAGTTG	TCATTTATGAGGGCTTCATTTCTCT
Klk5	CTCCTGCCAGGGTGATTCC	CAGGACACAAGGCCCTGTAAC
Klk6	GACATGAAAGAAGGCAACGATTC	GAGGCGACCCCCACATACTA
Klk7	GCATTCCTGACTCTAAGACCAACA	TTGGAGGGTGTCGTTGCA
Klk9	AGGCTCTTGCCAGGGTGACT	CCAGACACTATACCTGCCAAGGT
Klk10	ACGGCCGCACATTGCT	GCAAGTGGTCATCGCCAACT
NFATc1	CTGGGAGATGGAAGCAAAGACT	CGGAAAGGTGGTATCTCAACCA

Oligonucleotide primers for Real Time RT-PCR on human samples

Gene	**Forward primer (5'-3')**	**Reverse primer (5'-3')**
RPLP0	GACGGATTACACCTTCCCACTT	GGCAGATGGATCAGCCAAGA
TSLP	GCTATCTGGTGCCCAGGCTAT	TCTCCTCTTCTTCATTGCCTGAGT

KRT5	CCTCAACAATAAGTTT GCCTCCTT	GCAGCAGGGTCCACTTGGT

3.5 Primary keratinocytes and cell cultures

Newborn mice were placed in petri dishes with ice and inserted in an ice bucket. After 30-45' newborn mice were washed twice with 70% ethanol and twice with water to remove ethanol completely. Using sterile techniques, mice tails and limbs were amputated with sterile surgical scissors. Single skin was carefully separated from the rest of the viscera and flattened in a empty 6 well dish with the dermis facing down; 2 ml of Dispase solution (0.5mg Dispase-GIBCO, Na-bicarbonate 0.75%, Hepes 10mM, Antibiotic-Antimycotic in PBS) were added to each 6 well dish and incubated o/n at 4 °C. Next day epidermis was separated from the dermis and placed in a 100mm Petri dish in 2ml (for each epidermis) of 0.125% trypsin- 0.1mM EDTA. Epidermis was minced with tweezers and scissors until was reduced in very small fragments and placed at 37°C for 5-8 minutes. Then trypsin was inactivated with DMEM+10% FBS and filtered by applying it to cell strainer in order to remove the floating particles. Cells were placed into the centrifuge for 5 minutes at 1000 rpm; then were plated on collagen coated plates (1.2x106 cells/ml) and incubated at 34°C, 8% CO2. Primary mouse keratinocytes were isolated from newborn mice and cultured under low calcium conditions (0.05 mM) or treated with 2mM calcium chloride as previously described (Antonini et al, 2010).

Human keratinocytes obtained from AEC patients Q11X and T533P (kindly provided by J. Zhou, (Ferone et al, 2013)), as well as control keratinocytes obtained by unaffected individuals were plated at a density of 10^4cells/cm^2 and cultured in KBM Gold medium (Lonza) till they reach confluency. Confluent cells were treated with 0.3mM calcium for subsequent RNA analysis.

Knockdown was achieved by transient transfection of 100nM small interfering RNA (siRNA) for pan-p63, ΔNp63 (De Rosa et al, 2009), or negative control (Invitrogen).

3.6 Retroviral infection

Mouse primary keratinocytes were infected the day after plated with retroviruses carrying the GFP (GINCO), NFATc1 (Porter & Clipstone, 2002) for 2 hours. After the infection cells were washed with PBS and were cultured in LCM4% for a week at 34°C.

3.7 Gene expression microarrays

We measured the differential expression of 22000 RNA on freshly isolated epidermis from three mutants versus three wild-type newborn mice. We hybridized the RNA samples to the Affymetrix Mouse Genome 430A 2.0 chips. We processed the microarrays using the RMA algorithm. False

Discovery Rate (FDR) correction was performed on the estimated p-value to correct for multiple hypothesis test.

3.8 Histology and Immunostaining

Dorsal skin was dissected, fixed in 4% paraformaldehyde (PFA) and embedded in paraffin or in OCT, from which 7 μm sections were cut and stained with Haematoxylin and Eosin (H&E), Toluidine blue and immunofluorescence according to standard methods. For paraffin sections, permeabilization for antigen retrieval was performed by microwaving samples in 0.01 M citrate buffer at pH 6.0. The following antibodies were used: keratin 6, keratin 5, keratin 14 (Convance), p63 (4A4, Santa Cruz Biotechnology), Ecadherin (Zymed laboratories-Invitrogen), guinea pig antibody to keratin 15 (a gift from Doctor Langbein), FLAG M2 (Sigma), anti-TSLP antibody (R&D Systems), anti-F4/80 (Abcam), anti-CD45 (eBioscience), anti-HMGB1 (a gift from Doctor Marco Bianchi), anti-Ki67 (Dako), NFATc1 (clone 7A6 Santa Cruz Biotechnology), Klk6 (a gift from doct. Mari Kishibe).
The following secondary antibodies were used for immunofluorescence staining: Alexa Fluor ® 488 goat anti-mouse (Invitrogen), Alexa Fluor ® 594 goat anti-rabbit (Invitrogen), Alexa Fluor ® 594 goat anti-rat (Invitrogen). Fluorescent signals were monitored under a Zeiss Axioskop2 plus image microscope or under a Zeiss confocal microscope LSM510meta. Sections were counterstained with DAPI nuclear stain.

3.9 ELISA

Serum TSLP levels were determined using Quantikine mouse TSLP kit according to manufacturer's instructions (R&D Systems). Serum IgE levels were measured using Mouse IgE ELISA kit (Immunology Consultants Laboratory).

3.10 FACS Analysis

Single cell suspension from Bone Marrow (BM) and spleen were prepared for Flow cytometry (FC) analysis transferring the freshly dissected lymphoid organ to a 60 x 15-mm culture dish containing 4 ml of HBSS supplemented with 5% serum. Then the spleen was placed between the frosted ends of two glass microscope slides. The organ was disrupted by gently pressing the frosted ends in a circular motion until only the empty capsule remains. Instead, bone marrow was simply syringed. The resulting cell suspension were transferred to a 15-ml conical centrifuge tube and was resuspended with a combined total of 3 ml of 5% HBSS. The cell suspensions were centrifuged for 10 min at 200 x g, 4 °C, then the supernatant was discarded and the pellet resuspended in HBSS and labeled with the specific antibodies. The following antibodies were used: anti-B220/CD45R (RA3-6B2) conjugated to PE-Cy7, anti-CD43 (S7)

conjugated to FITC both from BD Pharmingen, anti-IgM conjugated to FITC (RMM-1) from Biolegend. Stained cells were studied using a BD FACS CANTO II, and the data were analyzed using FACS DIVA software.

3.11 Skin Barrier Assays

To perform X-gal staining, unfixed, untreated newborn mice or embryos were washed in PBS and then incubated overnight at 37°C in 5-bromo-4-chloro-3-indlyl-b-D-galactopyranoside (X-gal) reaction mix (100 mM NaPO4, 1.3 mM MgCl2, 3 mM K3Fe[CN]6, 3 mM K4Fe[CN]6, and 1 mg/ml X-gal [pH 4.5]). At pH 4.5, the skin exhibits endogenous b-galactosidase activity, so increased X-gal staining indicates epidermal permeability to X-gal, a sign of compromised barrier function (Hardman et al, 1998).

4. RESULTS

4.1 AEC conditional mouse model is characterized by an epidermal-specific L514F mutation that results in severe skin phenotype

To dissect the molecular defects occurring after birth in AEC syndrome and to overcome the lethality of the constitutive AEC mouse model (Ferone et al, 2012), we generated a conditional knock-in $p63^{floxL514F}$ mouse model, in which the L514F mutation was expressed only in the presence of the CRE recombinase and it is fused to a 3xFLAG tag at the C-terminus (Fig 12A). The knock-in strategy was designed to replace the wild-type amino acid leucine encoded by codon 514 with phenylalanine in the p63 protein in murine embryonic stem (ES) cells by homologous recombination. To overcome the neonatal lethality due to cleft palate we crossed $p63^{+/floxL514F}$ mice with K14-Cre knock-in mice, in which Cre is highly expressed by embryonic day 17.5 (E17.5) in the epidermis and in the hair follicle under the control of the endogenous keratin 14 (K14) promoter (K14-Cre Δneo) (Huelsken et al, 2001). Immunofluorescence analysis with anti-FLAG antibody, which specifically recognizes the mutant protein, revealed a nearly uniform expression of the mutant protein in the basal compartment of the interfollicular epidermis at postnatal day 2(P2) (Fig. 12B).

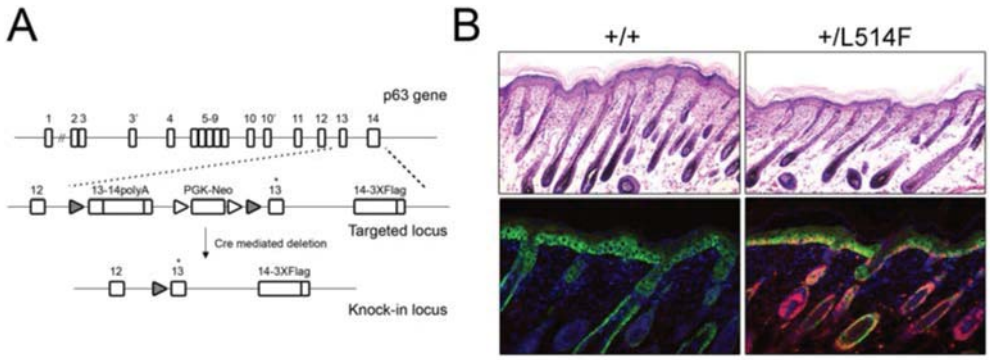

Figure 12. Generation of K14-Cre Δneo; $p63^{+/floxL514F}$ AEC mutant mice. A) Gene targeting strategy used to generate the K14-Cre Δneo; $p63^{+/floxL514F}$ (+/L514F) knock-in mice. The L514F mutation is indicated with *, the targeted locus contains two LoxP flanking wild-type exons 13 and 14 fused together and place upstream of a neomycin resistance cassette flanked by FRT loci. A mutant exon 13 followed by the exon 14 and a 3xFLAG epitope tag at the end of this is placed after the LoxP. Flag-tagged p63 gene is expressed upon Cre mediated deletion. B) H&E staining of dorsal skin of K14Cre; $p63^{+/floxL514F}$ (+/L514F) and control (+/+) mice at post-natal day 2 (P2) reveals hypoplasia (upper

panel). Immunofluorescence analysis of Flag and Krt14 on dorsal skin of +/L514F and +/+ mice at P2 reveals the proper expression of mutant p63 protein in the basal layers of the epidermis and confirms the hypoplasia (lower panel).

K14-Cre; $p63^{+/floxL514F}$ (+/L) newborn mice appeared normal at birth and exhibited in time a relatively mild but reproducible phenotype with partial and progressive hair loss (Fig. 13A). In adult mice (P50) histological analysis of the skin revealed epidermal abnormalities characterized by an overall reduction of epidermal thickness (Fig. 13B). Similarly to what observed in the constitutive AEC mouse model strong reduction of Krt15 in both hair follicles and interfollicular epidermis was observed (Ferone et al, 2012) (Fig. 13B).

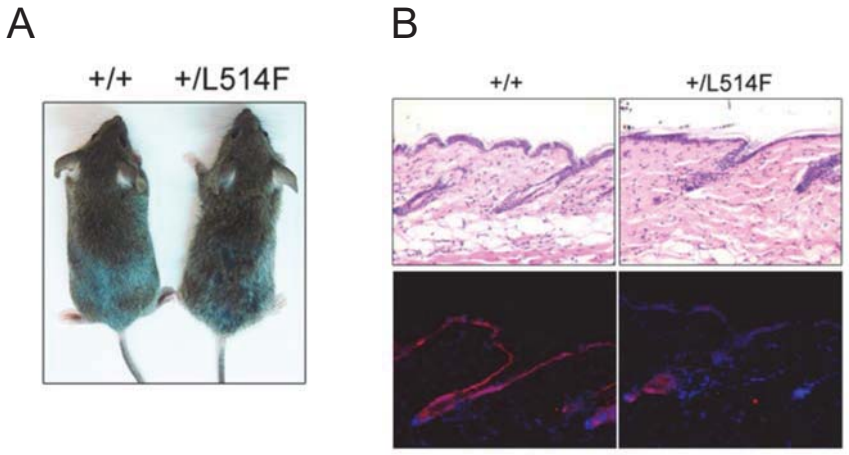

Figure 13. Characterization of +/L514F mouse model. A) Photographs were taken of +/L and L/L at 30 days. B) H&E staining of dorsal skin of +/L514F and +/+ mice at P50 revealed hyper-cellularized dermis and decreased fat layer in mutant skin (upper panel). Immunofluorescence analysis for Krt15 at P50 revealed a reduction of Krt15 in mutant mice compared to controls.

Given the relatively mild phenotype, heterozygous mutant mice were crossed to homozigosity to obtain K14-Cre Δneo; $p63^{floxL514F/floxL514F}$ mice (from here on referred as L514F mutant mice), in which wild-type p63 was virtually absent at P3, and mutant p63 was highly expressed in homozygous mice (Fig. 14A). Immunofluorescence analysis with anti-FLAG antibody revealed a uniform expression of the mutant protein in the basal compartment of the interfollicular epidermis at birth (Fig. 14B).

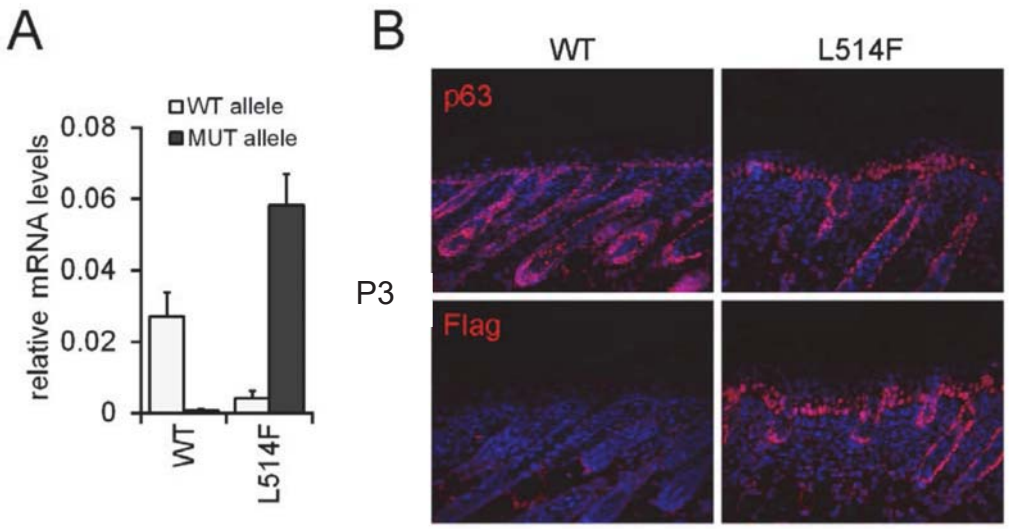

Figure 14. L514F conditional expression in AEC mutant mice. A) Real time RT-PCR for *p63* wt and mutant alleles in mouse epidermis derived from L514F mice and controls at P3 revealed the expression of mutant allele in L514F mice. Data are normalized for *β-actin* mRNA levels and are expressed relative to controls. Error bars denote SD. B) Immunofluorescence staining of L514F and control (WT) skin revealed the expression of the p63L514F-3xFLAG protein in the basal layer of the epidermis and hair follicle at P3 in mutant skin compared to wild-type mice. Nuclei are stained with DAPI.

AEC mutant mice were indistinguishable from their wild-type littermates at birth, but ~6% P2-P5 mice displayed areas of severe skin erosion with an otherwise apparently normal phenotype. Starting from P5-P7, all mutant mice developed a progressively severe phenotype, characterized by shallow skin erosions, exfoliative erythroderma, crusting, associated with dehydration, chronic skin inflammation, and stunted growth (Fig. 15A). Accordingly, 70% of mutant mice died between P7 and P20, and a significant reduction in body weight was observed both at P10 and P20. (Fig. 15B and C and data not shown).

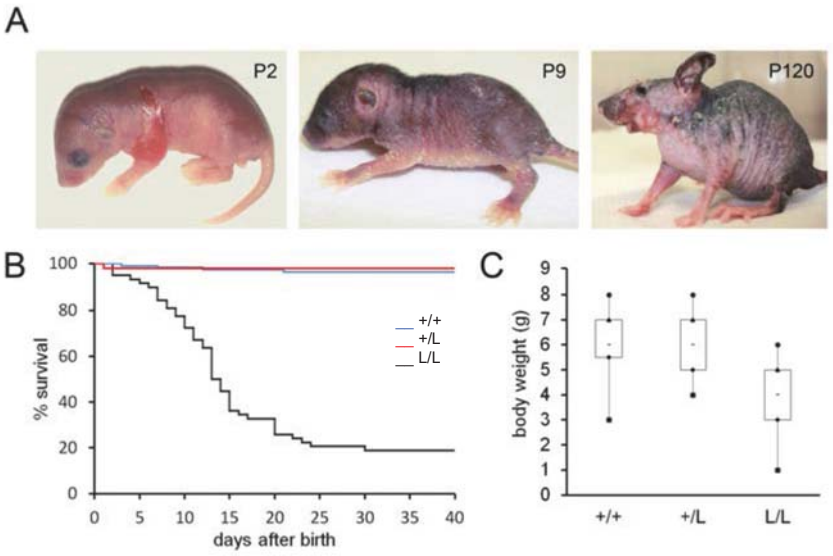

Figure 15. Phenotype of AEC mutant mice: A) Photographs are taken from controls and L514F mice at different stages, as indicated in the figure. From P2 L514F mice showed a progressively strong phenotype characterized at P9 by shallow skin erosions, skin crusting, hair loss and ulcerations that worsen throughout their life, as indicated at P120. B) Survival curve of L514F (L/L black line), +/L514F (+/L red line) and +/+ (blue line) mice (P-value= 3.71682E-22; n=276). C) Body weight at P10 of L514F, +/L514F and +/+ mice, (***P-value=2.6847E-07; n= 72).

4.2 Epidermal blistering and altered epidermal barrier characterized AEC mice

To test the hypothesis that the progressive dehydration observed in AEC mutant mice may be due to at least partially impaired integrity of the epidermal barrier, we employed a dye exclusion assay, a technique that stains areas with defective skin barrier. No abnormalities were observed at E17.5 when the AEC mutation starts to be expressed, whereas newborn mutant mice displayed focal loss of epidermal barrier (Fig. 16A). Histological analysis of the back skin revealed a mild epidermal hypoplasia at P0 in AEC mutant mice with apparently normal upper layers and an intact cornified layer (data not shown). While no obvious disruption of the epidermal barrier were observed in the upper layers, small and large areas of focal blistering were observed in the basal layer of mutant epidermis accompanied with cytolysis and to a lesser extent acantholysis as shown by H&E staining (Fig. 16B) and immunofluorescence with E-cadherin (Fig. 16C). Interestingly, similar intra-

epidermal blistering with areas of both acantholysis and cytolysis was previously reported in perilesional skin of an infant affected by AEC syndrome subjected to mild mechanical stress (Payne et al, 2005).

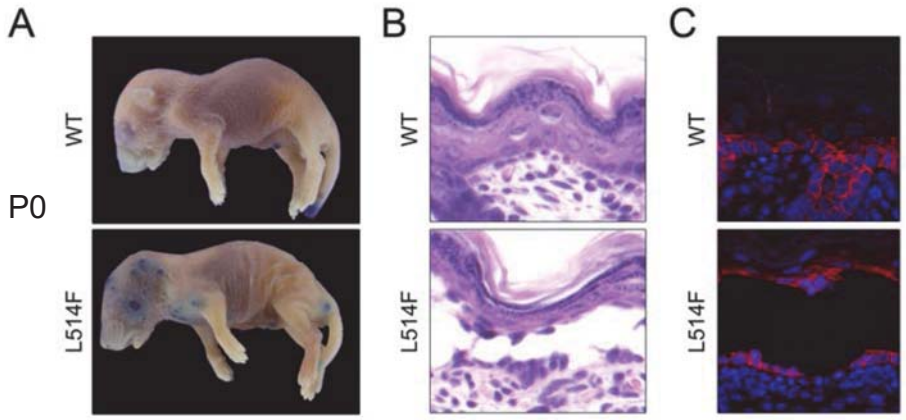

Figure 16. Epidermal blistering and skin fragility in AEC mutant mice. A) Barrier assay at P0 on L514F and control mice (WT) revealed the presence of focal gaps in mutant mice at P0 (***P-value=1.58596E-09; n= 34). B) H&E staining of the skin from newborn mice revealed blistering both between the basal lamina and the basal layer, and between basal layer and suprabasal compartment in mutant but not in wild-type epidermis at birth. C) Immunofluorescence analysis for E-cadherin (Cdh1) on newborn skin of L514F and WT mice revealed signs of both acantholysis and cytolysis.

Mutations or the complete absence of keratin proteins in the epidermis results in defective intermediate filament structure, mechanical stress-induced cytolysis and blistering (Coulombe et al, 2009). Consistent with the phenotype observed in AEC mutant mice, strong reduction of Krt5, Krt15 and to a lesser extent Krt10 expression was observed at the mRNA and protein levels in mutant epidermis compared to controls (Fig. 17A and B). Importantly, a similar reduced Krt5 and Krt15 expression was observed also in human samples derived from AEC patients at the RNA and protein levels (Fig. 17D and 17E, and (Ferone et al, 2012)). Krt14 was less abundant at the protein level as previously described (Fig. 17A) (Clements et al, 2012). Ultrastructural analysis obtained by transmission electron microscopy demonstrated reduces keratin bundles in the basal layer of the epidermis of mutant mice compared to controls (Fig. 17C). In conclusion these data indicate that the skin phenotype observed in AEC mutant mice is due to reduced mechanical strength of the

lower layers of the epidermis, rather than an impairment in the epidermal barrier.

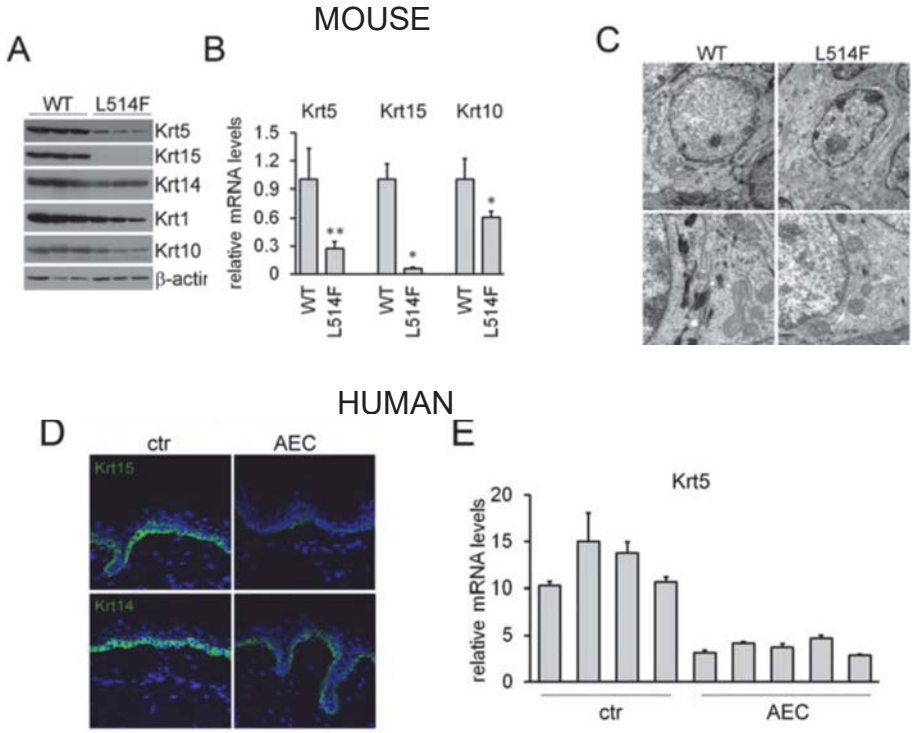

Figure 17. Focal epidermal barrier disruption in AEC mutant mice. A) Immunoblotting analysis for the indicated proteins in cell extracts of mouse epidermis derived from mutant and control mice at P3. Data are normalized for *β*-actin protein expression. B) Real time RT-PCR for *Krt5, Krt15* and *Krt10* in mouse epidermis derived from L514F mice and controls at P3. mRNA expression of the analyzed genes were strongly downregulated in mutant skin as compared to controls (Krt5:**P-value=0.001; n=26; Krt15:* P-value=0.006; n=13; Krt10 *P-value=0.005; n=13). Data are normalized for *β-actin* mRNA levels and are expressed relative to controls. Error bars denote SD. C) Transmission electron microscopy (TEM) of skin samples derived from newborn mice, scale bar: 2um. Reduced keratin bundles in mutant epidermis compared to controls is showed in the lower panel, scale bar: 500nm. D) Immunofluorescence analysis of human AEC patients and controls skin with antibodies against *KRT5* and *KRT14* reveals a reduction of both proteins in non lesional skin of AEC patients compared to controls. E) Real time RT-PCR for *KRT5* in human skin derived from AEC patients and healthy patients (P-value=0.003; n=9).

Data are normalized for *RPLP0* mRNA levels and and are represented as mean ± SD normalized mRNA levels.

4.3 Gene expression profile of AEC mouse epidermis

To obtain a global view of changes in gene expression of AEC mutant mice, we performed a comparison of gene expression profiling of mutant versus wild-type epidermis at P3 using Affymetrix gene chip. Analysis of the data revealed that a subset of genes, known to be p63 target genes, is downregulated by L514F mutation. Among the p63 targets affected in mutant epidermis we found the two fibroblast growth factor receptors *Fgfr2* and *Fgfr3* and *Krt15* (Ferone et al, 2012), *Col17a1* and *Dst*, two genes encoding for hemidesmosome junctions (Carroll et al, 2006), *Ddit4* gene, also called *Redd1*, a developmentally regulated transcriptional target of p63 and p53, involved in DNA damage (Ellisen et al, 2002), and *Notch1* and *Jag2*, two key components of the Notch signaling pathway (Nguyen et al, 2006)(Fig. 18A). By contrast, AEC mutant epidermis displayed increased focal expression of some keratins, including *Krt6* and *Keratin 16* (*Krt16*) that were essential to maintain keratinocyte integrity in wounded epidermis (18B).
Interestingly, we found a strong up-regulation of inflammatory genes. In particular, we found an up-regulation of one hundred fold of *Tslp*, an IL-7-like cytokine produced by epithelial cells, including keratinocytes that was highly expressed in the epidermis of atopic dermatitis and asthmatic patients (Ziegler & Artis, 2010) (Fig. 18B). TSLP is produced by epithelial cells and it is involved in several processes. Indeed, Tslp caused a polarization of dendritic cells to drive T helper (Th) 2 cytokine production, promoted T-cell proliferation in response to T-cell receptor activation and Th2 cytokines production, and supported B-cell expansion and differentiation. TSLP further amplifies Th2 cytokine production by mast cells and natural killer T cells.
In addition to Tslp induction, our microarray data revealed us also the induction of antimicrobial peptides such as the DAMPs (damage-associated molecular pattern molecules), alarmins involved in the inflammatory response in the event of disruption of skin barrier, such as the inflammatory complex of calprotectin (*S100a8*/ *S100a9* complex), and -to a lesser extent- *Defb4* and *Defb6* (Fig. 18B).

A

p63 target genes

Gene Symbol	Fold +/ctr
Fgfr2	0.43
Fgfr3	0.36
Krt15	0.30
Col17a1	0.44
Dst	0.57
Ddit4	0.49
Notch1	0.44
Jag2	0.63

B

Biological processes

Gene Symbol	Fold +/ctr
Defb4	2.58
Defb6	2.31
S100a8	9.03
S100a9	7.81
Tslp	112.93
Krt6a	11.09
Krt6b	14.18
Krt16	9.24

Figure 18. Gene expression analysis. A) Microarray data confirmed that a subsets of known p63 target genes are affected in the epidermis of L514F mice at P3 compared to ctr mice B) Microarray data showed that a subset of genes involved in different biological processes were up-regulated consistently with what we observed in AEC mutant mice.

4.4 Inflammation in AEC mouse model

While mutant epidermis was hypoplastic at birth, few days after (P7-P12) acanthosis and hyperkeratosis with neutrophils accumulation on the surface was observed accompanied by hypercellularization of the dermis (Fig. 19A). Increased cell proliferation was observed in mutant epidermis as determined by Ki67 immunostaining (Fig. 19A). In addition strong up-regulation of Krt6 was observed in mutant mice, indicating an altered balance between proliferation and differentiation (Fig. 19A). To determine whether hyperproliferation could be a consequence of an inflammatory state, skin sections were stained with antibodies against several immune cell markers. Immunostaining against CD45, a pan-leukocyte marker, revealed that the total number of leukocytes was strongly increased in mutant mice (Fig. 19B). A massive macrophage accumulation in mutant dermis was revealed using the macrophage-specific marker F4/80 antibody, and strong induction of mast cells was observed by toluidine blue staining (Fig. 19B). Therefore, the presence of infiltrating inflammatory cells in the dermis, with concomitant increase in cell proliferation and Krt6 up-regulation in the epidermis suggested that an inflammatory response may be implicated in the development of the severe skin phenotype observed in young mutant mice.

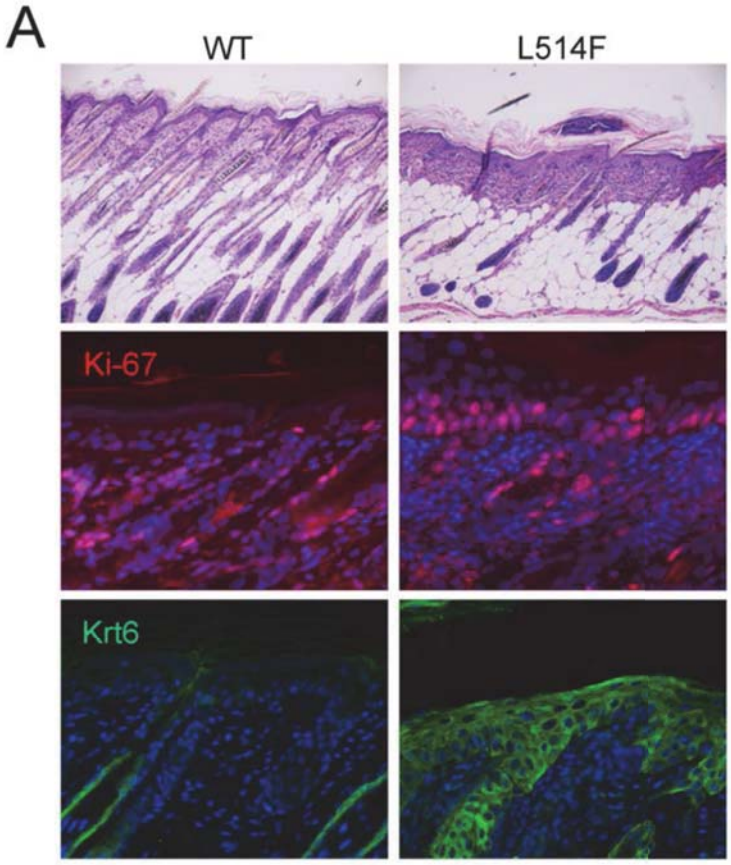
A
WT
L514F
Ki-67
Krt6
P8

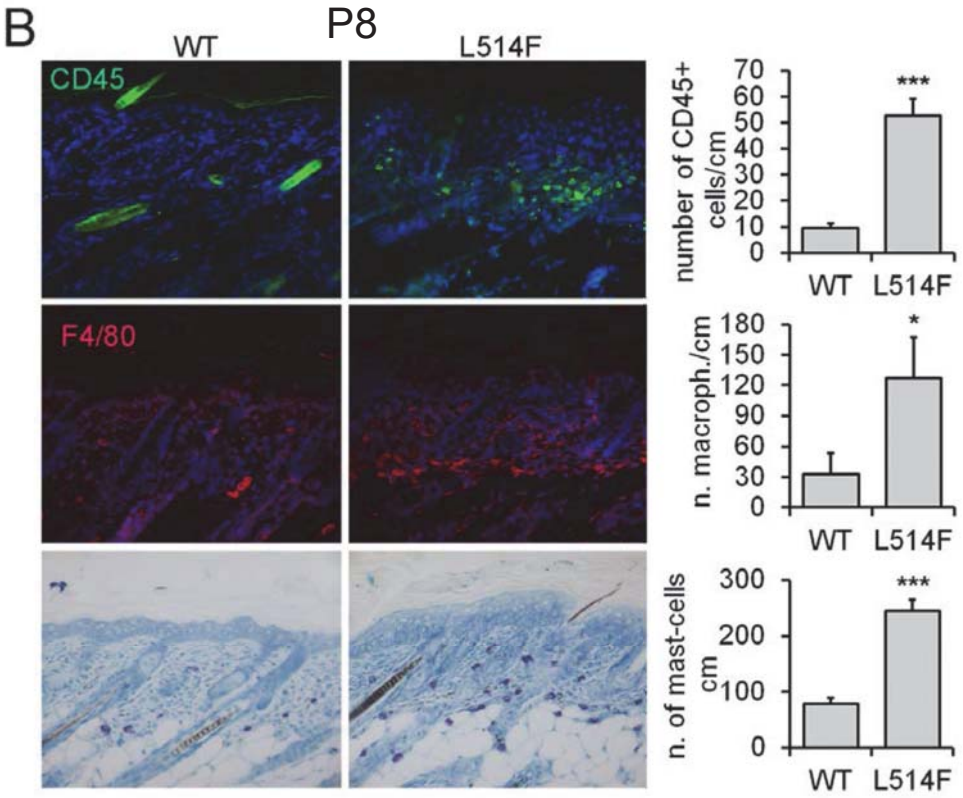

Figure 19. Clear signs of inflammation in L514F mice. A) H&E staining of dorsal skin of L514F mice at P8. Mutant epidermis is hyperplastic with infiltration of polymorphonuclear cells (neutrophils); mutant dermis displays a dense cellularization with few hair follicles. Ki-67 staining in the epidermis of a mutant mouse: only few proliferating cell located in the basal layer are present in control skin, whereas in mutant skin almost all of the cells in the basal layer and numerous suprabasal cells are in cell division. Immunofluorescence analysis for Krt6 in skin at P8 reveals a strong up-regulation in mutant epidermis respect to the control. B) Immunofluorescence analysis for CD45 in skin at P8 shows the presence of leukocytes in the dermis of mutant skin respect to the control. The number of CD45 positive cells is reported in the graph (right panel; ***P-value= 0.0003; n=6). Immunofluorescence analysis for F4/80 in skin at P8. Macrophage infiltration in the dermis of AEC mice calculated measuring F4/80 positive cells is reported in the column chart (right panel; *P-value=0.01; n=7). Histological analysis of mast cells with toluidine blue staining in skin at P8. Massive mast cell infiltration in the dermis of AEC mice calculated measuring toluidine blue positive cells is reported in the graph (right panel; ***P-value= 6.35928E-06; n=8).

To characterize the early steps of this inflammatory state, we firstly tested expression of alarmin also known as Damage-Associated Molecular Patterns (DAMPs), molecules that are upregulated and released in response to DNA damage in epithelial cells triggering inflammation (Hammad & Lambrecht, 2015). At the first time when the first signs of microscopic inflammation became evident (P3), the high mobility group box 1 protein (HMGB1), a prototypic DAMP molecule that can be passively released by damaged cells (Lu et al, 2012) (Kikuchi et al, 2011) was localized primarily in the nucleus of wild-type basal and suprabasal epidermal cells. By contrast, in basal mutant epidermal cells at P3 HMGB1 nuclear signal was lost, and weak cytoplasmic staining was detected, whereas nuclear staining was retained in the suprabasal layers, consistent with cell damage localized primarily in the basal layer (Fig. 20A). Consistent with cell damage, gene expression of the antimicrobial peptides S100A8 and S100A9, other DAMP proteins often induced in epidermal inflammation, that act as amplifiers of inflammatory responses in several inflammatory diseases, were strongly upregulated at the RNA level in mutant epidermis (respectively 22x and 21x) (Fig. 20B). Similarly antimicrobial peptides (AMPs), produced in damaged epithelia, such as β-defensins were respectively up-regulated (Defb4 2.58x; Defb6 1.28x). We next tested innate cytokines such as IL-25, IL-33, and thymic stromal lymphopoietin (Tslp) that activate dendritic cells to promote adaptive Th2 cell immunity, and license the innate type 2 cell response by activation of lymphoid cells, basophils, eosinophils, and mast cells (Hammad & Lambrecht, 2015). While a 4x increase was observed for IL-33, no changes were observed for IL-25 (0.98x). By contrast we observed a massive upregulation of Tslp (788x) at the RNA level in the epidermis, confirming the microarray data.

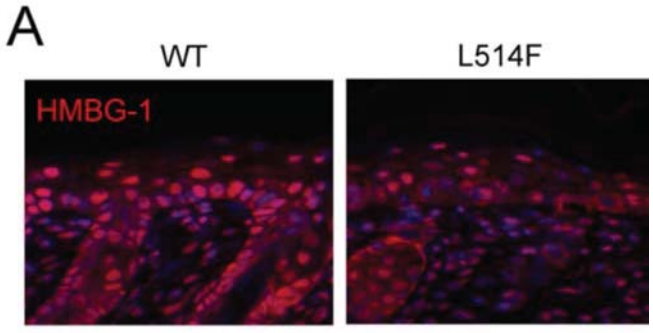

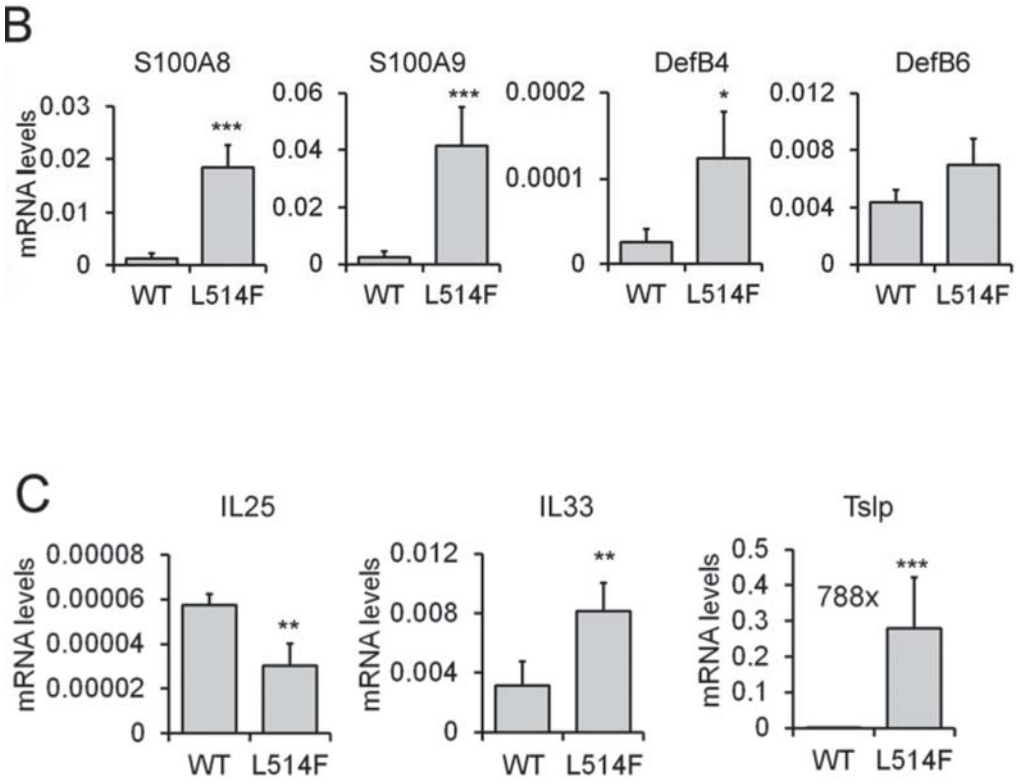

Figure 20. Inflammation in AEC mouse model. A) Immunofluorescence analysis for HMBG-1 in skin at P3 reveals a nuclear-cytoplasm translocation of the protein in mutant epidermis compared to controls. B) Real time RT-PCR for *S100A8, S100A9*, *DefB4* and *DefB6* in mouse epidermis derived from L514F mice and controls at P3. mRNA expression of the analyzed genes are strongly up-regulated in mutant skin as compared to controls (***P-value= 1.24E-05 and 0.0001 respectively; n=10; *P-value=0.01; n=7). Data are normalized for β-actin mRNA levels and are represented as mean ± SD normalized mRNA levels. C) Real time RT-PCR for *IL25*, *IL33* in mouse epidermis derived from L514F mice and controls at P3. mRNA expression of *IL33* are strongly up-regulated in mutant skin as compared to controls (**P-value= 5.13937E-05; n=15); by contrast, mRNA levels of *IL25* in L514F are down-regulated (**P-value= 0.33; n=15). *Tslp* mRNA levels are strongly up-regulated (788x) in mutant epidermis compared to controls (***P-value= 0.0002; n=18). Data are normalized for β-actin mRNA levels and are represented as mean ± SD normalized mRNA levels.

4.5 Tslp as the first biochemical sign of inflammation in AEC syndrome

Global gene expression profiling revealed a massive up-regulation of thymic stromal lymphopoietin (Tslp), whose induction may be the first biochemical sign of inflammation in fact it is considered an alarmin. qRT-PCR analysis in epidermis of mutant mice at P3 confirmed that Tslp mRNA expression was up-regulated 788x fold in mutant epidermis. Tslp was also able to reach the bloodstream and for this purpose we evaluated its expression also in blood serum derived from AEC mutant and control mice. ELISA assays revealed that TSLP levels >3500-fold above the normal levels in sera from mutant mice at P10 (Fig 21A). Interestingly Tslp protein expression was specifically detected in the basal and -to a lesser extent- the spinous layers of mutant epidermis at P8 (Fig 21B). Basal layer induction of Tslp indicates that was unlikely to be due to a canonical defect in epidermal barrier but was rather due to defects in the basal layer consistent with epidermal blistering and aberrant HMGB1 cytoplasmic localization in basal keratinocytes.
Being AEC syndrome a rare disorder with variable penetrance, extensive studies in patients have not been performed. Also in AEC patients in non lesional skin TSLP expression is doubled as compared to control individuals (Fig 21C).

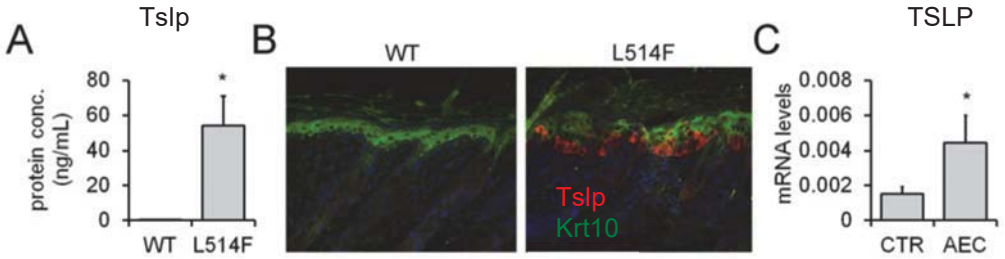

Figure 21. Tslp levels in human patients affected by AEC syndrome and in AEC conditional mouse model: A) Systemic accumulation of Tslp protein (ng/ml) in blood serum of mutant mice at P10 measured by ELISA (*P-value=0.04;n=6). B) Immunofluorescence analysis for Tslp and Krt10 at P8 reveals a strong expression in basal and suprabasal mutant epidermis respect to controls. C) Real time RT-PCR for *TSLP* in human skin derived from AEC patients and healthy controls (*P-value= 0.01; n=7). Data are normalized for *RPLP0* mRNA levels and are represented as mean ± SD normalized mRNA levels.

Consistent with previous reports (Yoo et al, 2005) implicating Tslp in an atopic dermatitis-like phenotype, we observed increased levels of CD4+ T-cells and of Th2 cytokines (IL-4 5.4x; IL-13 18.7x, IL-20 26.3x, IL33 2x, IL1F5 1.6x, Csf2 3.8x, Csf3 1.3x), Th1 cytokines (Cxcl5 14x, IL1b 3.7x, IFNγ 5.3x, IL1F6 13.13x, IL1F9 3.5x), Th17 cytokines (IL6 6.85x, IL17a 15.6x) and AMPs

(DefB1 1.4x, DefB3 574x, DefB4 300x, s100a8 100x, s100a9 106x) in skin at P8 (Fig. 22A), and we found elevated serum IgE levels at later stages (P90) (Fig. 22B).

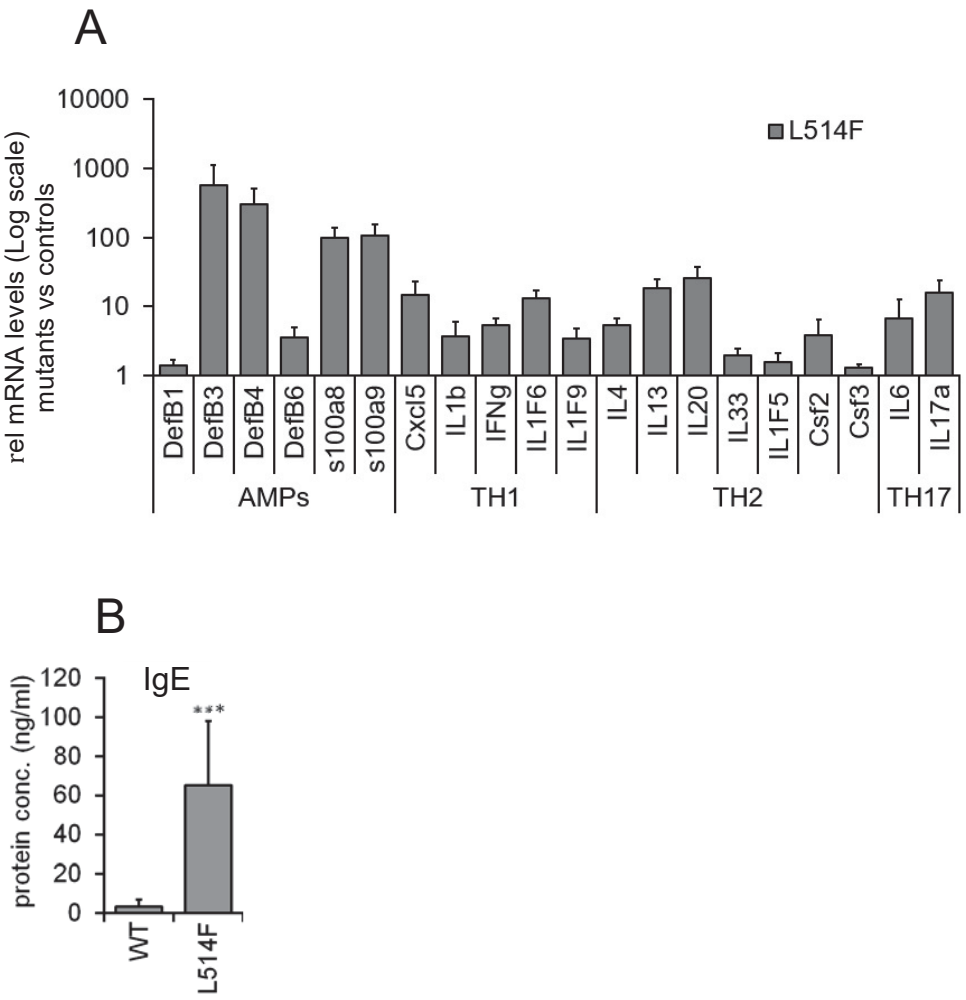

Figure 22. Inflammatory response in AEC conditional mouse model. A) mRNA levels of different inflammatory mediators in mutant skin at P8. B) Systemic accumulation of IgE (ng/ml) in blood serum of mutant mice at adult stage (P90) measured by ELISA (***P-value=0.001; n=16).

4.6 Autoimmune condition associated with AEC syndrome

AEC mutant mice had high white blood cells (WBC) counts (>15.000 cells/µl) at P16 (Fig. 23).

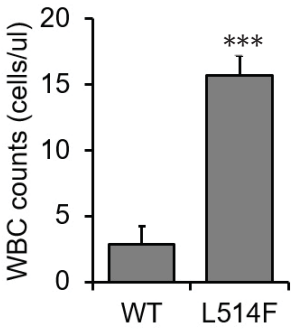

Figure 23. White blood cell counts in L514F mice and relatives controls: increase of WBC count in L514F animals measured at P16 (***P-value= 0.0003; n=8).

Since Tslp is able to reach the bloodstream and to influence the cell fate of different inflammatory and immune cell populations (Liu et al, 2007), the hematopoietic organs bone marrow and spleen were analysed.
Flow cytometry (FACS) analysis of bone marrow (BM) and spleen cells demonstrated a clear expansion of pre- (B220+ CD43- IgM-) and immature B cells in both central and peripheral compartments of the mutant mice (Fig. 24A and B). The expansion of Pre- and Immature B Cells caused a B-Lymphoproliferative Disorder (B-LPD) including B-cell infiltration into vital organ in AEC mice that could culminate in death, consistent with previous reports (Astrakhan et al, 2007) (Demehri et al, 2009b).

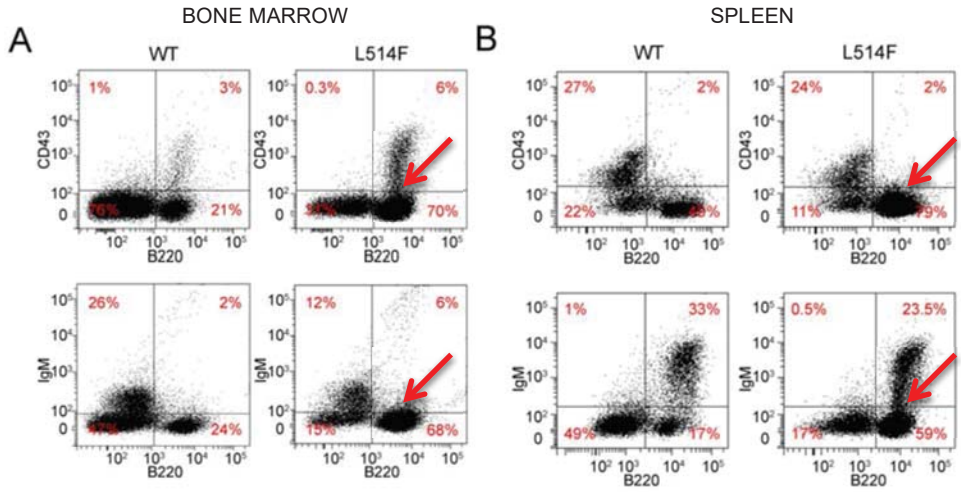

Figure 24. Expanding Pre- and Immature B cells cause a B-LPD in the mutant animals. Mature and immature B-lymphocytes were measured by FACS analysis in bone marrow (***P-value= 7.76267E-14; n=24) (Fig. 24A) and spleen (***P-value= 8.40796E-12; n=24)

(Fig. 24B) in mice at P10. Increased $CD43^{-}IgM^{-}B220^{+}$ revealed an enrichment in Pre-B cells in mutant mice.

4.7 Generation of AEC conditional mouse model in a Tslp null background

To evaluate whether the absence of Tslp in AEC conditional mouse model may lead to a reduced inflammatory state, AEC mice (L514F) were crossed with Tslp $^{floxL2/floxL2}$ conditional null mice (Tslp epidermal Knock-out [Tslp eKO]) (Li et al, 2009). Also the deletion of Tslp occurred in epidermis thanks to CRE recombinase (K14-Cre ΔNeo) and gave birth to L514F; Tslp eKO (Fig. 25B). At P0 L514F; Tslp eKO showed small and large areas of focal blistering in the basal layer (Fig. 25A), as we observed in L514F skin mice. Accordingly with the previous model, at P3 L514F; Tslp eKO are characterized also by a reduction of Krt10 and Krt15 at mRNA levels (Fig. 25B) suggesting that Tslp didn't interfere on p63 role.

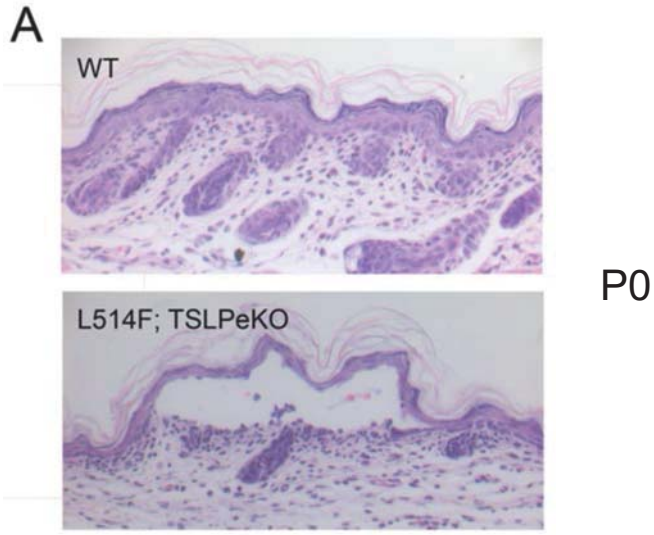

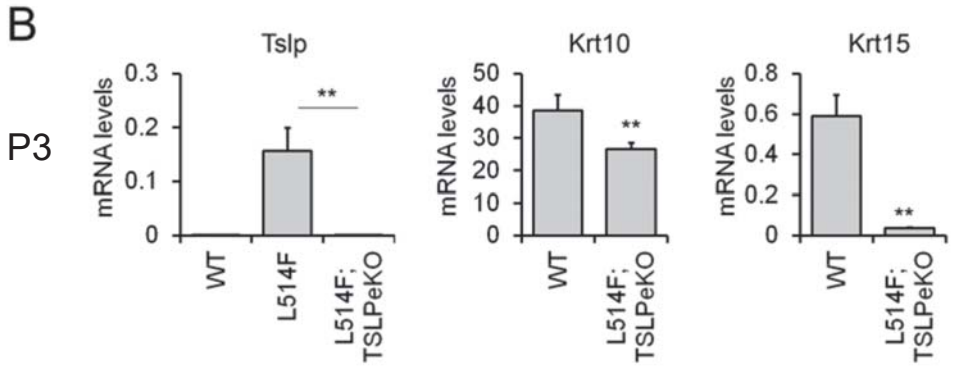

Figure 25. L514F; TSLPeKO histological analysis at P0 and keratin levels expression at P3 A) H&E staining of the skin from newborn mice reveals blistering between the basal lamina and the basal layer and between basal layer and suprabasal compartment in L514F;TSLPeKO skin but not in wild-type epidermis at birth, as reported for L514F mice. B) Real time RT-PCR for *Tslp* (*Tslp* ***P-value=0.000492162; n=14) in mouse epidermis derived from +/+; L514F and L514F; TSLPeKO mice confirmed the deletion of Tslp in epidermis of L514F;TSLPeKO mice. Real time RT-PCR for *Krt10* and *Krt15* reveals a downregulation for both keratins in L514F;TSLPeKO mice similarly observed in L514F mice (*Krt10* **P-value= 0.008484229; n=6; *Krt15* **P-value=0.000408351; n=6).

Interestingly, at P8 L514F; Tslp eKO didn't show shallow erosion or crusting, as we observed at the same stage in L514F mice (Fig 26A). Furthermore, we observed that L514F; Tslp eKO at P10 displayed an higher survival compared to L514F. In addition L514F; Tslp eKO presented a body weight at similar level of wild type controls (Fig 26B and C).
At P40 L514F; Tslp eKO showed a delayed hair loss, a milder phenotype compared to L514F mice', no erythema, no crusting and an amelioration of general health condition (Fig. 26D).

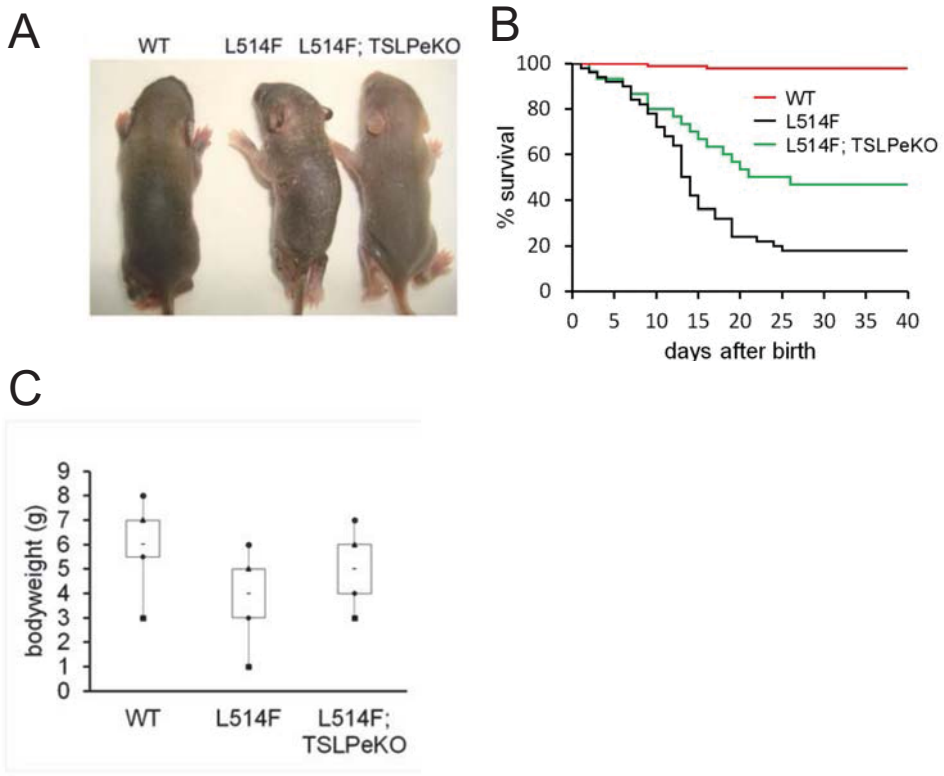

D

Figure 26. Characterization of conditional L514F; TSLPeKO mice: phenotype, survival and weight. A) Photographs are taken from +/+,+/L514F and L514F;TSLPeKO mice at 8 days. B) Survival curve of L514F; TSLPeKO (green line), L514F (black line), and +/+ (red line) mice (*P-value=0.018; n=80). C) Body weight at P10 of +/+, L514F and L514F; TSLPeKO. D) Photographs are taken from L514F and L514F; TSLPeKO mice at 40 days (P40).

4.8 Test the contribution of Tslp upregulation and inflammation in L514F; TSLPeKO conditional mice

The deletion of Tslp occurred in epidermis and reduced the severity of inflammation at P8 in the skin of L514F; TSLP eKO animals. Indeed, normal epidermal and dermal thickness (Fig. 27A), and the proper expression of Krt6 was observed in L514F; TSLPeKO mice (Fig. 27A). Also the immunostaining for CD-45 showed the reduction of leukocytes infiltration in L514F; TslpeKO mice skin and Ki-67 immunofluorescences showed a normal proliferation in AEC mouse model with a Tslp null background. Furthermore, macrophages and mast cells are expressed as in the control mice thus indicating an amelioration of the skin inflammatory phenotype (Fig. 27B).

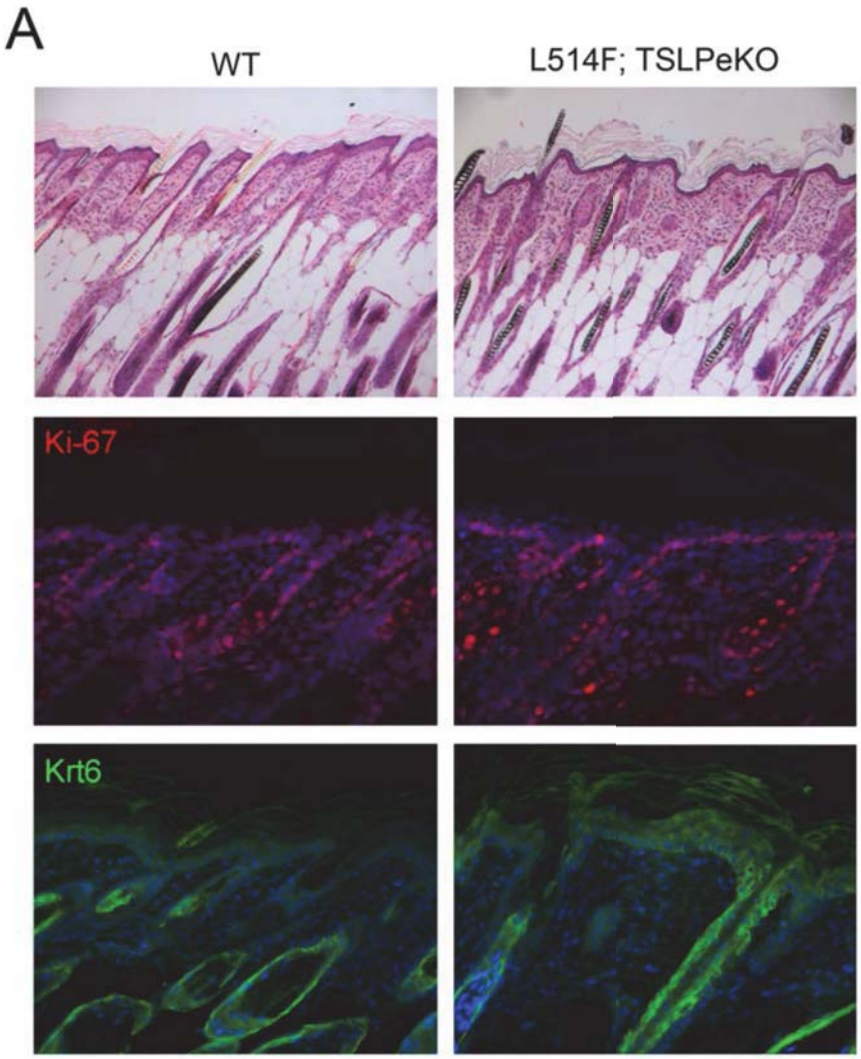
A
WT
L514F; TSLPeKO
Ki-67
Krt6
P8

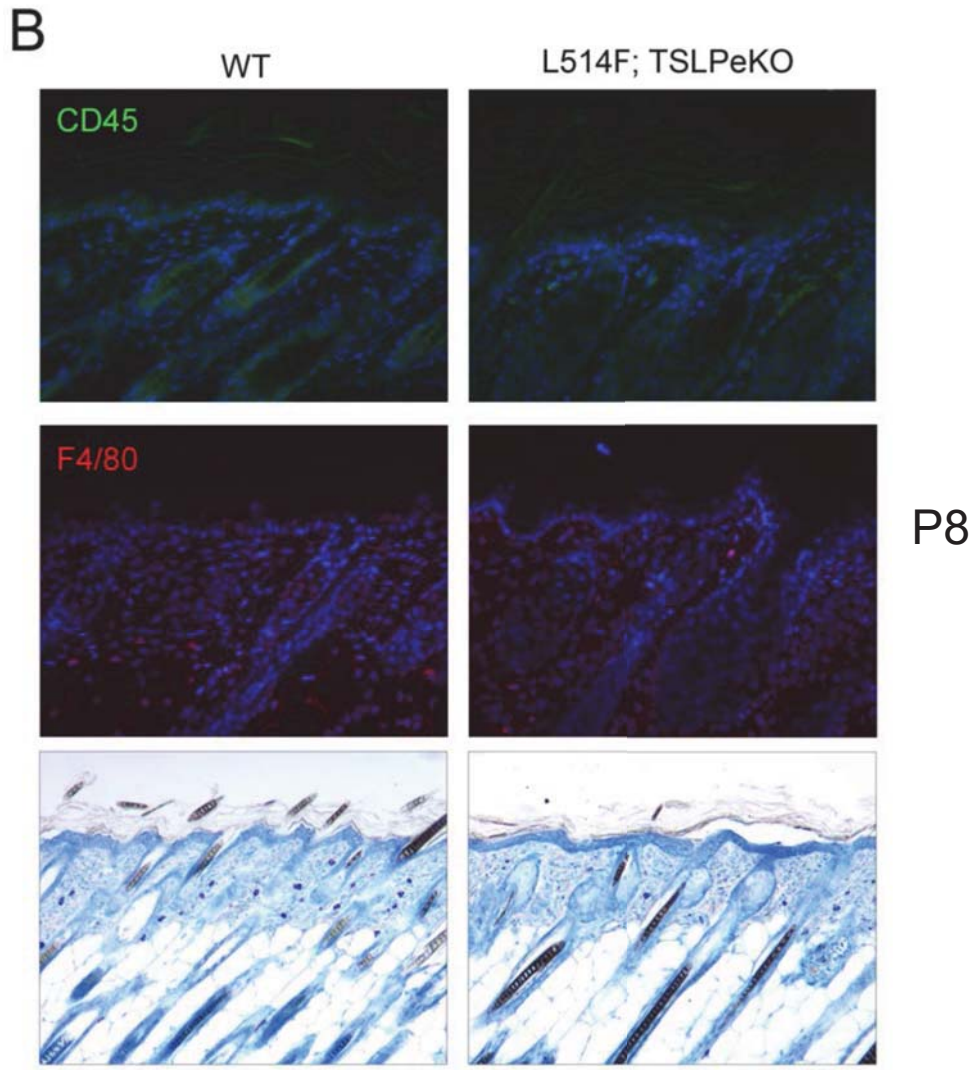

Figure 27. Rescue of the inflammatory state in L514F mice with a Tslp null background A) H&E staining of dorsal skin of L514F; TslpeKO mice at P8. L514F; TslpeKO epidermis is similar to controls. Ki-67 staining in the epidermis of L514F; TslpeKO mutant mouse presented no difference compared to controls. Immunofluorescence analysis for Krt6 in skin at P8 revealed its properly localization in L514F; TslpeKO epidermis. B) Immunofluorescence analysis for CD45 in skin at P8 showed no difference between L514F; TslpeKO and control animals. Immunofluorescence analysis for F4/80 in skin at P8 also showed no difference between L514F; TslpeKO and relative controls. Histological analysis of mast cells with toluidine blue staining in skin at P8 revealed no infiltration of mast cell in the dermis of L514F; TslpeKO mice.

The inflammatory response mediated by inflammatory cytokines and AMPs is also attenuated confirming that Tslp is involved in the insurgence of the inflammatory process and that inflammation occurred as secondary condition associated with AEC syndrome (Fig. 28).

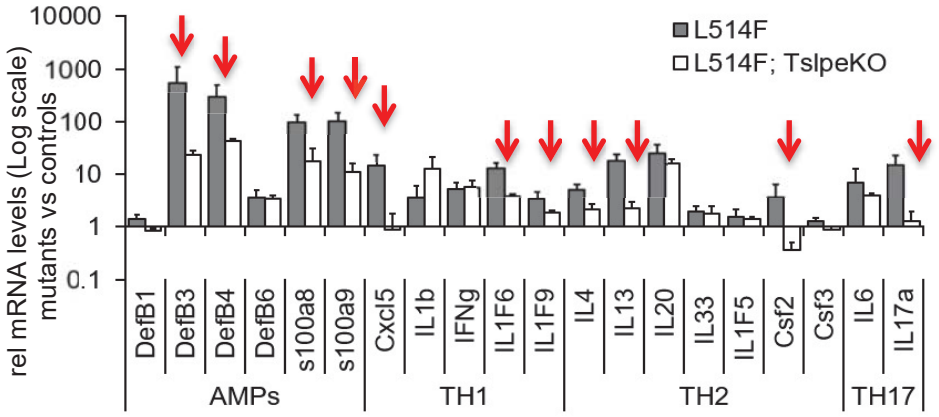

Figure 28. Rescue of the inflammatory cytokines and AMPs in L514F mice with a Tslp null background. mRNA levels of different inflammatory mediators in skin of L514F; TSLPeKO at P8 reveal the attenuation of the inflammatory response (red arrows) in L514F in a Tslp null background.

Consistent to these results in bone marrow of L514F; TSLPeKO mice B-cell development and maturation was not affected, pre-B cells developed normally and spleen size was equal to wild type mice, confirming the rescue in L514F with a Tslp null background (Fig. 29).

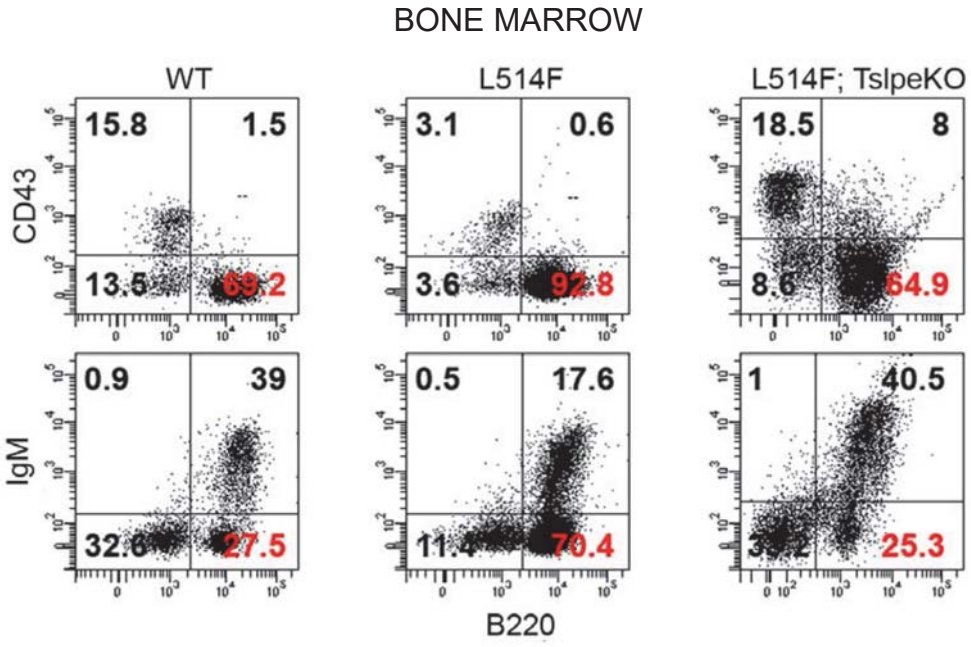

Figure 29. Rescue of the pre-B lymphocytes in spleen of L514F; TSLPeKO mice. B-lymphocytes maturation was measured by FACS analysis in spleen at P10. A rescue of the distribution between immature and mature B-cells was observed in L514F; TSLPeKO mice compared to L514F (CD43-, B220+: P-value <0.001***; n=10; IgM-, B220+: P-value= <0.001***; n=12).

4.9 Klks/PAR2/NFAT pathway regulates Tslp expression in AEC syndrome

Microarray data revealed us that kallikreins, enzymes with serine protease activity that regulate the desquamation of the epidermis (Candi et al, 2005) were strongly up-regulated at P3 thus indicating an altered equilibrium in epidermis structure (Fig. 30). In particular, Klk6 is the proteases most induced in AEC mutant mice compared to wild type.

Gene Symbol	Fold +/ctr
Klk10	3.36
Klk5	1.20
Klk6	5.12
Klk7	1.42
Klk9	1.56

Figure 30. Gene expression analysis. Microarray data showed that a subset of kallikrein proteases were up-regulated in AEC mutant mice.

Recently calcineurin/NFAT signaling has been implicated in Tslp expression downstream of the PAR2 receptor (Wilson et al, 2013). PAR2 activation by serine proteases such as kallikreins (KLKs) leads to calcineurin-dependent nuclear translocation of the transcription factor NFAT. In AEC mouse epidermis at P3 protease activity was induced as determined by in situ zymography (Fig. 31; in collaboration with A. Hovnanian).

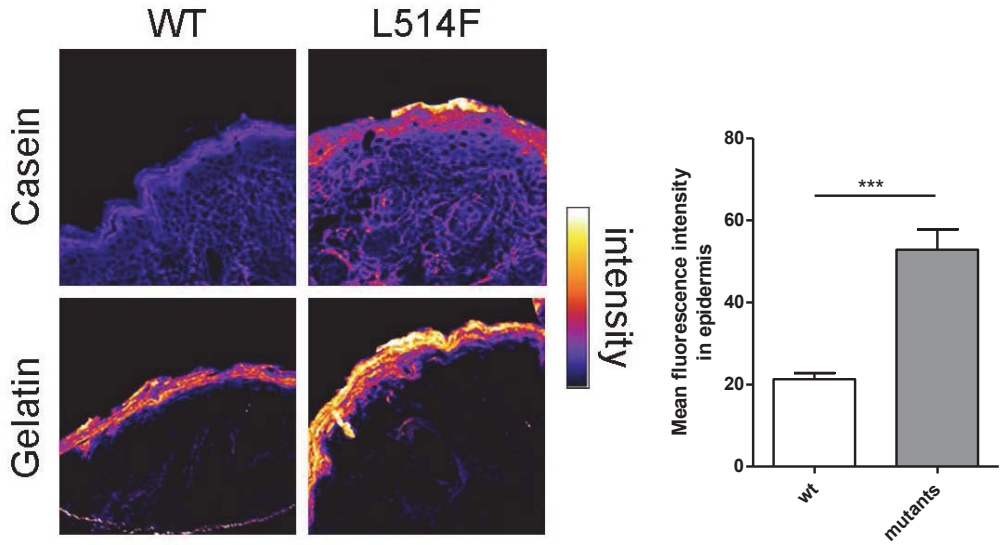

Figure 31. Proteolytic activity in AEC mutant epidermis. *In situ* gel zymography with casein as substrate demonstrate a strong induction of serine-protease protein activity in L514F mutant mice at P3.

Interestingly at P3 we confirmed the microarray data and observed that Klk6 mRNA and to a lesser extent Klk10 was strongly upregulated as compared to controls (Fig. 32A). These data were confirmed also by the immunofluorescence staining for Klk6 (Fig. 32B) and by protein levels (Fig. 32C). We observed a specific upregulation of Klk6 by western blot analysis, instead Klk5 and Klk7 protein levels are expressed equally in L514F mouse epidermis and relative controls.

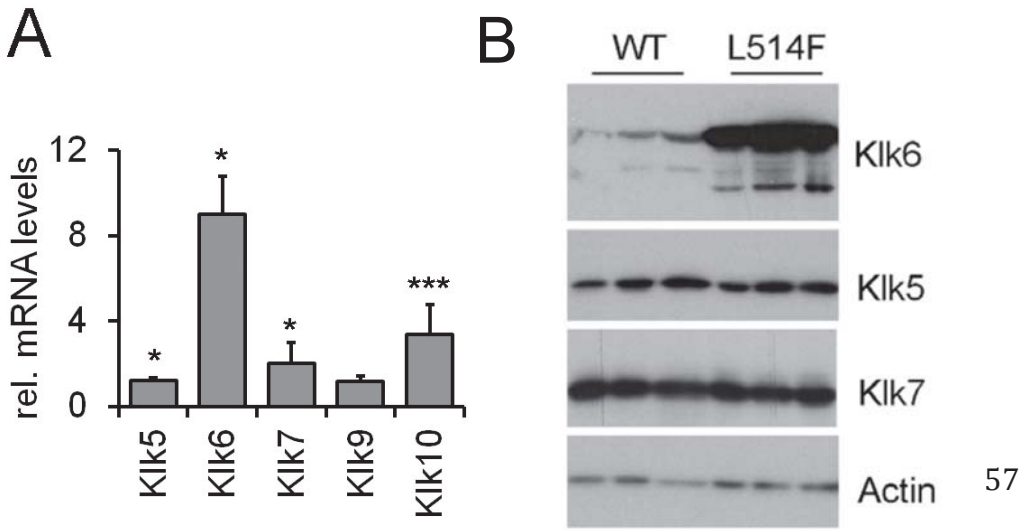

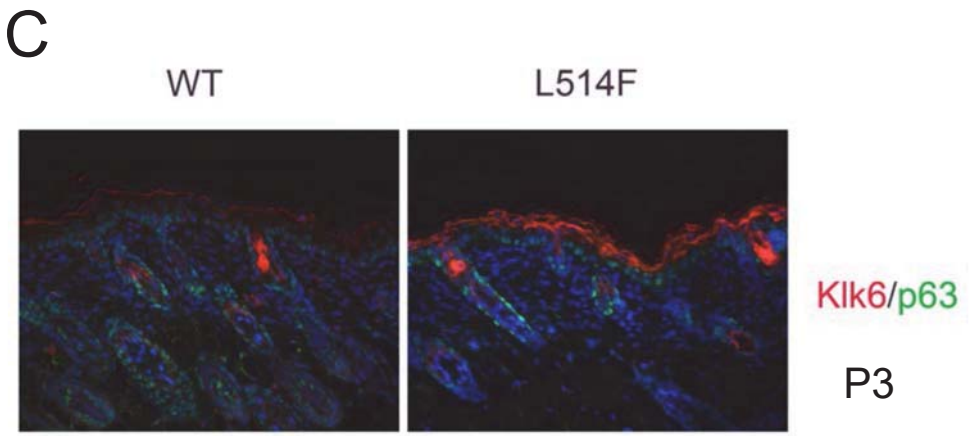

Figure 32. Klk6 upregulation in L514F mice. A) Relative mRNA expression of the indicated kallikreins shows a strong upregulation of Klk6 in the epidermis of L514F mutant mice at P3. B) Immunoblotting analysis for the indicated proteins in cell extracts of mouse epidermis derived from mutant and control mice at P3. Data are normalized for b-actin protein expression. C) Immunofluorescence analysis for Klk6/p63 in skin at P3 shows the strong upregulation of Klk6 in the stratum corneum of the epidermis of L514F mice compared to control animals.

p63 may directly regulate Klk6 since p63 depletion in keratinocytes leads to increase Klk6 expression (Fig. 33A). *In vivo,* in AEC mutant epidermis we observed at P3 that NFAT is highly expressed compared to wild-type (Fig. 33C). NFAT overexpression triggers Tslp induction in mouse keratinocytes (Fig. 33B), supporting the hypothesis that the axis KLK/PAR2/NFAT signaling may be involved in aberrant overexpression of TSLP in the AEC syndrome.

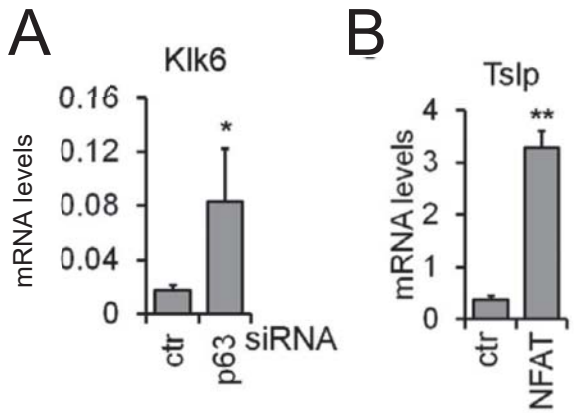

C

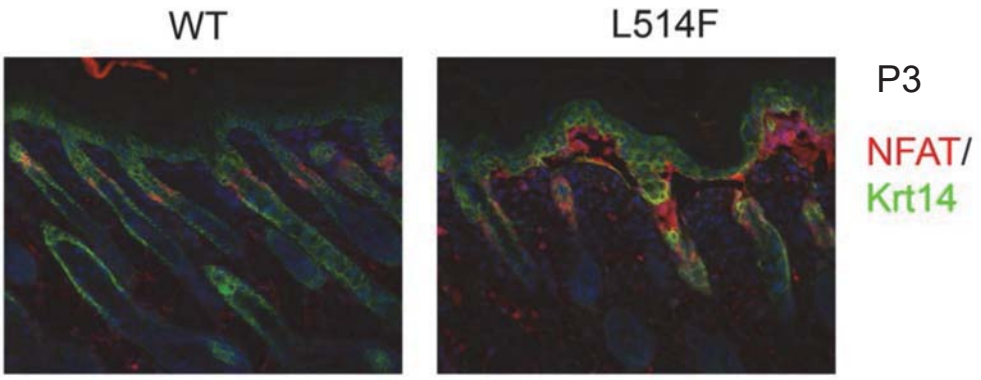

Figure 33. Klk6 upregulation in L514F mice. A) Klk6 mRNA levels is upregulated upon p63 depletion (P-values: <0.05 *; <0.01 **; <0.001 ***; n=8). B) Tslp mRNA is induced by a constitutive active form of NFAT. C) Immunofluorescence analysis for NFAT/Krt14 in skin at P3 shows the presence of NFAT in the basal layer of the epidermis of L514F mice compared to control animals.

5. DISCUSSION

AEC syndrome is an autosomal dominant disorder characterized by cleft palate, ectodermal dysplasia, and severe skin fragility and extensive erosions that are currently treated using generic wound care. Targeted treatments are highly desirable. The disorder is caused by mutations in the *p63* gene, coding for a transcription factor that is a master regulator of epidermal structure and function. AEC mutations lead to reduced mechanical strength by affecting desmosome and keratin expression, and causing severe skin inflammation. Most AEC causative mutations fall in the poorly characterized C-terminal domain of the p63 alpha isoform not shared by p63 beta.

Since little is known about the causes of AEC skin erosions, the histological and molecular defects, we previously generated a constitutive mouse model that carries a clinically relevant point mutation in the SAM domain of the p63 alpha isoform (L514F) reported in AEC patients.

$p63^{+/L514F}$ mice died at birth with severe cleft palate, skin defects and ectodermal dysplasia (Ferone et al, 2012), thus faithfully recapitulating the defects observed in AEC syndrome. The cause of death in $p63^{+/L514F}$ mice was cleft palate, which is lethal in mice but not in humans. $p63^{+/L514F}$ skin displayed an overall reduction in skin thickness, accompanied by a significant epidermal atrophy and hair follicle hypoplasia. At the molecular level we found that the AEC mutation affected proliferation of the epithelial cells of the palate and skin, and led to a reduced number of epidermal stem cells. These phenotypes were associated with aberrantly low FGF signaling due to reduced expression of the FGF receptor *Fgfr2*, a direct p63 target gene. Importantly, we obtained evidences that humans affected by AEC syndrome have similar defects of the epidermal stem cell compartment (Ferone et al, 2012). AEC mouse skin displayed focal blistering skin lesions, localized mainly between the basal and suprabasal layers of the epidermis accompanied with acantholysis (loss of intercellular adhesions) and only rarely by cytolysis (rupture of the cell membrane). These phenotypes were associated with reduced desmosomal contacts in AEC mutant skin. We demonstrated that skin fragility observed in the constitutive mouse model was caused by a strong reduction of desmosomes and that Dsg1, Dsc3 and Dsp were strongly reduced also in human keratinocytes derived from AEC patients and focal downregulation of DSP and DSC3 expression was observed in non-lesional skin of AEC patients (Ferone et al, 2013; Koster et al, 2014), confirming their possible causative role in the pathogenesis of AEC syndrome.

To overcome the lethality of the constitutive mouse model and to better characterize the molecular mechanisms underlined skin erosions and hypothetical in vivo treatments, we generated a conditional AEC mouse model. The conditional knock-in model ($p63^{+/floxL514F}$) expresses the L514F mutation only in the presence of the CRE recombinase. Thus the newly generated $p63^{+/floxL514F}$ mouse model expresses only the wild-type p63 and has no phenotype until a portion of the inserted DNA is removed by CRE-mediated

recombination. We cross $p63^{+/floxL514F}$ with a knock-in mouse expressing Cre by E17.5 in epidermis and hair follicle under the control of the endogenous Keratin 14 (K14) promoter (K14-Cre Δneo) to obtain both the heterozygous and the homozygous model (+/L and L/L) (Huelsken et al, 2001).

We begin to characterize the heterozygous model, +/L that show no gross abnormalities. We hypothesize that, since the expression of the mutation is late in the development a number of biological processes that required p63 presence are not affected because they happen when the mutation is still off and only one copy of mutant p63 is not able to negatively influence these processes later. Our observations are quite in contrast with what we observe in the constitutive model, in which gene expression analysis lead us to hypothesize that L514F mutation acts in a dominant negative fashion. To shed light on this discrepancy further analysis on the molecular mechanisms by which mutant p63 influences its transcriptional activity will be needed. On the other hand it has been reported that sometimes mouse model and human disorders are quite different in the genetic contest, therefore our model need to be in homozygosity to mimic the syndrome. Importantly, alteration of the p63 target genes in the conditional homozygous model is comparable to the constitutive heterozygous mutant in spite of nearly complete absence of the wild-type copy by P0, thus indicating that the L/L model is comparable to the constitutive one.

The conditional mouse model for AEC syndrome (L514F) is affected by a progressive skin phenotype characterized by focal skin erosions and scaling, skin crusting and hair loss, closely resembling the skin defects observed in humans affected by AEC syndrome. The severe skin phenotype leads to reduced body weight and survival. Histological analysis of newborn skin reveals focal disruption of cell-cell adhesion, as previously observed for the constitutive mouse model (Ferone et al, 2013) and cytolysis of the basal layer, even in the absence of a macroscopic phenotype. Consistent with local areas of mechanical disruption, focal loss of epidermal barrier is observed. Ultrastructural analysis demonstrated reduced keratin bundles in the basal layer of the epidermis, accompanied by reduced expression of several keratins, of which Krt5 and Krt15 are the most severely affected. Importantly reduced Krt5 and Krt15 are observed also in human samples derived from AEC patients at the RNA and protein levels (Ferone et al, 2012).

Few days after the first biochemical sign of inflammation, AEC mutant epidermis becomes hyperplastic and hyperkeratotic with neutrophils accumulation in the epidermis, Krt6 induction and massive infiltration of macrophages and mast cells in the dermis. Blister healing often involves the induction of keratins related to Krt5 (Krt6a and Krt6b) and Krt14 (Krt16 and Krt17) (Coulombe et al, 2009). By P3, Krt6 and Krt16 are strongly upregulated, whereas Krt17 is unaffected, suggesting a partial and selective compensation. Concomitant with Krt6 and Krt16 induction, we observed significant induction of damage-associated molecular pattern molecules (DAMPs) that initiate the inflammatory response in the event of a disruption of

the epidermal barrier, such as the inflammatory complex calprotectin (S100a8/ S100a9 complex), and -to a lesser extent- antimicrobial peptides (Defb). In addition, we observed massive upregulation of thymic stromal lymphopoietin (Tslp), an interleukin 7-like cytokine, which is markedly elevated in lesional skin of atopic dermatitis and asthmatic patients (Ziegler & Artis, 2010). TSLP is produced by epithelial cells and causes a polarization of dendritic cells to drive T helper (Th) 2 cytokines production. TSLP also directly promotes T-cell proliferation in response to T-cell receptor activation and Th2 cytokine production, and supports B-cell expansion and differentiation. TSLP further amplifies Th2 cytokine production by mast cells and natural killer T cells.
Several observations support the notion that TSLP is implicated in autoimmunity, promoting humoral autoimmunity by enhancing B cell population expansion (Astrakhan et al, 2007), indicating that signaling pathways triggering Tslp expression and their inhibitors may have therapeutic potential in a number of diseases. Consistently, massive Tslp induction precedes skin inflammation and is released into the blood circulation, likely causing the development of a B-Lymphoproliferative Disorder with massive increase of pre-B cells in the bone marrow and in the spleen as observed by Demehri et al, in Notch1; Notch2 conditional knock-out mice (Demehri et al, 2008).

The consequence of ablating Tslp was evaluated by crossing AEC mutant mice with conditional Tslp null mice (Li et al., 2009). Genetic ablation of Tslp in the epidermis of L514F mice ameliorates the general health condition of AEC mutant mice, significantly increasing survival, and reducing skin inflammation. Importantly deletion of Tslp in the epidermis is sufficient to rescue B-cell maturation. Taken together these data indicate that Tslp is likely to be a crucial mediator of skin and systemic inflammation in AEC syndrome.
Several pathways may be responsible for Tslp induction downstream of mutant p63. To begin to untangle the pathways regulating Tslp downstream of p63, we tested the following hypothesis: 2) Calcineurin/NFAT regulates Tslp expression in AEC syndrome. Calcineurin/NFAT signaling has been recently implicated in Tslp expression downstream of the PAR2 receptor (Wilson et al., 2013). PAR2 activation by serine proteases such as kallikreins (KLKs) leads to calcineurin-dependent nuclear translocation of the transcription factor NFAT. In AEC mouse epidermis at P3 Klk6 mRNA (and to a lesser extent Klk10) is strongly upregulated as compared to controls. We demonstrated that p63 might directly regulate Klk6 since p63 depletion in keratinocytes leads to increase Klk6 expression. In agreement with Klk6 upregulation, protease activity is induced in AEC mouse skin as determined by in situ zymography (Fig. 14D; in collaboration with A. Hovnanian). Furthermore we observed that NFAT overexpression triggers Tslp induction in mouse keratinocytes, supporting the hypothesis that the axis KLK/PAR2/NFAT signaling may be involved in aberrant overexpression of TSLP in AEC syndrome.
Being AEC syndrome a rare disorder with variable penetrance, extensive studies in patients have not been performed. However, we observed that TSLP

expression in the epidermis of AEC patients is doubled as compared to control individuals. Interestingly, an autoimmune disorder has been observed in at least one AEC patient with severe skin erosions occurring soon after birth in 70% of the body, indicating that the release of TSLP may be at basis of a systemic autoimmune condition also in individuals affected by AEC syndrome. This patient during the childhood was placed under prednisone, and at the age of 16 is still on a very low dose of mycophenolate mofetil (M. Atlas, MD Pediatric Hematology-Oncology doctor; personal comm.). We tested his levels of TSLP in the blood, but found no difference with matching controls, consistent with the remission of the disease. We are in the process of obtaining approval for systematic examination of blood levels of TSLP in AEC children, with the help of the American National Foundation for Ectodermal Dysplasia (NFED) to coordinate the enrollment of patients since the largest collection of families affected by AEC syndrome is done in the US.

Pharmacological Tslp inhibitors are not available yet, however identification of molecular pathways leading to Tslp induction in epidermis may help to identify specific inhibitors of upstream pathways. Several other pathways beyond the calcineurin/NFAT pathway may be responsible for Tslp induction downstream of mutant p63 such as the Notch signaling pathway or the NF-kB. In addition, other molecules such as the transcription factors NF-kB, AP-1, as well as the Ca2+-permeable ion channel TRPRV1 could be part of the Tslp regulation and they have to be analyzed. Understanding the pathways regulating Tslp expression is likely to lead to identification of additional pharmacological strategies.

6. CONCLUSIONS

In conclusion, we have demonstrated that the basal cell fragility and blistering observed in AEC mutant mice are due to alteration in adhesion molecules belonged to different categories. Interestingly, we have established a key role of intermediate filaments in the basal layer of the epidermis of AEC mouse model, which integrity is fundamental to give mechanical resilience to the epidermis. For the first time we have evaluated the contribution of Krt5 in the progression of skin erosions in AEC syndrome therefore paving the way for new feasible treatments aimed at restoration of keratins functionality.
Importantly, we have explored the possibility that altered skin barrier due to unbalanced keratin bundles in the basal layer leads to inflammation, driven by upregulation of Tslp. TSLP is at basis of a systemic autoimmune condition also in individuals affected by AEC syndrome. Genetic ablation of Tslp in the epidermis of L514F mice ameliorates the general health condition of AEC mutant mice. Mechanistically, massive Tslp induction was accompanied by strong induction of kallikrein-6 (Klk6) and NFAT accumulation in mutant epidermis. We have demonstrated that p63 might directly regulate Klk6 since p63 depletion in keratinocytes leads to increase Klk6 expression. Overall in AEC mutant epidermis, Klk6 upregulation leads to massive Tslp induction by an NFAT-dependent mechanism (Fig. 34). In addition, other molecules such as the transcription factor NF-kB could be part of the Tslp regulation and they have to be analyzed.

Taken together these data indicate that Tslp is likely to be a crucial mediator of skin and systemic inflammation in AEC syndrome, and controlling Tslp in severely affected patients may be therapeutically beneficial.

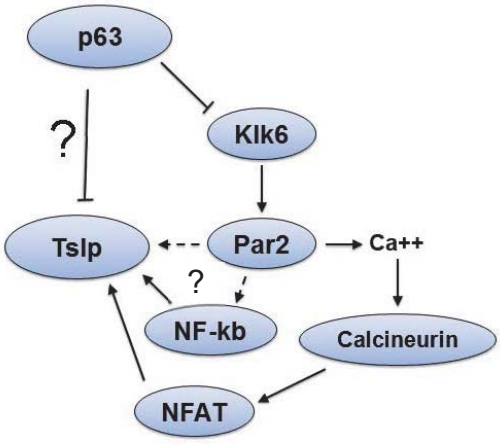

Figure 34. Proposed model: Tslp regulation and mechanism of action in keratinocytes. Proposed model for Tslp regulation by p63 and KLK/PAR2/NFAT or NFkB signaling pathway.

REFERENCES

Allakhverdi Z, Comeau MR, Jessup HK, Yoon BR, Brewer A, Chartier S, Paquette N, Ziegler SF, Sarfati M, Delespesse G (2007) Thymic stromal lymphopoietin is released by human epithelial cells in response to microbes, trauma, or inflammation and potently activates mast cells. *The Journal of experimental medicine* **204:** 253-258

Antonini D, Russo MT, De Rosa L, Gorrese M, Del Vecchio L, Missero C (2010) Transcriptional repression of miR-34 family contributes to p63-mediated cell cycle progression in epidermal cells. *J Invest Dermatol* **130:** 1249-1257

Astrakhan A, Omori M, Nguyen T, Becker-Herman S, Iseki M, Aye T, Hudkins K, Dooley J, Farr A, Alpers CE, Ziegler SF, Rawlings DJ (2007) Local increase in thymic stromal lymphopoietin induces systemic alterations in B cell development. *Nature immunology* **8:** 522-531

Barrow LL, van Bokhoven H, Daack-Hirsch S, Andersen T, van Beersum SE, Gorlin R, Murray JC (2002) Analysis of the p63 gene in classical EEC syndrome, related syndromes, and non-syndromic orofacial clefts. *Journal of medical genetics* **39:** 559-566

Bertola DR, Kim CA, Albano LM, Scheffer H, Meijer R, van Bokhoven H (2004) Molecular evidence that AEC syndrome and Rapp-Hodgkin syndrome are variable expression of a single genetic disorder. *Clinical genetics* **66:** 79-80

Candi E, Rufini A, Terrinoni A, Dinsdale D, Ranalli M, Paradisi A, De Laurenzi V, Spagnoli LG, Catani MV, Ramadan S, Knight RA, Melino G (2006) Differential roles of p63 isoforms in epidermal development: selective genetic complementation in p63 null mice. *Cell death and differentiation* **13:** 1037-1047

Candi E, Schmidt R, Melino G (2005) The cornified envelope: a model of cell death in the skin. *Nature reviews Molecular cell biology* **6:** 328-340

Carroll DK, Brugge JS, Attardi LD (2007) p63, cell adhesion and survival. *Cell cycle* **6:** 255-261

Carroll DK, Carroll JS, Leong CO, Cheng F, Brown M, Mills AA, Brugge JS, Ellisen LW (2006) p63 regulates an adhesion programme and cell survival in epithelial cells. *Nature cell biology* **8:** 551-561

Celli J, Duijf P, Hamel BC, Bamshad M, Kramer B, Smits AP, Newbury-Ecob R, Hennekam RC, Van Buggenhout G, van Haeringen A, Woods CG, van Essen AJ, de Waal R, Vriend G, Haber DA, Yang A, McKeon F, Brunner HG, van Bokhoven H (1999) Heterozygous germline mutations in the p53 homolog p63 are the cause of EEC syndrome. *Cell* **99:** 143-153

Chapiro E, Russell L, Lainey E, Kaltenbach S, Ragu C, Della-Valle V, Hanssens K, Macintyre EA, Radford-Weiss I, Delabesse E, Cave H, Mercher T, Harrison CJ, Nguyen-Khac F, Dubreuil P, Bernard OA (2010) Activating mutation in the TSLPR gene in B-cell precursor lymphoblastic leukemia. *Leukemia* **24:** 642-645

Chi SW, Ayed A, Arrowsmith CH (1999) Solution structure of a conserved C-terminal domain of p73 with structural homology to the SAM domain. *The EMBO journal* **18:** 4438-4445

Clements SE, Techanukul T, Lai-Cheong JE, Mee JB, South AP, Pourreyron C, Burrows NP, Mellerio JE, McGrath JA (2012) Mutations in AEC syndrome skin reveal a role for p63 in basement membrane adhesion, skin barrier integrity and hair follicle biology. *The British journal of dermatology* **167:** 134-144

Coulombe PA, Kerns ML, Fuchs E (2009) Epidermolysis bullosa simplex: a paradigm for disorders of tissue fragility. *The Journal of clinical investigation* **119:** 1784-1793

De Moerlooze L, Spencer-Dene B, Revest JM, Hajihosseini M, Rosewell I, Dickson C (2000) An important role for the IIIb isoform of fibroblast growth factor receptor 2 (FGFR2) in mesenchymal-epithelial signalling during mouse organogenesis. *Development* **127:** 483-492

De Rosa L, Antonini D, Ferone G, Russo MT, Yu PB, Han R, Missero C (2009) p63 Suppresses non-epidermal lineage markers in a bone morphogenetic protein-dependent manner via repression of Smad7. *The Journal of biological chemistry* **284:** 30574-30582

Demehri S, Liu Z, Lee J, Lin MH, Crosby SD, Roberts CJ, Grigsby PW, Miner JH, Farr AG, Kopan R (2008) Notch-deficient skin induces a lethal systemic B-lymphoproliferative disorder by secreting TSLP, a sentinel for epidermal integrity. *PLoS biology* **6:** e123

Demehri S, Morimoto M, Holtzman MJ, Kopan R (2009a) Skin-derived TSLP triggers progression from epidermal-barrier defects to asthma. *PLoS biology* **7:** e1000067

Demehri S, Turkoz A, Kopan R (2009b) Epidermal Notch1 loss promotes skin tumorigenesis by impacting the stromal microenvironment. *Cancer cell* **16:** 55-66

Deutsch GB, Zielonka EM, Coutandin D, Weber TA, Schafer B, Hannewald J, Luh LM, Durst FG, Ibrahim M, Hoffmann J, Niesen FH, Senturk A, Kunkel H, Brutschy B, Schleiff E, Knapp S, Acker-Palmer A, Grez M, McKeon F, Dotsch V (2011) DNA damage in oocytes induces a switch of the quality control factor TAp63alpha from dimer to tetramer. *Cell* **144:** 566-576

Di Meglio P, Perera GK, Nestle FO (2011) The multitasking organ: recent insights into skin immune function. *Immunity* **35:** 857-869

Dohn M, Zhang S, Chen X (2001) p63alpha and DeltaNp63alpha can induce cell cycle arrest and apoptosis and differentially regulate p53 target genes. *Oncogene* **20:** 3193-3205

Dombrowski Y, Peric M, Koglin S, Kammerbauer C, Goss C, Anz D, Simanski M, Glaser R, Harder J, Hornung V, Gallo RL, Ruzicka T, Besch R, Schauber J (2011) Cytosolic DNA triggers inflammasome activation in keratinocytes in psoriatic lesions. *Science translational medicine* **3:** 82ra38

Duijf PH, Vanmolkot KR, Propping P, Friedl W, Krieger E, McKeon F, Dotsch V, Brunner HG, van Bokhoven H (2002) Gain-of-function mutation in ADULT syndrome reveals the presence of a second transactivation domain in p63. *Human molecular genetics* **11:** 799-804

Dumortier A, Durham AD, Di Piazza M, Vauclair S, Koch U, Ferrand G, Ferrero I, Demehri S, Song LL, Farr AG, Leonard WJ, Kopan R, Miele L, Hohl D, Finke D, Radtke F (2010) Atopic dermatitis-like disease and associated lethal myeloproliferative disorder arise from loss of Notch signaling in the murine skin. *PloS one* **5:** e9258

Ellisen LW, Ramsayer KD, Johannessen CM, Yang A, Beppu H, Minda K, Oliner JD, McKeon F, Haber DA (2002) REDD1, a developmentally regulated transcriptional target of p63 and p53, links p63 to regulation of reactive oxygen species. *Molecular cell* **10:** 995-1005

Fallon PG, Ballantyne SJ, Mangan NE, Barlow JL, Dasvarma A, Hewett DR, McIlgorm A, Jolin HE, McKenzie AN (2006) Identification of an interleukin (IL)-25-dependent cell population that provides IL-4, IL-5, and IL-13 at the onset of helminth expulsion. *The Journal of experimental medicine* **203:** 1105-1116

Feldmeyer L, Werner S, French LE, Beer HD (2010) Interleukin-1, inflammasomes and the skin. *European journal of cell biology* **89:** 638-644

Ferone G, Mollo MR, Thomason HA, Antonini D, Zhou H, Ambrosio R, De Rosa L, Salvatore D, Getsios S, van Bokhoven H, Dixon J, Missero C (2013) p63 control of desmosome gene expression and adhesion is compromised in AEC syndrome. *Human molecular genetics* **22:** 531-543

Ferone G, Thomason HA, Antonini D, De Rosa L, Hu B, Gemei M, Zhou H, Ambrosio R, Rice DP, Acampora D, van Bokhoven H, Del Vecchio L, Koster MI, Tadini G, Spencer-Dene B, Dixon M, Dixon J, Missero C (2012) Mutant p63 causes defective expansion of ectodermal progenitor cells and impaired FGF signalling in AEC syndrome. *EMBO molecular medicine* **4:** 192-205

Friend SL, Hosier S, Nelson A, Foxworthe D, Williams DE, Farr A (1994) A thymic stromal cell line supports in vitro development of surface IgM+ B cells and produces a novel growth factor affecting B and T lineage cells. *Experimental hematology* **22:** 321-328

Fuchs E (2007) Scratching the surface of skin development. *Nature* **445:** 834-842

Fuchs E, Green H (1980) Changes in keratin gene expression during terminal differentiation of the keratinocyte. *Cell* **19:** 1033-1042

Furio L, Pampalakis G, Michael IP, Nagy A, Sotiropoulou G, Hovnanian A (2015) KLK5 Inactivation Reverses Cutaneous Hallmarks of Netherton Syndrome. *PLoS genetics* **11:** e1005389

Gebhardt T, Wakim LM, Eidsmo L, Reading PC, Heath WR, Carbone FR (2009) Memory T cells in nonlymphoid tissue that provide enhanced local immunity during infection with herpes simplex virus. *Nature immunology* **10:** 524-530

Gebhardt T, Whitney PG, Zaid A, Mackay LK, Brooks AG, Heath WR, Carbone FR, Mueller SN (2011) Different patterns of peripheral migration by memory CD4+ and CD8+ T cells. *Nature* **477:** 216-219

Ghioni P, Bolognese F, Duijf PH, Van Bokhoven H, Mantovani R, Guerrini L (2002) Complex transcriptional effects of p63 isoforms: identification of novel activation and repression domains. *Molecular and cellular biology* **22:** 8659-8668

Glaser R, Harder J, Lange H, Bartels J, Christophers E, Schroder JM (2005) Antimicrobial psoriasin (S100A7) protects human skin from Escherichia coli infection. *Nature immunology* **6:** 57-64

Gonfloni S, Di Tella L, Caldarola S, Cannata SM, Klinger FG, Di Bartolomeo C, Mattei M, Candi E, De Felici M, Melino G, Cesareni G (2009) Inhibition of the c-Abl-TAp63 pathway protects mouse oocytes from chemotherapy-induced death. *Nature medicine* **15:** 1179-1185

Halim TY, Krauss RH, Sun AC, Takei F (2012) Lung natural helper cells are a critical source of Th2 cell-type cytokines in protease allergen-induced airway inflammation. *Immunity* **36:** 451-463

Hammad H, Lambrecht BN (2015) Barrier Epithelial Cells and the Control of Type 2 Immunity. *Immunity* **43:** 29-40

Harder J, Schroder JM (2005) Antimicrobial peptides in human skin. *Chemical immunology and allergy* **86:** 22-41

Hardman MJ, Sisi P, Banbury DN, Byrne C (1998) Patterned acquisition of skin barrier function during development. *Development* **125:** 1541-1552

Hay RJ, Wells RS (1976) The syndrome of ankyloblepharon, ectodermal defects and cleft lip and palate: an autosomal dominant condition. *The British journal of dermatology* **94:** 277-289

Helton ES, Zhu J, Chen X (2006) The unique NH2-terminally deleted (DeltaN) residues, the PXXP motif, and the PPXY motif are required for the transcriptional activity of the DeltaN variant of p63. *The Journal of biological chemistry* **281:** 2533-2542

Huelsken J, Vogel R, Erdmann B, Cotsarelis G, Birchmeier W (2001) beta-Catenin controls hair follicle morphogenesis and stem cell differentiation in the skin. *Cell* **105:** 533-545

Ikoma A, Steinhoff M, Stander S, Yosipovitch G, Schmelz M (2006) The neurobiology of itch. *Nature reviews Neuroscience* **7:** 535-547

Iseki M, Omori-Miyake M, Xu W, Sun X, Takaki S, Rawlings DJ, Ziegler SF (2012) Thymic stromal lymphopoietin (TSLP)-induced polyclonal B-cell activation and autoimmunity are mediated by CD4+ T cells and IL-4. *International immunology* **24:** 183-195

Kantaputra PN, Hamada T, Kumchai T, McGrath JA (2003) Heterozygous mutation in the SAM domain of p63 underlies Rapp-Hodgkin ectodermal dysplasia. *Journal of dental research* **82:** 433-437

Kashyap M, Rochman Y, Spolski R, Samsel L, Leonard WJ (2011) Thymic stromal lymphopoietin is produced by dendritic cells. *Journal of immunology* **187:** 1207-1211

Kemp CJ, Wheldon T, Balmain A (1994) p53-deficient mice are extremely susceptible to radiation-induced tumorigenesis. *Nature genetics* **8:** 66-69

Kerr JB, Hutt KJ, Michalak EM, Cook M, Vandenberg CJ, Liew SH, Bouillet P, Mills A, Scott CL, Findlay JK, Strasser A (2012) DNA damage-induced primordial follicle oocyte apoptosis and loss of fertility require TAp63-mediated induction of Puma and Noxa. *Molecular cell* **48:** 343-352

Kikuchi K, Uchikado H, Miura N, Morimoto Y, Ito T, Tancharoen S, Miyata K, Sakamoto R, Kikuchi C, Iida N, Shiomi N, Kuramoto T, Miyagi N, Kawahara KI (2011) HMGB1 as a therapeutic target in spinal cord injury: A hypothesis for novel therapy development. *Experimental and therapeutic medicine* **2:** 767-770

Koster MI, Dai D, Marinari B, Sano Y, Costanzo A, Karin M, Roop DR (2007) p63 induces key target genes required for epidermal morphogenesis. *Proceedings of the National Academy of Sciences of the United States of America* **104:** 3255-3260

Koster MI, Dinella J, Chen J, O'Shea C, Koch PJ (2014) Integrating animal models and in vitro tissue models to elucidate the role of desmosomal proteins in diseases. *Cell communication & adhesion* **21:** 55-63

Koster MI, Roop DR (2004) The role of p63 in development and differentiation of the epidermis. *Journal of dermatological science* **34:** 3-9

LeBoeuf M, Terrell A, Trivedi S, Sinha S, Epstein JA, Olson EN, Morrisey EE, Millar SE (2010) Hdac1 and Hdac2 act redundantly to control p63 and p53 functions in epidermal progenitor cells. *Dev Cell* **19:** 807-818

Leonard WJ (2002) TSLP: finally in the limelight. *Nature immunology* **3:** 605-607

Leoyklang P, Siriwan P, Shotelersuk V (2006) A mutation of the p63 gene in non-syndromic cleft lip. *Journal of medical genetics* **43:** e28

Levin SD, Koelling RM, Friend SL, Isaksen DE, Ziegler SF, Perlmutter RM, Farr AG (1999) Thymic stromal lymphopoietin: a cytokine that promotes the development of IgM+ B cells in vitro and signals via a novel mechanism. *Journal of immunology* **162:** 677-683

Li M, Hener P, Zhang Z, Ganti KP, Metzger D, Chambon P (2009) Induction of thymic stromal lymphopoietin expression in keratinocytes is necessary for generating an atopic dermatitis upon application of the active vitamin D3 analogue MC903 on mouse skin. *J Invest Dermatol* **129:** 498-502

Liu YJ, Soumelis V, Watanabe N, Ito T, Wang YH, Malefyt Rde W, Omori M, Zhou B, Ziegler SF (2007) TSLP: an epithelial cell cytokine that regulates T cell differentiation by conditioning dendritic cell maturation. *Annual review of immunology* **25:** 193-219

Lu B, Nakamura T, Inouye K, Li J, Tang Y, Lundback P, Valdes-Ferrer SI, Olofsson PS, Kalb T, Roth J, Zou Y, Erlandsson-Harris H, Yang H, Ting JP, Wang H, Andersson U, Antoine DJ, Chavan SS, Hotamisligil GS, Tracey KJ (2012) Novel role of PKR in inflammasome activation and HMGB1 release. *Nature* **488:** 670-674

McGrath JA, Duijf PH, Doetsch V, Irvine AD, de Waal R, Vanmolkot KR, Wessagowit V, Kelly A, Atherton DJ, Griffiths WA, Orlow SJ, van Haeringen A, Ausems MG, Yang A, McKeon F, Bamshad MA, Brunner HG, Hamel BC, van Bokhoven H (2001) Hay-Wells syndrome is caused by heterozygous missense mutations in the SAM domain of p63. *Human molecular genetics* **10:** 221-229

Mills AA, Zheng B, Wang XJ, Vogel H, Roop DR, Bradley A (1999) p63 is a p53 homologue required for limb and epidermal morphogenesis. *Nature* **398:** 708-713

Moon PD, Choi IH, Kim HM (2011) Naringenin suppresses the production of thymic stromal lymphopoietin through the blockade of RIP2 and caspase-1 signal cascade in mast cells. *European journal of pharmacology* **671:** 128-132

Nestle FO, Di Meglio P, Qin JZ, Nickoloff BJ (2009) Skin immune sentinels in health and disease. *Nature reviews Immunology* **9:** 679-691

Nguyen BC, Lefort K, Mandinova A, Antonini D, Devgan V, Della Gatta G, Koster MI, Zhang Z, Wang J, Tommasi di Vignano A, Kitajewski J, Chiorino G, Roop DR, Missero C, Dotto GP (2006) Cross-regulation between Notch

and p63 in keratinocyte commitment to differentiation. *Genes & development* **20:** 1028-1042

Payne AS, Yan AC, Ilyas E, Li W, Seykora JT, Young TL, Pawel BR, Honig PJ, Camacho J, Imaizumi S, Heymann WR, Schnur RE (2005) Two novel TP63 mutations associated with the ankyloblepharon, ectodermal defects, and cleft lip and palate syndrome: a skin fragility phenotype. *Archives of dermatology* **141:** 1567-1573

Petiot A, Conti FJ, Grose R, Revest JM, Hodivala-Dilke KM, Dickson C (2003) A crucial role for Fgfr2-IIIb signalling in epidermal development and hair follicle patterning. *Development* **130:** 5493-5501

Porter CM, Clipstone NA (2002) Sustained NFAT signaling promotes a Th1-like pattern of gene expression in primary murine CD4+ T cells. *Journal of immunology* **168:** 4936-4945

Prassas I, Eissa A, Poda G, Diamandis EP (2015) Unleashing the therapeutic potential of human kallikrein-related serine proteases. *Nature reviews Drug discovery* **14:** 183-202

Qiao F, Bowie JU (2005) The many faces of SAM. *Science's STKE : signal transduction knowledge environment* **2005:** re7

Reardon C, Lechmann M, Brustle A, Gareau MG, Shuman N, Philpott D, Ziegler SF, Mak TW (2011) Thymic stromal lymphopoetin-induced expression of the endogenous inhibitory enzyme SLPI mediates recovery from colonic inflammation. *Immunity* **35:** 223-235

Reche PA, Soumelis V, Gorman DM, Clifford T, Liu M, Travis M, Zurawski SM, Johnston J, Liu YJ, Spits H, de Waal Malefyt R, Kastelein RA, Bazan JF (2001) Human thymic stromal lymphopoietin preferentially stimulates myeloid cells. *Journal of immunology* **167:** 336-343

Rice R, Spencer-Dene B, Connor EC, Gritli-Linde A, McMahon AP, Dickson C, Thesleff I, Rice DP (2004) Disruption of Fgf10/Fgfr2b-coordinated epithelial-mesenchymal interactions causes cleft palate. *The Journal of clinical investigation* **113:** 1692-1700

Rinne T, Bolat E, Meijer R, Scheffer H, van Bokhoven H (2009) Spectrum of p63 mutations in a selected patient cohort affected with ankyloblepharon-ectodermal defects-cleft lip/palate syndrome (AEC). *American journal of medical genetics Part A* **149A:** 1948-1951

Rinne T, Brunner HG, van Bokhoven H (2007) p63-associated disorders. *Cell cycle* **6:** 262-268

Rinne T, Clements SE, Lamme E, Duijf PH, Bolat E, Meijer R, Scheffer H, Rosser E, Tan TY, McGrath JA, Schalkwijk J, Brunner HG, Zhou H, van Bokhoven H (2008) A novel translation re-initiation mechanism for the p63 gene revealed by amino-terminal truncating mutations in Rapp-Hodgkin/Hay-Wells-like syndromes. *Human molecular genetics* **17:** 1968-1977

Rizzo JM, Romano RA, Bard J, Sinha S (2014) RNA-seq Studies Reveal New Insights into p63 and the Transcriptomic Landscape of the Mouse Skin. *J Invest Dermatol*

Roll JD, Reuther GW (2010) CRLF2 and JAK2 in B-progenitor acute lymphoblastic leukemia: a novel association in oncogenesis. *Cancer research* **70:** 7347-7352

Romano RA, Ortt K, Birkaya B, Smalley K, Sinha S (2009) An active role of the DeltaN isoform of p63 in regulating basal keratin genes K5 and K14 and directing epidermal cell fate. *PloS one* **4:** e5623

Schmitz J, Owyang A, Oldham E, Song Y, Murphy E, McClanahan TK, Zurawski G, Moshrefi M, Qin J, Li X, Gorman DM, Bazan JF, Kastelein RA (2005) IL-33, an interleukin-1-like cytokine that signals via the IL-1 receptor-related protein ST2 and induces T helper type 2-associated cytokines. *Immunity* **23:** 479-490

Senoo M, Pinto F, Crum CP, McKeon F (2007) p63 Is essential for the proliferative potential of stem cells in stratified epithelia. *Cell* **129:** 523-536

Shen Q, Jin H, Wang X (2013) Epidermal stem cells and their epigenetic regulation. *International journal of molecular sciences* **14:** 17861-17880

Simpson CL, Patel DM, Green KJ (2011) Deconstructing the skin: cytoarchitectural determinants of epidermal morphogenesis. *Nature reviews Molecular cell biology* **12:** 565-580

Sims JE, Williams DE, Morrissey PJ, Garka K, Foxworthe D, Price V, Friend SL, Farr A, Bedell MA, Jenkins NA, Copeland NG, Grabstein K, Paxton RJ (2000) Molecular cloning and biological characterization of a novel murine lymphoid growth factor. *The Journal of experimental medicine* **192:** 671-680

Sonnenberg GF, Fouser LA, Artis D (2011) Border patrol: regulation of immunity, inflammation and tissue homeostasis at barrier surfaces by IL-22. *Nature immunology* **12:** 383-390

Soumelis V, Reche PA, Kanzler H, Yuan W, Edward G, Homey B, Gilliet M, Ho S, Antonenko S, Lauerma A, Smith K, Gorman D, Zurawski S, Abrams J, Menon S, McClanahan T, de Waal-Malefyt Rd R, Bazan F, Kastelein RA, Liu YJ (2002) Human epithelial cells trigger dendritic cell mediated allergic inflammation by producing TSLP. *Nature immunology* **3:** 673-680

Straub WE, Weber TA, Schafer B, Candi E, Durst F, Ou HD, Rajalingam K, Melino G, Dotsch V (2010) The C-terminus of p63 contains multiple regulatory elements with different functions. *Cell death & disease* **1:** e5

Su X, Chakravarti D, Cho MS, Liu L, Gi YJ, Lin YL, Leung ML, El-Naggar A, Creighton CJ, Suraokar MB, Wistuba I, Flores ER (2010) TAp63 suppresses metastasis through coordinate regulation of Dicer and miRNAs. *Nature* **467:** 986-990

Suh EK, Yang A, Kettenbach A, Bamberger C, Michaelis AH, Zhu Z, Elvin JA, Bronson RT, Crum CP, McKeon F (2006) p63 protects the female germ line during meiotic arrest. *Nature* **444:** 624-628

Takeuchi O, Akira S (2010) Pattern recognition receptors and inflammation. *Cell* **140:** 805-820

Tasian SK, Loh ML (2011) Understanding the biology of CRLF2-overexpressing acute lymphoblastic leukemia. *Critical reviews in oncogenesis* **16:** 13-24

Truong AB, Kretz M, Ridky TW, Kimmel R, Khavari PA (2006) p63 regulates proliferation and differentiation of developmentally mature keratinocytes. *Genes & development* **20:** 3185-3197

van Bokhoven H, Brunner HG (2002) Splitting p63. *American journal of human genetics* **71:** 1-13

van Bokhoven H, Hamel BC, Bamshad M, Sangiorgi E, Gurrieri F, Duijf PH, Vanmolkot KR, van Beusekom E, van Beersum SE, Celli J, Merkx GF, Tenconi R, Fryns JP, Verloes A, Newbury-Ecob RA, Raas-Rotschild A, Majewski F, Beemer FA, Janecke A, Chitayat D, Crisponi G, Kayserili H, Yates JR, Neri G, Brunner HG (2001) p63 Gene mutations in eec syndrome, limb-mammary syndrome, and isolated split hand-split foot malformation

suggest a genotype-phenotype correlation. *American journal of human genetics* **69:** 481-492

Watanabe N, Hanabuchi S, Soumelis V, Yuan W, Ho S, de Waal Malefyt R, Liu YJ (2004) Human thymic stromal lymphopoietin promotes dendritic cell-mediated CD4+ T cell homeostatic expansion. *Nature immunology* **5:** 426-434

Wilson SR, The L, Batia LM, Beattie K, Katibah GE, McClain SP, Pellegrino M, Estandian DM, Bautista DM (2013) The epithelial cell-derived atopic dermatitis cytokine TSLP activates neurons to induce itch. *Cell* **155:** 285-295

Yang A, Kaghad M, Caput D, McKeon F (2002) On the shoulders of giants: p63, p73 and the rise of p53. *Trends in genetics : TIG* **18:** 90-95

Yang A, Kaghad M, Wang Y, Gillett E, Fleming MD, Dotsch V, Andrews NC, Caput D, McKeon F (1998) p63, a p53 homolog at 3q27-29, encodes multiple products with transactivating, death-inducing, and dominant-negative activities. *Molecular cell* **2:** 305-316

Yang A, Schweitzer R, Sun D, Kaghad M, Walker N, Bronson RT, Tabin C, Sharpe A, Caput D, Crum C, McKeon F (1999) p63 is essential for regenerative proliferation in limb, craniofacial and epithelial development. *Nature* **398:** 714-718

Yang A, Walker N, Bronson R, Kaghad M, Oosterwegel M, Bonnin J, Vagner C, Bonnet H, Dikkes P, Sharpe A, McKeon F, Caput D (2000) p73-deficient mice have neurological, pheromonal and inflammatory defects but lack spontaneous tumours. *Nature* **404:** 99-103

Ying S, O'Connor B, Ratoff J, Meng Q, Mallett K, Cousins D, Robinson D, Zhang G, Zhao J, Lee TH, Corrigan C (2005) Thymic stromal lymphopoietin expression is increased in asthmatic airways and correlates with expression of Th2-attracting chemokines and disease severity. *Journal of immunology* **174:** 8183-8190

Yoo J, Omori M, Gyarmati D, Zhou B, Aye T, Brewer A, Comeau MR, Campbell DJ, Ziegler SF (2005) Spontaneous atopic dermatitis in mice expressing an inducible thymic stromal lymphopoietin transgene specifically in the skin. *The Journal of experimental medicine* **202:** 541-549

Ziegler SF, Artis D (2010) Sensing the outside world: TSLP regulates barrier immunity. *Nature immunology* **11:** 289-293

Research Techniques Made Simple: Skin Carcinogenesis Models: Xenotransplantation Techniques

Maria Rosaria Mollo[1], Dario Antonini[2], Luisa Cirillo[1,3] and Caterina Missero[1,4]

Xenotransplantation is a widely used technique to test the tumorigenic potential of human cells in vivo using immunodeficient mice. Here we describe basic technologies and recent advances in xenotransplantation applied to study squamous cell carcinomas (SCCs) of the skin. SCC cells isolated from tumors can either be cultured to generate a cell line or injected directly into mice. Several immunodeficient mouse models are available for selection based on the experimental design and the type of tumorigenicity assay. Subcutaneous injection is the most widely used technique for xenotransplantation because it involves a simple procedure allowing the use of a large number of cells, although it may not mimic the original tumor environment. SCC cell injections at the epidermal-to-dermal junction or grafting of organotypic cultures containing human stroma have also been used to more closely resemble the tumor environment. Mixing of SCC cells with cancer-associated fibroblasts can allow the study of their interaction and reciprocal influence, which can be followed in real time by intradermal ear injection using conventional fluorescent microscopy. In this article, we will review recent advances in xenotransplantation technologies applied to study behavior of SCC cells and their interaction with the tumor environment in vivo.

Journal of Investigative Dermatology (2016) **136,** e13–e17; doi:10.1016/j.jid.2015.12.015

INTRODUCTION

Establishing human tissue cancer models is essential to elucidate fundamental mechanisms underlying cancer development and progression, and to develop novel therapies. Humanized mouse models, in which human tumor cells or tissue are engrafted into immunodeficient mice (xenotransplantation), are frequently used to understand tumor biology in the presence of a tissue environment, and to study tumor responses to gene modulation and pharmacological treatments in vivo.

This article will focus primarily on xenotransplantation models for skin squamous cell carcinomas (SCCs). In most cases, this process involves growth in culture of neoplastic keratinocytes or genetically modified keratinocytes, fibroblasts, and other skin cell types that can be admixed with keratinocytes and used for in vivo tissue regeneration.

To establish SCC cell lines, primary tumor tissue is physically dissociated into either small explant pieces or single cell suspensions to be expanded in culture on a feeder layer of 3T3 fibroblasts, but SCC cells soon become feeder independent (Purdie et al., 2011). Defined genetic lesions contributing to SCC formation, such as proto-oncogene or tumor suppressor mutations, can be studied by manipulating human primary keratinocytes using retroviral- or lentiviral-mediated gene modulation (Khavari, 2006), allowing the introduction of putative oncogenes, knockdown of tumor suppressor genes, or gene ablation or mutation using genome editing tools such as the CRISPR/Cas9 system.

BENEFITS

- Allows measurement of the tumorigenic potential of human skin cancer cells in a complex in vivo environment.
- Allows study of the consequences of specific genetic alterations in vivo.
- Can be used for screening the therapeutic potential of novel chemical compounds on human tissues.
- Interactions between epithelial tumor cells, stroma, and other cell types can be studied in combination.
- Recent techniques allow growth of primary SCC tissue and SCC single-cell suspensions, and/or monitoring growth in real time using in vivo imaging.

LIMITATIONS

- Only partially recapitulates tumor organization and function, and its interaction with the immune, vasculature, and lymphatic systems.
- As with other in vivo assays, it is subject to high variability, and appropriate statistical analyses must be used to obtain reliable results.
- Tumor development occurs slowly, and may take up to or more than 4 months.

[1]CEINGE Biotecnologie Avanzate, Scarl, Napoli, Italy; [2]IRCCS SDN, Napoli, Italy; [3]Department of Molecular Medicine and Medical Biotechnology, University of Naples Federico II, Napoli, Italy; and [4]Department of Biology, University of Naples Federico II, Napoli, Italy

Correspondence: Caterina Missero, Department of Biology, University of Naples Federico II, Via Cinthia, 80126 Napoli, Italy. E-mail: caterina.missero@unina.it

IMMUNODEFICIENT MOUSE MODELS FOR XENOTRANSPLANTATION

Immunodeficient mouse strains are used for human cell studies to avoid rejection of the human cells. Here we will focus on immunodeficient mouse models that have been used in dermatological research for studying SCC (for a more comprehensive description of recipient mouse strains, see Russell et al., 2015). Athymic *Foxn1*^{nu} (nude) mice lack functional T cells, but have an intact humoral adaptive and innate immune system (Price, 2014). In spite of only partial impairment of the immune system, nude mice effectively support tumor growth because of a paradoxical role of both the adaptive and innate immune responses in inducing inflammation, which can be protumorigenic (Patel et al., 2012). In severe combined immune deficiency (SCID) mice, the development of mature T- and B-lymphocytes is abolished, but innate immunity is conserved. Similarly, RAG1/2 null mice lack both functional T and B cells. Crossing SCID mice with nonobese diabetic (NOD) mice confers partially defective innate immunity. To further weaken the innate immune system, immunodeficient mice carrying a targeted mutation in the IL2 receptor common gamma chain gene (*IL2r* γ) have been crossed with NOD/SCID or NOD/RAG1/2 mice, generating the NOD/SCID/*IL2r* γ null or NOD/RAG1/2/*IL2r* γ null mice. Adaptive immunity is completely lacking in NOD/SCID/*IL2r* γ null and NOD/RAG1/2/*IL2r* γ null mice, and they are severely deficient in innate immunity, thus being highly receptive to the engraftment of human cells, tissues, and primary tumors.

INJECTIONS OF HUMAN CELLS IN IMMUNODEFICIENT MICE

The most widely used tumorigenicity assay involves ectopic injection of neoplastic cells into the subcutaneous space on the back of immunodeficient mice. Depending on the experimental design, tumor cells and relative controls are frequently injected into the two dorsal flanks to compare their tumorigenicity in the same biological environment.

A range of 0.5×10^5 to 5×10^6 tumor cells are injected, depending on their tumorigenic potential and the experimental plan. A smaller number of cells can be utilized when testing the tumor-initiating capability of selected cell populations. In this case, it is crucial to use NOD/SCID/*IL2r* γ null mice where adaptive immunity is completely lacking, because a small number of cells are more prone to be destroyed by the immune system. In addition, tumorigenic cells are mixed with Matrigel, a complex mixture of extracellular matrix proteins that enhances the engraftment of primary epithelial cancer cells by promoting perfusion of nutrients and holding cells in place in the subcutaneous tissue (Quintana et al., 2008). Matrigel is used at a high concentration (20 mg/ml) with the cells mixed in a 1:1 ratio. After injection, tumor size is monitored once a week, and two diameters of the tumors are measured to estimate changes in tumor volume over time. Immunohistological and immunohistochemical analysis is required to determine the tumor grade by examining tissue morphology, degree of cell proliferation, differentiation, and number of cells undergoing senescence or apoptosis.

ADVANCES IN SCC XENOTRANSPLANTATION

Established SCC cell lines are mostly tumorigenic and retain features of primary cutaneous SCC with variable degree of differentiation, ranging from well-differentiated cysts to more aggressive tumors, whereas grafting of freshly isolated SCC cells is more challenging. Recently, Patel et al. (2012) established a method to obtain reproducible and robust growth of xenografted primary SCC tissue and SCC single-cell suspensions in athymic nude mice by preimplantation of a humanized stromal bed. In this assay, a glass disk or Gelfoam dressing is implanted into the dorsal subcutaneous space, together with 10^6 primary human dermal fibroblasts (HDFs) suspended in Matrigel. After 2 weeks, the glass disk is removed and intact tumor tissue or primary human SCC cells suspended in Matrigel are injected into the subcutaneous space or into the in situ Gelfoam dressing (Patel et al., 2012). The glass disk promotes a stromal reaction and vascularization sufficient to induce reproducible tumor growth from SCC cell lines. However, preimplantation of HDFs is essential to achieve robust growth of primary SCC cells. With this method, xenografts from all tumor grades maintain the histological and growth characteristics of the original tumors even through serial transplantation (Figure 1). Interestingly, xenografts of freshly isolated SCC cells are consistently larger in athymic nude mice than in more immunocompromised mice (SCID), possibly due to a higher inflammatory response elicited in athymic nude mice, in which only T cells are compromised, but the humoral and innate responses are still active.

Subepidermal injections

Although subcutaneous injections are widely used, the subcutaneous microenvironment is different from the one in which skin tumors originally develop. To promote the interaction of cancer cells with a more physiological environment, SCC cells can be mixed with Matrigel and injected at the dermal-epidermal junction. An advantage of this technique is that SCC cells diffuse less, and proliferative centers originating from single cells can be counted (Wu et al., 2010). Although injecting in the subepidermal environment is insufficient to enhance SCC tumorigenic potential, it can be useful to test cancer-inducing factors. Indeed, using this assay, Wu and co-workers demonstrated that inhibition of the calcineurin/nuclear factor of activated T-cell pathway induced a more aggressive, moderately infiltrating tumor phenotype with high cellularity, thus suggesting a reason for why treatment with calcineurin inhibitors, used as immunosuppressive treatment for organ transplantation recipients, leads to an increased risk of SCC formation.

Ear injections

More recently, Procopio et al. (2015) described a novel assay for studying SCC and stromal cell expansion by intradermal ear injection in NOD/SCID/*IL2r* γ null mice. The ear thinness enables tumor formation to follow in real time and quantification of its growth rate by in vivo imaging using conventional fluorescence stereomicroscopy (Figure 2). A very low volume can be injected, allowing a low number of cells (10^5) to be used. This novel technique has proven useful to test the function of the Notch effector

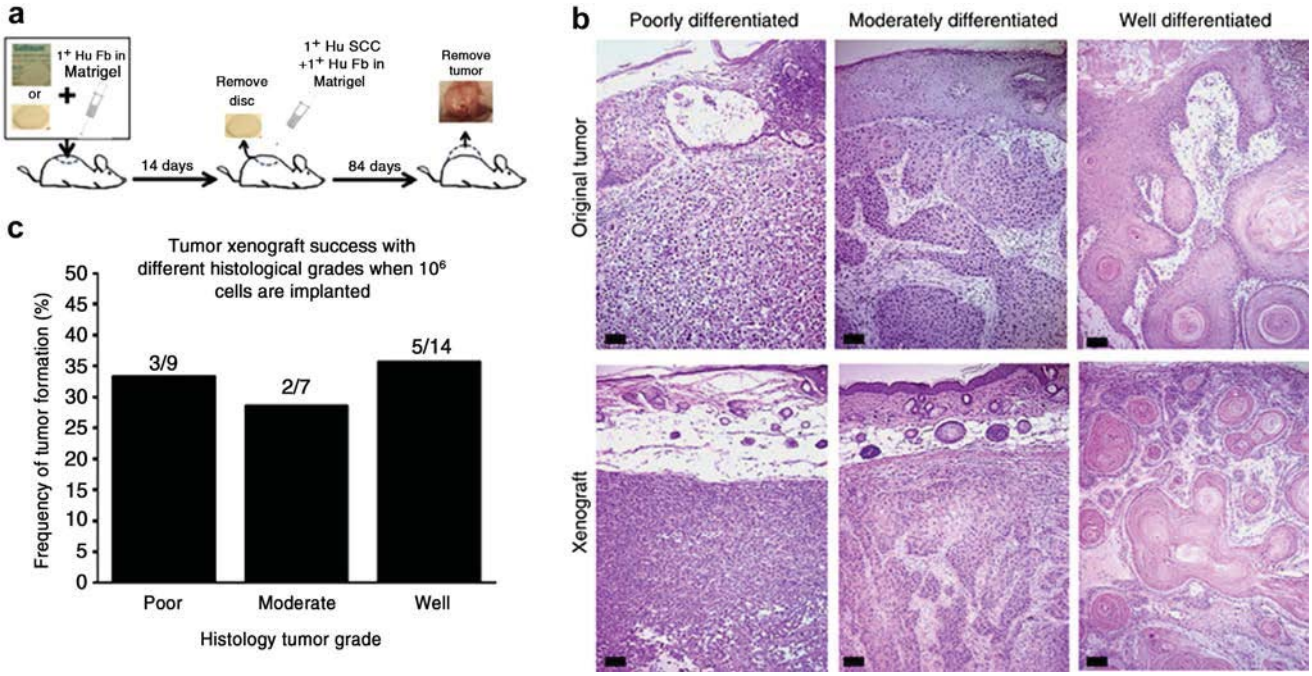

Figure 1. Xenografts from cell suspensions can accurately recapitulate human squamous cell carcinoma (SCC). (**a**) Schematic of the technique. (**b**) SCC xenografts from cell suspensions recreated the original tumor morphology and (**c**) growth based on the original tumor histological grade. Reprinted with permission from Patel et al. (2012).

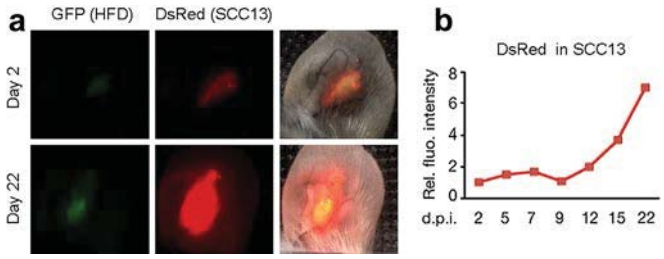

Figure 2. Tumor and stromal cell expansion in an ear injection assay. (**a**) DsRed2-expressing SCC13 cells were admixed with green fluorescence protein-expressing human dermal fibroblasts (HDFs), followed by injection into mouse ears and imaging every 2–3 days under a fluorescence dissection microscope. Shown are representative images from a mouse ear at the indicated times after injection. (**b**) Quantification of digital images for relative red (SCC cells) fluorescence intensity values (intensity × surface area) at different days after injections. SCC, squamous cell carcinoma. Photo courtesy of G.P. Dotto and M.G. Procopio.

(suppressor of hairless or RBP-J in mammalian cells) CSL in the stromal component of the tumor. The expansion of SCC13 cells admixed with HDFs depleted for CSL, p53, or both was monitored in time. Cancer cell expansion was significantly enhanced in the presence of HDFs with concomitant silencing of CSL and p53, as compared with CSL or p53 alone. Interestingly, stromal cells themselves missing both CSL and p53 expanded to a much greater extent than those with silencing of CSL alone. Thus, loss or reduction of CSL in HDFs coupled with p53 inactivation induces SCC expansion, demonstrating a crucial contribution of stromal CSL in tumor formation. Similar to the observations obtained by Patel et al. (2012), these findings demonstrate a fundamental role of the stroma in SCC expansion.

Grafting of human engineered skin

To study specific genetic contributors to SCC, genetic manipulation of primary human keratinocytes using high-efficiency gene transfer can be achieved using retroviral infections repeated at 8- to 12-hour intervals in rapidly dividing cells (Lazarov et al., 2002), which can then be seeded onto devitalized human dermis containing extracellular matrix and stromal proteins (Khavari, 2006). In contrast to subcutaneous or subepidermal injections where an underlying extracellular matrix and intact epithelial basement membrane is lacking, this method allows reconstitution of a human skin-like environment, although it does not fully recapitulate the stochastic nature of mutations that occur in spontaneous cancers and the genomic instability typical of most human cancers.

Recently, Monteleon et al. (2015) used this model to study the function of the protein domains of the IQ motif-containing GTPase-activating protein (IQGAP1), a modulator of mitogen-activated protein kinase signaling, using exogenous expression of IQGAP1 decoy peptides. Ras/CDK4 transformed keratinocytes were infected with lentiviruses designed to drive expression of a single IQGAP structural domain to interfere with specific IQGAP functions. Using this model, a single decoy peptide designed to interfere with binding to the Ras effector Raf (IQGAP-IQM) was found to significantly suppress tumor formation and mitogen-activated protein kinase phosphorylation (Figure 3), whereas the other peptides were ineffective.

CONCLUDING REMARKS

In conclusion, xenotransplantation represents a unique tool to study human SCC progression in an in vivo environment. Recent advances in this technique focus on reproducing the

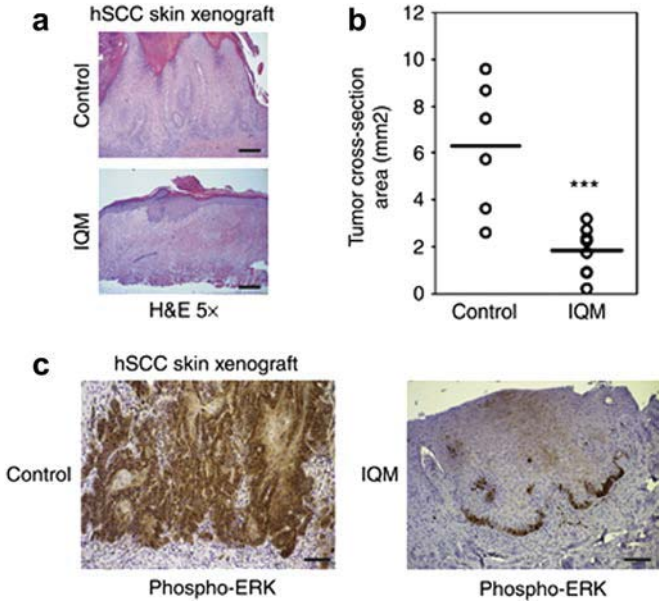

Figure 3. Expression of the IQGAP1-IQM decoy peptide inhibits invasive squamous cell carcinoma (SCC). (**a**) IQGAP1-IQM expression inhibits keratinocyte proliferation and invasion in an SCC skin xenograft, bar = 250 μm. (**b**) Relative tumor cross-sectional area of xenograft control versus IQGAP1-IQM SCC tumors. (**c**) MAPK signaling as indicated by phospho-ERK expression is markedly diminished in the IQM-expressing tissue, bar = 100 μm. ERK, extracellular signal-regulated kinase; IQGAP; IQ motif-containing GTPase-activating protein; MAPK, mitogen-activated protein kinase. Reprinted with permission from Monteleon et al. (2015).

tumor microenvironment and following tumor growth in real time. In the future, engineered human skin and subepidermal and ear injections may become increasingly useful for preclinical investigations of novel therapies, because these models are amenable to topical treatments.

MULTIPLE CHOICE QUESTIONS

1. Which of the following murine models is more receptive for the engraftment of human tumor cells?
   - A. NOD/SCID
   - B. SCID
   - C. NOD/SCID/IL2rγ null (NSG)
   - D. Athymic Foxn1^{nu} (nude)
2. Are SCC cells highly tumorigenic when used in xenotransplantation assays?
   - A. SCC cells are less tumorigenic when injected with human dermal fibroblasts
   - B. SCC cells form aggressive tumors when injected at high concentration
   - C. SCC cells form aggressive tumors when injected in the ear
   - D. Freshly isolated SCC cells are not highly tumorigenic when injected subcutaneously in nude mice without a stromal bed
3. Which of the following sentences is false?
   - A. Subepidermal injections enhance SCC tumorigenic potential and can be used to test cancer inhibiting small compounds
   - B. Ear injections can be used to monitor expansion of tumorigenic cells in real time using conventional fluorescence stereomicroscopy
   - C. In subcutaneous injections, the presence of human dermal fibroblasts enhances tumor growth of human SCC primary cells
   - D. Grafting of human engineered skin onto mice reconstitutes a human skin-like environment
4. What is the advantage of injecting SCC cells in the subepidermal compartment?
   - A. Allows injection of a low number of cells
   - B. Allows interaction of cancer cells with a more physiological environment
   - C. Induces a higher inflammatory response
   - D. Promotes rapid tumor growth
5. Why does preimplantation of a glass disk or Gelfoam improve tumorigenicity of SCC cells in subcutaneous injections in nude mice?
   - A. It generates a wound-like environment, allowing easier access for implantation of SCC cells
   - B. It induces secretion of T-lymphocyte–secreted chemokines, thus favoring tumor growth
   - C. It allows the SCC cells to grow more efficiently in clusters
   - D. It creates a favorable environment by generating a stromal reaction

This article has been approved for 1 hour of Category 1 CME credit. To take the quiz, with or without CME credit, follow the link under the "CME ACCREDITATION" heading.

CONFLICT OF INTEREST
The authors state no conflict of interest.

CME ACCREDITATION
This activity has been planned and implemented by the Duke University Health System Department of Clinical Education and Professional Development and Society for Investigative Dermatology for the advancement of patient care. The Duke University Health System Department of Clinical Education & Professional Development is accredited by the American Nurses Credentialing Center (ANCC), the Accreditation Council for Pharmacy Education (ACPE), and the Accreditation Council for Continuing Medical Education (ACCME) to provide continuing education for the health care team. Duke University Health System Department of Clinical Education and Professional Development designates this enduring activity for a maximum of 1.0 *AMA PRA Category 1 Credits*™. Physicians should claim only credit commensurate with the extent of their participation in the activity.

To participate in the CE activity, follow the link provided.
http://continuingeducation.dcri.duke.edu/sid-journal-based-translational-education-dermatology-research-techniques-made-simple-2015

SUPPLEMENTARY MATERIAL
Supplementary material is linked to this paper.

REFERENCES

Khavari PA. Modelling cancer in human skin tissue. Nat Rev Cancer 2006;6:270–80.

Lazarov M, Kubo Y, Cai T, Dajee M, Tarutani M, Lin Q, et al. CDK4 coexpression with Ras generates malignant human epidermal tumorigenesis. Nat Med 2002;8:1105–14.

Monteleon CL, McNeal A, Duperret EK, Oh SJ, Schapira E, Ridky TW. IQGAP1 and IQGAP3 serve individually essential roles in normal epidermal homeostasis and tumor progression. J Invest Dermatol 2015;135:2258–65.

Patel GK, Yee CL, Yuspa SH, Vogel JC. A humanized stromal bed is required for engraftment of isolated human primary squamous cell carcinoma cells in immunocompromised mice. J Invest Dermatol 2012;132:284–90.

Price JE. Spontaneous and experimental metastasis models: nude mice. Methods Mol Biol 2014;1070:223–33.

Procopio MG, Laszlo C, Al Labban D, Kim DE, Bordignon P, Jo SH, et al. Combined CSL and p53 downregulation promotes cancer-associated fibroblast activation. Nat Cell Biol 2015;17:1193–204.

Purdie KJ, Pourreyron C, South AP. Isolation and culture of squamous cell carcinoma lines. Methods Mol Biol 2011;731:151–9.

Quintana E, Shackleton M, Sabel MS, Fullen DR, Johnson TM, Morrison SJ. Efficient tumour formation by single human melanoma cells. Nature 2008;456:593–8.

Russell L, Griffin B, Kupper T, Divito SJ. Humanized mice in dermatology research. J Invest Dermatol 2015;135:e39.

Wu X, Nguyen BC, Dziunycz P, Chang S, Brooks Y, Lefort K, et al. Opposing roles for calcineurin and ATF3 in squamous skin cancer. Nature 2010;465:368–72.